SOIL NITROUS ACID EMISSIONS: MECHANISMS, IMPACT FACTORS, AND THEIR EFFECTS ON AIR QUALITY

PhD

YANAN WANG

The Hong Kong Polytechnic University

2024

The Hong Kong Polytechnic University
Department of Civil and Environmental Engineering

Soil nitrous acid emissions: mechanisms, impact factors, and their effects on air quality

Yanan Wang

A thesis submitted in partial fulfillment of the requirements for the Degree of Doctor of Philosophy

July 2023

CERTIFICATE OF ORIGINALITY

I hereby declare that this thesis is my own work and that, to the best of my knowledge and belief, it reproduces no material previously published or written, nor material that has been accepted for the award of any other degree or diploma, except where due acknowledgement has been made in the text.

_____ (Signed)

_____Yanan Wang_____ (Name of student)

Abstract

Nitrous acid (HONO) plays a crucial role in the production of the highly reactive hydroxyl radical (OH), which acts as a major oxidant to remove various gases emitted into the atmosphere and produce secondary air pollutants. Previous studies have revealed the significant contribution of HONO emissions from soil to atmospheric HONO. The release of HONO from soil is mainly attributed to nitrification and denitrification processes, in which microbial communities and genes play a vital role. These processes are influenced by various environmental factors, including soil moisture, temperature, nitrogen (N) content, etc.

As a major factor, the effects of N fertilizers on HONO emissions have not been studied. In addition to HONO emissions introduced by fertilizers, emissions from unfertilized soils also accounted for a large part of total soil emissions due to their long duration. However, limited research has been conducted to quantify HONO emissions for different soil types, resulting in a lack of parameterization schemes to assess their impact on air quality. To address these research gaps, parameterization schemes linking HONO emissions from both fertilized and unfertilized soils to soil water content (SWC) and temperature were developed and implemented in a chemical transport model. This improved the simulation of atmospheric HONO levels.

We conducted experiments to measure soil HONO emissions after applying three commonly used fertilizers and found high HONO emissions from soils at high soil moisture, which contrasts to previous lower predictions at high soil moisture. This source is missing from current state-of-the-art air quality models. The effects of fertilization on HONO release lasted for approximately one week. Based on laboratory results, we developed a parameterization scheme and incorporated it into a chemical transport model. The inclusion of post-fertilization soil HONO emissions improved HONO predictions and demonstrated the significant impact of this emission source on air quality. Additionally, we found that the use of urea fertilizer resulted in the highest release of HONO compared to other commonly used fertilizers (ammonium bicarbonate and ammonium nitrate). Therefore, we propose that adjusting fertilizer structures may help to reduce HONO emissions and improve air quality in polluted regions with intense agriculture.

We also measured soil background (unfertilized) HONO and NO emission fluxes of 48 soil samples collected from diverse soil types across China. The results show much higher emissions of HONO than those of NO, which were caused by the higher promotion effects of long-term fertilization on the abundance of HONO-producing genes than NO-producing genes. This enhancement was greater in northern China than in southern China, which accounts for the higher emission fluxes in the former region than in the latter region. Simulations using a chemical transport model with the lab-derived parametrization show greater impacts of soil background HONO emissions on

air quality than NO emissions, and larger impacts in the regions with lower anthropogenic emissions. With the projected continuous reduction of anthropogenic emissions, the contribution of soil emissions to reactive nitrogen levels is expected to increase substantially. Our study highlights the necessity for quantification of HONO emissions from soil together with NO emissions to improve the estimates of reactive N emissions and their impact on air quality.

Overall, this thesis measured both fertilized and unfertilized soil HONO emissions. The derived parameterization schemes improved the performance of the HONO simulations and demonstrated the important role of soil HONO emissions in atmospheric oxidative capacity and atmospheric chemistry.

Publications

1. **Wang, Y.**, Fu, X., Wu, D., Wang, M., Lu, K., Mu, Y., Liu, Z., Zhang, Y., and Wang, T.: Agricultural Fertilization Aggravates Air Pollution by Stimulating Soil Nitrous Acid Emissions at High Soil Moisture, Environ Sci Technol, 55, 14556-14566, 10.1021/acs.est.1c04134, 2021.
2. **Wang, Y.**, Fu, X., Wang, T., Ma, J., Gao, H., Wang, X., and Pu, W.: Large Contribution of Nitrous Acid to Soil-Emitted Reactive Oxidized Nitrogen and Its Effect on Air Quality, Environ Sci Technol, 57, 3516-3526, 10.1021/acs.est.2c07793, 2023.
3. Jia, C., **Wang, Y.**, Li, Y., Huang, T., Mao, X., Mo, J., Li, J., Jiang, W., Liang, X., Gao, H., and Ma, J.: Oxidative capacity and radical chemistry in a semi-arid and petrochemical-industrialized city, northwest China, Aerosol and Air Quality Research, 18(6), 1391-1404, 2018.
4. Gu, R., Zheng, P., Chen, T., Dong, C., **Wang, Y.**, Liu, Y., Liu, Y., Luo, Y., Han, G., Wang, X., Zhou, X., Wang, T., Wang, W., and Xue, L.: Atmospheric nitrous acid (HONO) at a rural coastal site in North China: Seasonal variations and effects of biomass burning, Atmospheric Environment, 229, 10.1016/j.atmosenv.2020. 117429, 2020.
5. Gu, R., Wang, W., Peng, X., Xia, M., Zhao, M., Zhang, Y., **Wang, Y.**, Liu, Y., Shen, H., Xue, L., Wang, T., and Wang, W.: Nitrous acid in the polluted coastal

atmosphere of the South China Sea: Ship emissions, budgets, and impacts, Sci Total Environ, 826, 153692, 10.1016/j.scitotenv.2022.153692, 2022.

6. Peng, X., Wang, T., Wang, W., Ravishankara, A. R., George, C., Xia, M., Cai, M., Li, Q., Salvador, C. M., Lau, C., Lyu, X., Poon, C. N., Mellouki, A., Mu, Y., Hallquist, M., Saiz-Lopez, A., Guo, H., Herrmann, H., Yu, C., Dai, J., **Wang, Y.,** Wang, X., Yu, A., Leung, K., Lee, S., and Chen, J.: Photodissociation of particulate nitrate as a source of daytime tropospheric Cl_2, Nat Commun, 13, 939, 10.1038/s41467-022-28383-9, 2022.

Acknowledgements

Time flies, and the fleeting four-year journey of the PhD student has been filled with growth and learning. Throughout these past years, I have not only cultivated a profound interest in scientific research but also acquired the valuable skills of discovering, critical thinking, and problem-solving under the guidance of Prof. Tao Wang. I have encountered numerous setbacks during this period, which have instilled in me the ability to confront challenges with an optimistic mindset. On the occasion of the completion of this thesis, I would like to sincerely express my heartfelt gratitude to those who have supervised, assisted, and inspired me along the way.

First, I would like to express my sincere gratitude to my supervisor, Prof. Tao Wang, for his inspiration and support in my scientific research. His enthusiasm for academics and rigorous logical thinking have greatly influenced me. Under his supervision, I have learned to analyze data from multiple perspectives and approach it from different angles. Moreover, Prof. Wang has opened my eyes to new possibilities and expectations for future research endeavors. I am also immensely grateful for his patience. Whenever I encountered obstacles or difficulties in my experiments, he always made time out of his busy schedule to help me explore and resolve issues together in the laboratory. His patient encouragement played a pivotal role in rebuilding my confidence and fortitude, especially during moments when I contemplated giving up.

I also want to thank Dr. Xiao Fu for her help in my work. Collaboration with her enabled the implementation of laboratory-derived parameterization schemes into models to assess the impact of soil emissions on air quality at a regional scale. Dr. Fu's profound scientific knowledge and innovative ideas continually inspire me to reconsider and refine my research. Collaborating with her has also allowed me to perceive the broader implications and significance of my work. I would also like to extend my thanks to Steven for his assistance during my experiments and for his continuous support in both my professional and personal life. His encouragement has been instrumental in helping me persevere during challenging times. A special mention goes to Dr. Wei Pu, who has been like a warm-hearted brother to me throughout my research journey. From accompanying me during soil sample collection to conducting experiments, Dr. Pu has been a constant source of support. He has also patiently listened to my frustrations and provided solace during my hardest time. I would like to express my gratitude to the other members of my research group as well, including Dr. Chuan Yu, Dr. Yi Chen, Dr. Rongrong Gu, Penggang Zheng, Dr. Yiming Liu, Dr. Qianjie Chen, Dr. Xiaorui Chen, Zhouxing Zou, Yue Tan, and others.

I extend my heartfelt appreciation to all of the collaborators who have played a pivotal role in supporting and advancing my research endeavors. Thanks Prof. Dianming Wu (East China Normal University) for helping me build the experimental equipment. Thanks Prof. Keding Lu (Peking University) and Prof.

Yuanghang Zhang (Peking University) for providing field data for validation of model. Thanks Prof. Yujing Mu (Research Center for Eco-Environmental Sciences, Chinese Academy of Sciences), Prof. Jianmin Ma (Peking University), Prof. Hong Gao (Lanzhou University), and Prof. Xin Wang (Tianjin University) for providing soil samples across China.

I would like to sincerely thank my family. Their unconditional love and support keep me with a kind and grateful heart. They are my strongest backing and the source of my courage and strength to persist in pursuing my dreams.

Finally, I acknowledge the financial support from The Hong Kong Research Grants Council (T24-504/17-N) and the National Natural Science Foundation of China (91844301).

July 2023

Hong Kong

Table of contents

List of tables

List of figures

Figure 5.6 Model-simulated monthly average soil background emissions of NO, HONO (ng N m^{-2} s^{-1}) in August 2016, and anthropogenic emissions of NO_x in 2015 in China.

Figure 5.7 Simulated effects of soil background emissions on air quality.

Figure 5.8 Simulated impacts of soil background on air quality in the future with the reduction of anthropogenic emissions under the low-carbon energy policies and maximal end-of-pipe control strategies.

Chapter 1 Introduction and Motivation

This chapter is an overall introduction to my graduation thesis, including the background and the importance of my Ph.D. research, the knowledge gaps and the objectives, and the new findings and significances of this study.

1.1 Introduction

Nitrous acid (HONO) is a key precursor of the highly reactive hydroxyl radical (OH) (Alicke et al., 2003;Kim et al., 2014). OH is the most important oxidant to remove many gases emitted into the atmosphere and, in the process, produces air pollutants such as ozone (O_3) and secondary aerosols (Lu et al., 2019a;Stone et al., 2012). Accordingly, exploring the sources and sinks of HONO is a hot topic in atmospheric chemistry and air pollution control. The sources of HONO we presently know contain direct emission from vehicles and ships, gas phase oxidation, and heterogeneous reactions occurring on the ground and aerosol surface, and photolysis of nitric acid and particulate nitrate (Gu et al., 2022;Liu et al., 2019b;Xue et al., 2020). However, these sources are insufficient to explain the observed HONO concentrations in the ambient atmosphere, especially during the daytime. Over the past ten years, several research studies have identified soil microbial emissions as a significant contributor to the missing source of HONO (Oswald et al., 2013;Ermel et al., 2018;Wu et al., 2019;Bhattarai et al., 2021).

Soil HONO emissions are mainly produced through the nitrification and denitrification processes in the soil, which are regulated by different microbial communities. The long-term fertilization enhances soil microbial abundance and activity by increasing soil nitrogen (N) content (Kautz et al., 2004;Tian et al., 2015), thereby affecting the release of reactive N, including HONO and NO, to the atmosphere. However, the impact of long-term fertilization on the mechanism and magnitude of HONO emission are not well studied.

Total soil N emissions comprise both emissions from fertilization and those from unfertilized sources (Yan et al., 2003b). To assess the impact of soil HONO emissions on air quality over different time periods, it is crucial to accurately quantify the emissions from soil under both fertilized and unfertilized conditions. Fertilization plays a significant role in supplying N to the soil and can also lead to N loss from fertilized soils into the atmosphere. Typically, N fertilizers are applied as a basal dressing and 1-3 rounds of top dressing during the crop growth period (Ministry of Agriculture and Rural Affairs of the People's Republic of China, 2010). The continuous use of N fertilizers and crop rotation increase the potential for reactive nitrogen production in fertilized soils. Although the agricultural sector recognizes fertilization as a major source of atmospheric reactive nitrogen, there is limited knowledge regarding its impact on HONO emissions. Consequently, the current state-of-the-art models lack an appropriate parameterization scheme to accurately quantify the impact of post-fertilization soil HONO emissions on air quality.

The emissions from unfertilized soil in current year or season are defined as the background emissions(Gu et al., 2007;Gu et al., 2009;Kim et al., 2013). Although post-fertilization N emissions are significantly higher than those during non-fertilization period, the boosting effect of nitrogen fertilization only lasts for one to two weeks, and nitrogen emissions from agricultural soils stay at a low level as background emissions for most of the time (Tian et al., 2020;Zhang et al., 2014). Thus, accurately quantifying background emissions is crucial for simulating their impact on air quality. Since the proposal of soil microbial emissions of HONO in 2013 by Oswald et al (Oswald et al., 2013), numerous studies have carried out laboratory experiments and field measurements of HONO emissions. However, most of these studies have been conducted at individual or sparse sites, resulting in limited measurements of HONO emissions from diverse soil types. Consequently, there is a lack of parameterization to quantify HONO emissions from different soil types and their impact on air quality.

1.2 Aims and objectives

It is essential to address these issues in order to accurately quantify soil HONO emissions and assess their impact on air quality. The detailed objectives of this study are listed below.

1. To investigate the responses of post-fertilization HONO emissions to different fertilizer types.

2. To quantify soil background emissions of HONO from a wide range of soil types in different regions of China.

3. To develop a parameterization scheme suitable for regional transport models.

4. To evaluate the effects of soil HONO emissions on regional air quality.

1.3 Findings and significances

We quantified soil HONO emissions after treatment using three common fertilizers (urea, ammonium bicarbonate, and ammonium nitrate) in laboratory. Additionally, we investigated the relationship between HONO emissions and the time since fertilization. Our laboratory experiments reveal high HONO emissions from fertilized soils at high soil moisture, which contrasts to previous lower predictions at this soil water content for agricultural or natural soils. This source is missing from current state-of-the-art air quality models. Urea leads to the largest HONO emissions compared to the other two common fertilizers. A parameterization is developed and implemented in a chemical transport model that improves post-fertilization HONO prediction and demonstrates significant impact of this HONO source on atmospheric chemistry. As the most consumed chemical fertilizer, nitrogen fertilizers have been extensively used in the world. Considering that nitrogen fertilizers are widely used worldwide and play a crucial role in agricultural practices, the high potential for post-fertilization HONO emissions and their impact on air quality should be of global

concern. The findings are likely of great interest to a wide range of readers, including atmospheric chemists, soil scientists, agricultural researchers, farmers, chemical engineers, and environmental policy makers.

Through the measurement of soil background HONO and NO emissions from diverse soil types in different regions of China, we find that the emission fluxes from cropland soils are higher than those from forest soils, and the emission fluxes from soil samples in northern China were found to be higher than those in southern China. In addition, the soil background emission fluxes of HONO are generally higher than that of NO, revealing a significant contribution of HONO to the reactive oxidized nitrogen. We conducted a statistical analysis of 52 previous field studies on the long-term fertilization impact on gene abundance in China. We found that the long-term fertilization can significantly increase the soil microbial gene abundances involved in soil nitrogen cycling, and the enhancement of HONO-producing genes abundances is much higher than that of NO-producing genes. The promotion effect in northern China is higher than that in southern China. We also derive a lab-based parametrization of soil background emissions to quantify the HONO emissions and their impact on air quality in a chemical transport model. Results show that high emissions are mainly concentrated in regions with dense cropland and that soil background emissions have a significant effect on atmospheric oxidation capacity and secondary pollutants, particularly in regions with low anthropogenic emissions and dense cropland. Soil background HONO emissions have a larger impact on air quality than NO. This study

highlights the need for considering HONO in the assessment of reactive nitrogen loss from soils to the atmosphere and their impact on air quality.

1.4 Thesis structure

1) The thesis is organized into nine chapters as follows: Chapter 1 provides an introduction to the background, knowledge gaps, objectives, and findings and significances of this study.

2) Chapter 2 reviews the HONO chemistry and its impact on air quality, the sources and sinks of HONO that we currently know, measurement techniques, and impact factors of soil HONO emissions.

3) Chapter 3 introduces the setup of dynamic chamber, measurement techniques, preparation of soil samples, and the process of measuring soil emission fluxes.

4) Chapter 4 reports the post-fertilization HONO emissions after using three commonly used fertilizers and reveals their significant impact on air quality.

5) Chapter 5 presents the background emissions from different soil types across China and quantifies their impact on air quality.

6) Chapter 6 summarizes the key findings and the implications of this thesis, the limitations of this study, and proposes the directions for future research.

Chapter 2 Literature review

OH is the most important oxidant in the atmosphere, removing and determining the lifetime of most trace gases in the troposphere and leading to the formation of secondary pollutants such as O_3 and secondary aerosols (Finlayson-Pitts and Pitts J., 1997;Stone et al., 2012;Elshorbany et al., 2010). The OH concentration level can be used as an indicator of atmospheric oxidation capacity. HONO plays important role in atmospheric chemistry due to its contribution to OH (Alicke et al., 2003;Kleffmann et al., 2005), and the research on the sources of HONO and its effects on air quality has become one of the hot topics of atmospheric chemistry. Despite numerous studies exploring the HONO budget and its effect on atmospheric oxidation capacity, many controversies remain (Gu et al., 2021;Zhang et al., 2019a;Xue et al., 2020;Zhang et al., 2020). In recent decade, soil microbial emissions have been identified as a significant source of HONO, which is regulated by various environmental factors (Oswald et al., 2013;Wu et al., 2019;Ermel et al., 2018). In this chapter, we reviewed the atmospheric chemistry and sources of HONO. Also, the research status of soil HONO emissions, measurement techniques, as well as the impact factors are also reviewed.

2.1 The atmospheric chemistry and impact of HONO

HONO is one of the relatively active trace gases in the atmosphere. Due to its important contribution to OH and significant role in nitrogen deposition and nitrogen cycle, HONO has received extensive attention. The measurement of HONO began in

the late 1970s (Perner and Platt, 1979), and its concentration is generally higher in heavily polluted urban areas, reaching as high as several to about a dozen ppb at night (Yun et al., 2017;Kleffmann, 2007;Spataro and Ianniello, 2014). In terms of diurnal variation, HONO usually accumulates continuously at night and peaks in the early morning, while rapidly declining during the day and reaching a minimum value at noon and afternoon due to photolysis (Qu et al., 2019;Nie et al., 2015;Michoud et al., 2014;Liu et al., 2019b;Gu et al., 2021). The photolysis of HONO occurs at a wavelength range of 300 - 405 nm (Stockwell and Calvert, 1978;Stutz et al., 2000), as shown below:

$$HONO + hv \rightarrow NO + OH(300\ nm < \lambda < 405nm) \quad (R1)$$

Early research believed that the contribution of HONO to OH was primarily concentrated in the early morning, while during the noon and afternoon, when sunlight is strong, HONO could not accumulate due to the rapid photolysis reaction (Platt et al., 1980;Alicke et al., 2003;Winer and Biermann, 1994), and its contribution to OH can therefore be ignored. With the improvement of measurement technology and the reduction in the detection limit of HONO (Kleffmann et al., 2002;Heland et al., 2001), the lower HONO concentration in the daytime can now be accurately quantified. In recent years, many studies have observed high concentrations of HONO both in urban and suburban areas, revealing that HONO can also make an important contribution to OH formation throughout the all daytime, with a contribution of 20-80% in different

regions around the world (Kleffmann et al., 2005;Zha et al., 2014;Fu et al., 2019;Elshorbany et al., 2009;Acker et al., 2006;Alicke et al., 2003;Kim et al., 2014).

Many studies have been conducted to understand the sources of HONO and assess its impact on atmospheric oxidation. A consistent finding from these studies is that even when considering the currently known sources of HONO (Section 2.2), there are still missing sources, particularly during the daytime with strong sunlight (Huang et al., 2017;Gu et al., 2020;Zhang et al., 2020;Liu et al., 2021;Hou et al., 2016;Villena et al., 2011). Several studies have proposed new mechanisms and sources to explain these missing sources (Stemmler et al., 2006;George et al., 2005;VandenBoer et al., 2014;Zhang and Tao, 2010), but there is still ongoing debate and controversy surrounding the reasons for the missing sources. Therefore, further investigation is needed to fully understand the sources of HONO and their implications for air quality. In the following section, we will review the widely accepted sources of HONO.

2.2 HONO sources and sinks

2.2.1 HONO sources

The sources of HONO in the atmosphere are very extensive, including homogeneous reactions, heterogeneous reactions of nitrogen dioxide (NO_2) on various surface, photolysis of nitric acid (HNO_3) and particulate nitrate (pNO_3), as well as direct emissions.

2.2.1.1 Gas phase homogeneous reactions

Homogeneous reactions refer to chemical reactions that occur in the same phase. The homogeneous reactions of NO and OH, as described in R2, have been shown to produce HONO (Nguyen et al., 1998;Pagsberg et al., 1997). This pathway is well established, and it is typically included in model mechanisms as a default HONO source (Fu et al., 2019;Zhang et al., 2016a). Another process, R3, also produces HONO. However, its reaction rate is quite low, with a small rate constant of 1.2×10^{-34} cm^3 $molecules^{-1}$ s^{-1} (Chan et al., 1976). As a result, its contribution to HONO concentration is not significant, especially in environments with low nitrogen oxides (NO_x).

$$NO + OH + M \rightarrow HONO + M \quad \text{(R2)}$$

$$NO + NO_2 + H_2O \rightarrow 2HONO \quad \text{(R3)}$$

2.2.1.2 Heterogeneous reactions

Heterogeneous chemical reactions take place at two-phase interfaces (e.g. gas-liquid, gas-solid, and liquid-solid). A large number of field observations have shown that HONO can be generated through heterogeneous processes of NO_2 on various surface (Harrison et al., 1996;Kleffmann et al., 1999;Finlayson-Pitts et al., 2003;Notholt et al., 1992;Reisinger, 2000). Due to absence of photochemical reactions at night, heterogeneous reactions become the most important sources of HONO at night. Heterogeneous reactions as sources of HONO can be divided into hydrolysis reactions and reduction reactions of NO_2 occurring on the surface of reducing substances.

Hydrolysis of NO_2 on various surfaces (R4), including the ground, buildings, vegetation, and aerosol, is an important pathway of heterogeneous formation source of HONO (Lammel and NeiláCape, 1996;Harrison et al., 1996;Kleffmann et al., 1999). On the basis of both field and laboratory studies, R4 is identified as a significant HONO source (Sakamaki et al., 1983;Finlayson-Pitts et al., 2003). However, the contribution of R4 to HONO varies greatly in different environments, depending on the concentration of NO_2, surface area, and moisture content (Finlayson-Pitts et al., 2003).

$$2NO_2 + H_2O \xrightarrow{\text{surface}} HONO + HNO_3 \quad \text{(R4)}$$

In addition, heterogeneous reactions of NO_2 on the surfaces of reducing matters (R5) (e.g., soot, humid acid, mineral dust, and other organic substrates) can also produce HONO, and this process has been shown to be photo enhanced (Ammann et al., 1998;Kalberer et al., 1999;Monge et al., 2010;Stemmler et al., 2006).

$$NO_2 + A^{red} \rightarrow HONO + A^{ox} \quad \text{(R5)}$$

where A^{red} and A^{ox} represent reducing and oxidizing substances, respectively. Although these reactions are related to previous findings, i.e., the unknown daytime source of HONO is correlated with NO_2 concentrations and radiation intensity, none of them can fully explain the high concentration of HONO observed during the daytime.

2.2.1.3 Photolysis of nitric acid/ nitrate

Previous field and laboratory experiments demonstrated that the photolysis of HNO_3 and nitrate deposited on the ground and vegetation surface was an important source of HONO (R6) (Zhou et al., 2003;Zhou et al., 2011). Both natural and artificial surfaces, like vegetation surfaces, roads, and buildings, could provide large surface areas for surface photolysis. The photolysis rate constant ($J_{HNO3(s)}$) of the surface HNO_3/nitrate is higher than that of the gaseous HNO_3, with a range of 6.0×10^{-6} s^{-1} to 3.7×10^{-4} s^{-1} (Ye et al., 2016a). A study conducted in the Pearl River Delta, China (Li et al., 2012) found that the photolysis of HNO_3 adsorbed on the ground surface was an important contributor to HONO formation.

$$HNO_3/NO_3^- + hv \rightarrow HONO/NO_2^- + O \quad \text{(R6)}$$

2.2.1.4 Photolysis of particulate nitrate

Ye et al. (2016b) conducted an airborne measurement in the marine boundary layer, the results showed that the HONO unknown source was strongly correlated with the product of the pNO_3 concentrations and its photolysis frequency, suggesting a significant contribution of pNO3 photolysis to HONO concentrations. Subsequent laboratory experiments demonstrated the important role of pNO_3 photolysis in HONO formation (Ye et al., 2017;Bao et al., 2018) and determined its photolysis rate constants (J_{pNO3}) are in the range of 6.2×10^{-6} s^{-1} to 5.0×10^{-4} s^{-1}.

$$pNO_3 + hv \rightarrow HONO + O \quad \text{(R7)}$$

2.2.1.5 Direct emissions

In addition to secondary generation, primary direct emissions also contribute significantly to HONO levels. Fossil fuel combustion and biomass burning are well-known primary sources of HONO (Kurtenbach et al., 2001;Kirchstetter et al., 1996;Nie et al., 2015;Gu et al., 2020). The quantification of HONO direct sources and mainly concentrated on vehicle exhaust. The HONO/NO_x ratio is often used to characterize the emission coefficient of HONO in vehicle exhaust. The type of vehicle and its operating state, the type of fuel used and whether it is equipped with a catalytic converter have a greater impact on HONO emissions. HONO emissions from diesel vehicles generally exceed those from gasoline vehicles. Kurtenbach et al. (2001) and Kirchstetter et al. (1996) measured the emission factors of HONO for different types of vehicles in Wuppertal, Germany and a tunnel in San Francisco, U.S., respectively, with the HONO/ NO_x ratios ranging from 0.3% to 0.8%. Trinh et al. (2017) found the emission ratio of HONO/NO_x was in a range of 0.16–1% with an average of 0.8%. Rappengluck et al. (2013) observed an emission factor of 1.7% for HONO at a heavily trafficked intersection in Houston. Generally, the HONO/NO_x ratios in the vehicle are within a range of 0.29–1.7% (Rappengluck et al., 2013;Xu et al., 2015). Modeling studies often employ HONO/NOx ratios of 0.8% for gasoline vehicles and 2.3% for diesel vehicles (Zhang et al., 2016a;Fu et al., 2019).

Apart from fossil fuel combustion, previous experiments have indicated that biomass burning can also directly emit HONO and generate it indirectly through NO_2 heterogeneous reactions on soot (Burling et al., 2010;Yokelson et al., 2009). The results of Nie et al. (2015) showed that the direct emission of biomass burning accounted for 17% of the observed HONO concentration, and more than 80% of the HONO was produced by the conversion of NO_2 in the nighttime biomass burning plume.

In the recent decade, the direct HONO emissions from soil have been recognized as an important source of HONO. The research status of soil HONO emissions will be reviewed in detail in Section 2.3.

2.2.2 HONO sinks

The main HONO mechanism for HONO removal is through the photolysis of HONO (R1). This reaction determines the lifetime of HONO in the daytime, which is generally 15-20 min at noon. Another significant chemical loss occurs through the reaction of HONO with OH (R8), with a reaction rate constant of 6×10^{-12} cm^3 $molecules^{-1}$ s^{-1} (Atkinson et al., 2006). Due to the low concentrations of OH in the nighttime, R8 is only important in the daytime with high OH concentrations. In addition, HONO can also be removed by wet and dry deposition.

$$HONO + OH \rightarrow H_2O + NO_2 \quad \text{(R8)}$$

2.3 Soil HONO emissions

2.3.1 Development of soil HONO emissions measurements

In 2011, Su et al. (2011) measured the direct emission of HONO from soil for the first time, and proposed that soil nitrite (NO_2^-) can emit a large amount of HONO to the atmosphere. This mechanism was proposed to explain sources of HONO that were previously unaccounted for during daylight hours. This study proposed that HONO can be released in equilibrium with soil NO_2^-. In 2013, Maljanen et al. (2013) measured the emission flux of reactive oxidized nitrogen gases from acidic soils in northern Finland and found that high nitrous oxide (N_2O) and nitric oxide (NO) emissions were accompanied by high HONO emissions.

Also in 2013, Oswald et al. (2013) measured HONO and NO emissions of 17 soil samples across the world and found that the fluxes of HONO and NO are comparable, even in samples from non-acidic soils. Their findings revealed that the nitrification caused by ammonia-oxidizing bacteria (AOB) can release HONO and NO directly. Building upon this discovery, many laboratory incubation experiments and field measurements were conducted to measure the soil microbial emissions of HONO. Ermel et al. (2018) investigated the HONO emissions from pure cultures of AOB and ammonia-oxidizing archaeon (AOA). The results demonstrated that in addition to AOB, AOA also contributes to biogenic HONO emissions, and all measured AOB and AOA strains emitted more HONO than NO; however, AOB appears to be the major

contributor to HONO and NO in their pure culture experiments. Scharko et al. (2015) utilized isotopic techniques to demonstrate the conversion of $^{15}NH_4^+$ in soil to $HO^{15}NO$. They also conducted gene sequence analysis, linking the peak HONO flux to the abundance of AOB and AOA. The results of forest soil sampled from the eastern United States by Mushinski et al. (2019) showed low emissions from forest soils, with fluxes of HONO about twice and six times that of NO for soils stands dominated by arbuscular mycorrhizal and ectomycorrhizal, respectively. And they proposed that soil NO_y ($HONO + NO_x$) production is largely mediated by AOB. Bhattarai et al. (2018) revealed that agricultural soil HONO and NO emissions highly depend on the concentration of soil NO_2^-, and in their laboratory measurements, the average NO emission flux was significantly higher than that of HONO. HONO flux from bare soil in the Mediterranean island measured by Meusel et al. (2018) are about twice as high as NO flux. Wu et al. (2022) measured HONO emissions from soil samples collected from different land use types in Shanghai, China, and scaled up their findings to estimate global HONO emissions.

In addition to nitrification, HONO is also produced in soil through denitrification. Wu et al. (2019) found the high soil HONO emissions at high soil water content. Through the gene expression analyses, they attributed this phenomenon to biological nitrate reduction, which is a step in the denitrification process. The study of Bhattarai et al. (2021) also revealed that microbial nitrate reduction is an important pathway of HONO generation in soil, and its contribution to HONO emissions even exceeded that

of nitrification in their study. In summary, the main mechanisms responsible for soil HONO emissions are nitrification and nitrate reduction in denitrification process.

2.3.2 Mechanisms of soil nitrogen emissions

Soil microbes are crucial drivers of N cycling in ecosystems, with various microbial communities regulating specific key steps in this process (Levy-Booth et al., 2014;Huang et al., 2013). Soil emissions of HONO and NO are mainly related to the nitrification and denitrification processes (Oswald et al., 2013;Ermel et al., 2018;Wu et al., 2019). Nitrification is the biological oxidation of ammonium (NH_4^+) to nitrate (NO_3^-), including two steps of ammonium oxidation and nitrite oxidation (Li et al., 2020b;Martens-Habbena et al., 2009;Zhang et al., 2018) performed by two distinct groups of microbes: ammonia-oxidizers (encoded by *amoA* genes of ammonia-oxidizing archaea (*AOA*) and ammonia-oxidizing bacteria (*AOB*)) and nitrite-oxidizers (encoded by *nxrA*) (Levy-Booth et al., 2014;Wertz et al., 2008) (Figure 2.1). Denitrification is the biological reduction of NO_3^- to dinitrogen gas (N_2); this occurs via a four-step process ($NO_3^- \rightarrow NO_2^- \rightarrow NO \rightarrow N_2O \rightarrow N_2$), with each step controlled by different microbiomes (Correa-Galeote et al., 2017;Philippot, 2002) and catalyzed by a different enzyme: nitrate reductase (encoded by *narG* and *napA*), nitrite reductase (encoded by *nirK* and *nirS*), nitric oxide reductase (encoded by *norB*), and nitrous oxide reductase (encoded by *nosZ*), respectively (Figure 2.1) (Tang et al., 2016;Geets et al., 2007). The emission fluxes of HONO during nitrification and denitrification are largely

related to NO_2^- produced in the soil, so *AOA amoA*, *AOB amoA*, *narG*, and *napA* can be used as functional gene markers of HONO emission. Similarly, *nirK* and *nirS* are gene markers of NO production and emission.

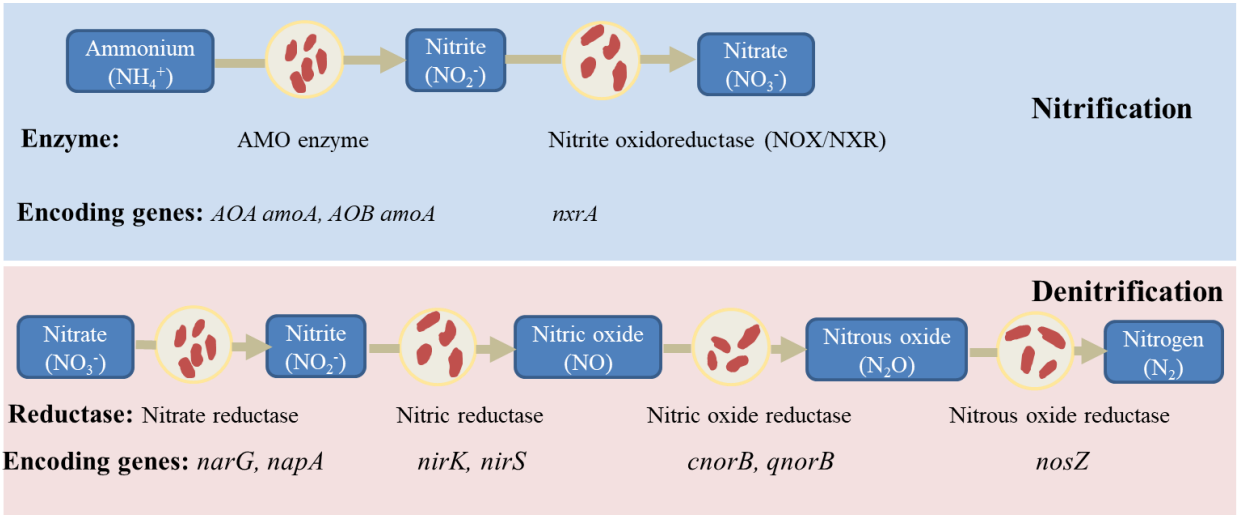

Figure 2.1 Soil microbial nitrification and denitrification processes, which are responsible for soil HONO and NO productions.

2.3.3 Measurement technologies of soil trace gas emissions

The technologies used for flux measurement mainly include micrometeorological methods and chamber methods (Smith et al., 1994;Harper et al., 2011). Micrometeorological techniques include various approaches such as the mass balance method, vertical flux techniques (aerodynamic gradient technique, eddy covariance, and relaxed eddy accumulation method), and inverse dispersion analysis (Harper et al., 2011). Micrometeorological methods are widely used in the measurement of gas emission fluxes in ecosystems or farmland. However, they have certain limitations,

such as being applicable only to large areas, requiring uniformity of the underlying surface, and demanding high analytical sensitivity and response speed of the analyzers (Muller et al., 2010;Horst and Weil, 1994;Harper et al., 2011). Sörgel et al. (2015) measured the flux of HONO in a forest in Germany by using the aerodynamic gradient technique and found that the forest soil was a sink of HONO, while the net emissions were observed for clearing soil in the daytime.

Chamber methods are commonly employed to measure the exchange of trace gases between the ground surface and the atmosphere (Behrendt et al., 2014;Smith et al., 1994;Xue et al., 2019;Tang et al., 2019b;van Dijk et al., 2002). Compared to micrometeorological techniques, chamber methods are less expensive, easier to deploy, and less demanding on the environment. There are two types of chamber methods: static chamber and dynamic chamber. The static chamber involves covering the soil with a closed chamber and calculating fluxes by measuring the concentration change of the gas inside the chamber. Since the static chamber is closed, the environment inside the chamber changes, which affects the emission processes of soil. This method is currently used for the measurement of inert gases. The dynamic chamber method considers the flow process of the gas inside the chamber and is better suited for measuring fluxes of reactive gases (Meixner, 1994). Previous studies have demonstrated that the dynamic chamber system can simulate field fluxes accurately (Plake et al., 2015;Remde et al., 1993). Also, several research groups have utilized the dynamic chamber method to measure soil HONO emissions (Ermel et al., 2018;Oswald et al., 2013;Wu et al., 2019).

2.3.4 Impact factors of soil HONO emissions

2.3.4.1 Soil moisture

Soil moisture is a major driver of HONO emissions (Oswald et al., 2013;Wu et al., 2019) by regulating the availability of oxygen (O_2) in soil that influences microbial activity (Bollmann and Conrad, 1998;Butterbach-Bahl et al., 2013). At lower soil water content (SWC), the nitrification process becomes dominant. In contrast, higher SWC limits the diffusion of O_2, creating an anaerobic environment in the soil that favors the denitrification process (Bollmann and Conrad, 1998). Oswald et al. (2013) found that the emission peak of HONO occurred under the condition of low SWC (0-40% water holding capacity, WHC), which is more conducive to the nitrification reaction and the diffusion of gas to the soil surface. Subsequent isotopic and genetic experiments further confirmed the significant contribution of nitrification to HONO emissions at low SWC (Ermel et al., 2018;Scharko et al., 2015). In addition to the dry peak at low SWC, Wu et al. (2019) found high HONO emissions (wet peak) under high SWC conditions, attributing it to the denitrification process in the soil through gene-expression analyses.

2.3.4.2 Soil temperature

The temperature range of 25-30 ℃ is generally considered optimal for the activities of nitrifying and denitrifying microorganisms, with microbial activity decreasing as temperatures increase. However, research by Myers demonstrated that

soil nitrifying bacteria adapt to their local climate. In tropical Australian soils, the optimum temperature for nitrification is 35°C, and nitrification occurs even at soil temperatures as high as 60°C, which is well above the reported maximum temperature for temperate soils (Myers, 1975). Many studies have found that between 5 and 25 °C, as the temperature increases by 10 °C, the nitrogen gas loss increases by 1.5 to 2 times. It is widely accepted that there is an exponential increase in soil N emissions in response to temperature, which has been observed in biological systems within a specific temperature range (O'Connel, 1990;Thierron and Laudelout, 1996;Winkler et al., 1996). At high temperature, the sensitivity of soil emissions to temperature may be reduced. This could be due to the deactivation or destruction of enzymes caused by further increases in temperature.Accurately quantifying the impact of soil HONO emissions on air quality requires understanding how these emissions respond to temperature. Despite this importance, there are currently only a limited number of studies on the temperature effect on HONO emissions. Oswald et al. (2013) investigated the relationship between soil temperature and soil HONO emissions and found that HONO flux increased exponentially with temperature. The activation energy they reported by fitting the experiment results using Arrhenius equation was 80 kJ mol^{-1}. Wu et al. (2019) found that both the wet and dry emission peaks of HONO increased with rising temperature, suggesting that biological processes drive HONO emissions.

2.3.4.3 Soil nitrogen content

N fertilizer plays a key role in sustaining food production and the world population (FAO (Food and Agriculture Organization), 2019;Mulvaney et al., 2009). The global N fertilizer consumption has increased from 11.3 Tg N yr^{-1} in 1961 to 109.1 Tg N yr^{-1} in 2017 (Lu and Tian, 2017;FAOSTAT (Food and Agriculture Organization Corporate Statistical Database), 2019). Due to low crop N use efficiency (<50% on average globally) (Zhang et al., 2015a;Mueller et al., 2017), a substantial fraction of surplus N is lost to the environment mainly through emissions and runoff, which causes adverse effects on water and air quality (Gheysari et al., 2009;Sepaskhah and Tafteh, 2012;Tafteh and Sepaskhah, 2012;Ju and Zhang, 2017). N loss from fertilized soils is a major source of reactive N species in the atmosphere, including HONO.

Soil nitrogen sources mainly include fertilization, nitrogen deposition, and biological nitrogen fixation (Bøckman, 1997;Zhu et al., 2015). The type, amount, method, and timing of nitrogen fertilizers affect soil N emissions. Many types of nitrogen fertilizers are available for fertilization. It can be divided into ammonium nitrogen (NH_4^+) fertilizer, nitrate nitrogen (NO_3^-) fertilizer, and amide nitrogen fertilizer, according to the form of compounds. Soil NH_4^+ and NO_3^- are the substrates of soil nitrification and denitrification, respectively. The availability of NH_4^+ and NO_3^- is an important factor controlling the nitrification and denitrification, respectively, and will cause differences in N emissions caused by different processes. The application of

different fertilizers would result in distinct promotion effects on HONO emissions from the soil. However, the differences in the effects of different fertilizer types on HONO emissions have not been reported yet.

Tang et al. (2019b) set up a dual dynamic chamber system and used it for field observations in a farmland in the North China Plain (NCP). Their study found that agricultural fertilization increased soil emissions of HONO. Similarly, Xue et al. (2019) also found the promoting effect of fertilization on HONO emissions in the NCP. The field observation results suggested that the high HONO flux is mainly from the direct emission of soil rather than from the heterogeneous reaction of NO_2. Agricultural fertilization will affect the balance of the HONO budget, and then affect the atmospheric oxidation in the NCP. Their subsequent research revealed the high HONO emissions from the fertilized fields enhanced atmospheric HONO concentrations and thus accelerated the local and the regional O_3 pollution (Xue et al., 2021).

2.3.4.4 Soil pH

Soil pH is a crucial factor that affects the emission of HONO by altering the chemical balance of NO_2^- and H^+ (Su et al., 2011). However, Oswald et al. (2013) found that high HONO emissions were observed from some non-acidic soils. Scharko et al. (2015) also found that the HONO emission flux in low pH soil was very low, which was caused by low soil pH leading to a low nitrification rate. It is generally believed that the optimum pH range of soil nitrifying microorganisms for nitrification

is about 8.5. When soil pH<6.0, the nitrification rate decreased significantly, and when pH>10.0, nitrification was hindered. The optimum pH range for denitrification reaction is 6 ~ 8, and some people think it is 7 ~ 8.

In summary, soil emissions play a significant role in atmospheric HONO levels. Nonetheless, there remains a need for further research to understand the fundamental mechanisms, factors influencing HONO emissions, and their effects on the atmosphere.

Chapter 3. Methodology

3.1 Dynamic chamber setup

A dynamic chamber system has been designed to measure the soil emissions of HONO and NO. As shown in Figure 3.1, The entire system consists of a zero gas generator, a dynamic chamber, and analyzers of HONO and NO. The diameter and height of the Teflon chamber are 20 cm and 30 cm, respectively, and the total volume is 9.4 L. The air inlet was evenly distributed at the bottom of the chamber, and a small fan was placed inside the chamber to completely mix the gas. A relative humidity (RH) sensor was used to measure the real-time RH inside the chamber. The entire sampling unit, including the chamber and LOPAP inlet, was placed in a dark and temperature-controlled cabinet to exclude photosensitized interferences.

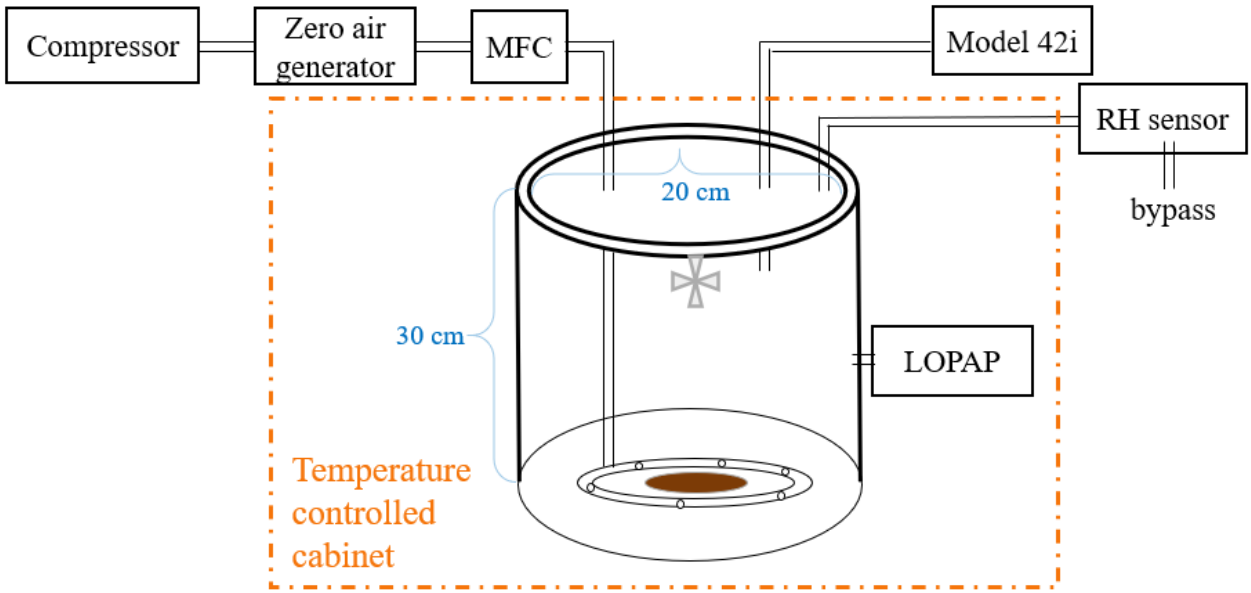

Figure 3.1 Schematic setup of the dynamic system.

3.2 Long path absorption photometry

The mixing ratio of HONO emitted from the soil samples was measured by a long path absorption photometer (LOPAP) (QUMA Elektronik & Analytik GmbH, Wuppertal, Germany) (Heland et al., 2001). Because of its high accuracy, low detection limit, simple operation, high time resolution, and relatively low cost, LOPAP is the most widely used instrument for measuring HONO.

The LOPAP is a wet chemical instrument that quantitatively converts HONO to an azo dye. The concentration of this dye is determined by measuring absorption photometry, and thus to quantify the HONO concentration (Kleffmann et al., 2002). LOPAP consists of three separate units: sampling unit, reaction unit, and detection unit. As shown in Figure 3.2, the sampling air first pumped through R1 (10 g L^{-1} sulfanilamide in 1 M hydrochloric acid (HCl)) in a stripping coil. In this step, HONO and are absorbed into solution. Then, the solution is transferred into the instrument and mixed with reagent R2 (a 0.1g L^{-1} n-(1-naphthyl) ethylenediamine-dihydrochloride solution) to yield the azo dye, which is subsequently detected by long-path absorption. Two parallel channels are set to avoid the influences of interfering species. In Channel 1, HONO and interfering species are determined, while in Channel 2, only the interferences are quantified. The difference between the two channels is the concentration of HONO.

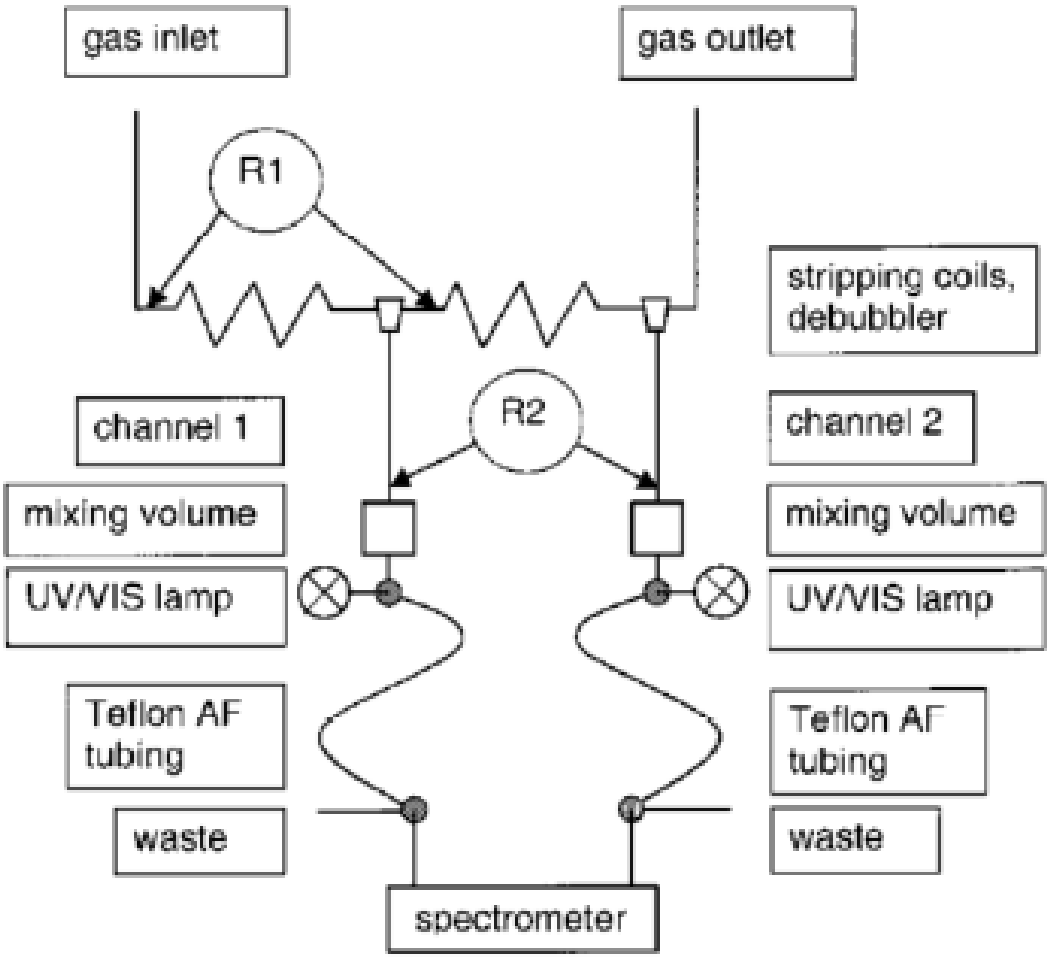

Figure 3.2 Schematic diagram of the LOPAP instrument (Heland et al., 2001).

3.3 NO_x chemiluminescence analyzer

The NO mixing ratio emitted from the soils was measured by a NO_x chemiluminescence analyzer (Model 42i, Thermo Scientific, USA). The principle of the 42i is that NO reacts with O_3 and produces electronically excited NO_2. The decay of electronically excited NO_2 molecules to lower energy states results in infrared light. The intensity is linear to the NO concentration. NO_2 must first be transformed into NO

before it can be measured using the chemiluminescent reaction. The NO_x emitted from soil is mainly NO (Yan et al., 2003a), so the measurement of NO_2 will not be described in detail here.

3.4 Preparation of soil samples

The 48 soil samples used in this study were collected from various regions in China (Figure 3.3), including 24 cropland samples and 24 forest samples. Among these samples, the soil samples used for fertilization experiments were collected from two typical agricultural regions in China. S_{WD} was collected from a maize field (38.66° N, 115.25° E) in Wangdu County located in the NCP, which is one of the highest agricultural productivity regions in China (Ma et al., 2016), producing more than 50% and 33% of wheat and maize, respectively, in the country (Wang et al., 2012). S_{HK} was collected from a vegetable field (22.43° N, 114.11° E) in Hong Kong, Southern China, which has a subtropical humid climate and produces of 10–15 vegetables and grains (Wong et al., 2001). The soil properties and crop species in these two regions differ significantly and are representative of typical north–south differences in Chinese agriculture.

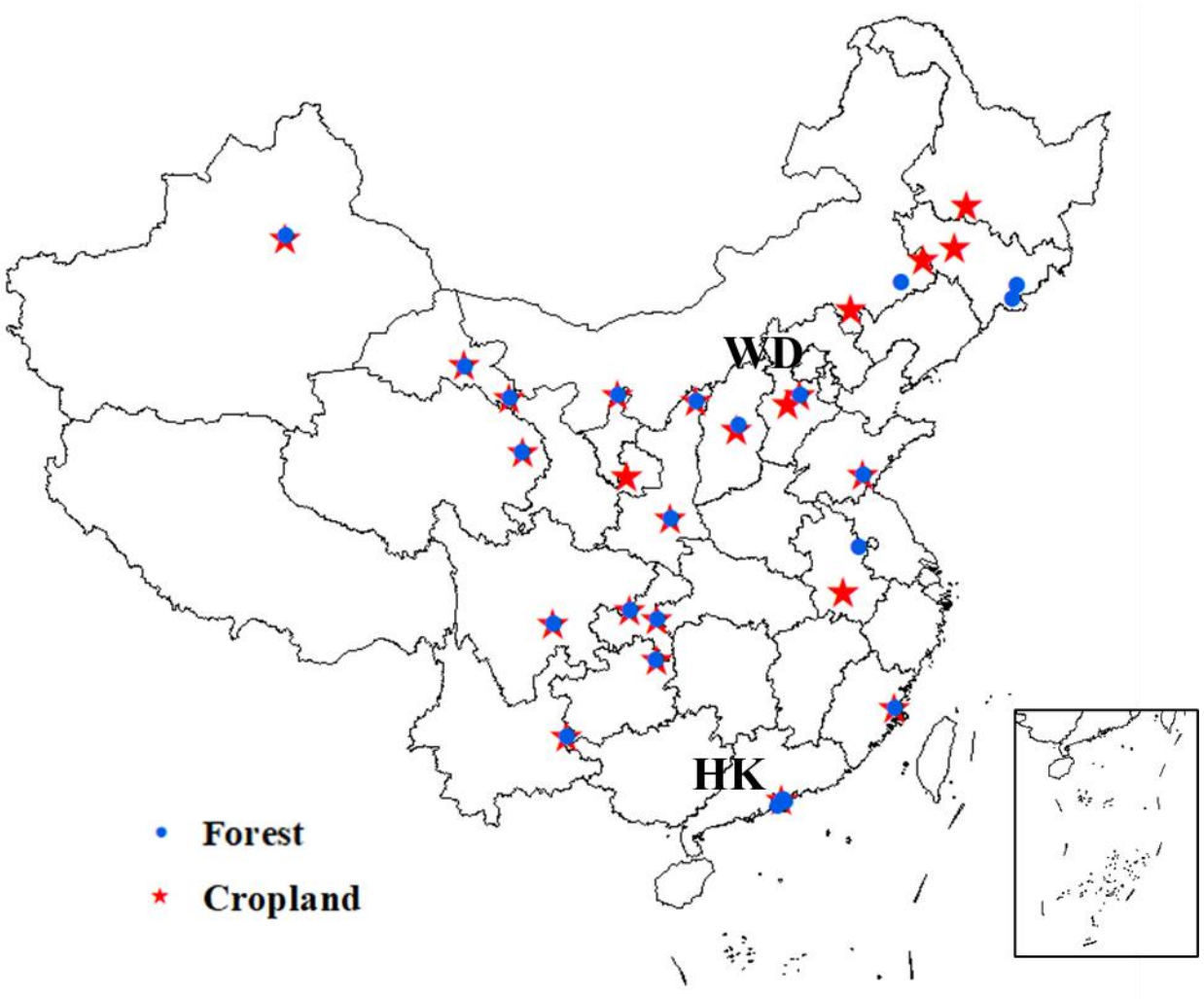

Figure 3.3 Sampling sites in China. Red stars and blue dots represent cropland sites and forest sites, respectively. The samples of cropland soil collected from WD and HK were used for fertilization experiments.

Each sample was a uniform mixture of five subsamples that were taken from the upper layer (0–5 cm) of soil at different locations within a 100 m^2 area to account for spatial inhomogeneity of soil properties. The SWC of the field soil samples (SWC_{field}) was measured immediately after soil samples being shipped to the laboratory of the Hong Kong Polytechnic University. The gravel, roots, and litter were removed from

the samples, and they were then air-dried at room temperature, homogenized by passage through a 2 mm sieve, and finally stored in a refrigerator at 4 °C until analysis.

3.5 HONO emission flux measurements

The HONO and NO emission fluxes of samples were measured using a dynamic chamber (Figure 3.1). 15.5 g of a prepared dry soil sample was placed in a glass petri dish (diameter = 50 mm) and wetted with ultrapure water (resistivity > 18 MΩ·cm) to its WHC value. WHC is the ratio of the water mass in soil at saturation point to dry soil mass. We used the filter method that is commonly used in soil laboratory incubation studies to determine the soil WHC. The detail steps are as follows (Bhadha et al., 2017). We first placed 25g dry soil sample in a funnel equipped with filter paper that was wetted before. The funnel was attached to a rubber hose with a stopper attached to the neck. Water was slowly added to the soil in the funnel until the soil was submerged, and the amount of water added (W0) was recorded. After 30 mins, we removed the stopper from rubber hose and collected all the water that drained from the funnel for 30 mins, recorded the amount of water drained from the funnel (W1). Water holding capacity is the ratio of the mass of water retained in the soil to dry soil mass, given in below equation:

$$\mathrm{WHC}=\frac{\mathrm{W0}-\mathrm{W1}}{25}\times 100\% \qquad (3.1)$$

The petri dish was then immediately placed into the chamber to measure the HONO and NO emission fluxes of the sample. A constant stream of purified dry air was passed through the chamber at a flow rate of 6.3 L min^{-1} until the sample was dry (i.e., no water vapor could be detected). The change in the RH value in the chamber was then calculated and used to determine the real-time SWC (Oswald et al., 2013) of the sample by using the formula:

$$SWC_{(t)} = 1 - \frac{\int_{t=0}^{t} RH(t)\cdot dt}{\int_{t=0}^{t_{max}} RH(t)\cdot dt} \frac{Mass_{water}}{Mass_{dry\ soil}} \cdot \frac{100}{WHC} \quad (3.2)$$

where SWC(t) and RH(t) is the SWC and the relative humidity in the chamber, respectively, at time t. $Mass_{water}$ is the water mass (g) evaporated from the soil during experiment, $Mass_{dry\ soil}$ is the mass of dry soil (g), WHC is soil water holding capacity (equation (3.1)).

The mixing ratios of HONO and NO in the chamber were measured using a LOPAP and a NO_x chemiluminescence analyzer, respectively. The emission fluxes of HONO or NO were calculated using the following formulae(Oswald et al., 2013):

$$F_{N(HONO)} = \frac{Q}{A} \cdot [HONO]_{measure} \cdot \frac{M_N}{V_m} = \frac{Q}{A} \cdot \left(C_{out(HONO)} - C_{in(HONO)}\right) \cdot \frac{M_N}{V_m} \quad (3.3)$$

$$F_{N(NO)} = \frac{Q}{A} \cdot [NO]_{measure} \cdot \frac{M_N}{V_m} = \frac{Q}{A} \cdot \left(C_{out(NO)} - C_{in(NO)}\right) \cdot \frac{M_N}{V_m} \quad (3.4)$$

where F_N is the HONO or NO emission flux in terms of N (ng N m^{-2} s^{-1}); Q and A are the chamber inlet flow rate (L s^{-1}) and the area of the soil surface (m^2),

respectively; $[HONO]_{measured}$ and $[NO]_{measured}$ are the measured HONO and NO mixing ratios (ppb), respectively; C_{out} and C_{in} are the mixing ratios of HONO or NO (ppb) at the chamber outlet and inlet, respectively; M_N is molar mass of N (g mol^{-1}); and V_m is the molar volume of the air (L mol^{-1}). The temperature in the chamber was regulated between 5 °C and 55 °C with a step of 10 °C. The flux measurement procedure was the same as that described above.

3.5.1 Measurements of fertilized soil emissions

We investigated the responses of HONO and NO emissions to different N fertilizers by applying urea, ammonium bicarbonate (NH_4HCO_3) and ammonium nitrate (NH_4NO_3). As shown in Figure 3.4, for each fertilizer, we added 250 g of the soil sample to a glass beaker and calculated the water required by the soil samples to reach the target SWC_{field}. Next, a fertilizer equivalent to 100 kg N ha^{-1} (urea: 24.3 mg for S_{WD}, 19.7 mg for S_{HK}; NH_4HCO_3: 64.2 mg for S_{WD}, 51.9 mg for S_{HK}; NH_4NO_3: 32.5 mg for S_{WD}, 26.3 mg for S_{HK}) was dissolved in the water, added to the beaker and well mixed with the soil. The beaker was then covered by parafilm punctured with small holes to reduce the evaporation of water and ensure gas exchange between the beaker and air. During the experimental period after fertilization, 15.5 g of fertilized soil subsamples were taken from the beaker at 8–24 hr intervals to measure the emission fluxes following the step described above, until the emission flux reached the pre-fertilization levels. These set of experiments aimed to determine the emission flux in

different days after fertilization. A total of 9, 6 and 5 subsamples were taken for S_{WD} and 14, 11 and 10 subsamples for S_{HK} after urea, NH_4HCO_3 and NH_4NO_3 application, respectively.

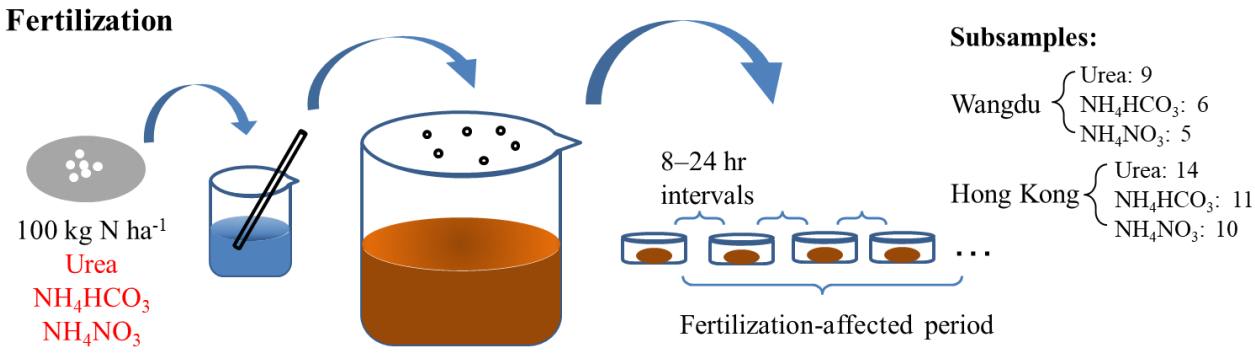

Figure 3.4 Flow chart of fertilization experiment.

3.6 Methods of meta-analysis

We conducted a meta-analysis of previous studies to summarize what has been determined about the effects of long-term fertilization on the abundance of HONO- and NO-producing genes in soil microbes. Meta-analysis is a statistical method that combines individual studies addressing the same question by giving different weights to each study according to their sampling size and variance, rather than simply averaging the results of these studies.

The first step of the meta-analysis involved a literature search for relevant studies, followed by the extraction of six types of data from these studies: the sample size, mean, and standard deviation (SD) of the abundances of HONO- and NO-producing genes

(Figure 2.1) with long-term fertilization (the treatment group) and without fertilization (the control group). We searched the Web of Science and Google Scholar for studies published from 2010 to 2021, using the following keywords: “fertilization” (or “fertilizer application”); “genes”; “*amoA*” or “*narG*” or “*napA*” or “*nirK*” or “*nirS*” (functional genes relevant to HONO and NO production; Figure 2.1); and “soil”. A study was included if (1) it was a field experiment; (2) it involved fertilization experiments that were conducted for more than 3 years with fertilization and control plots located on the same soil and subjected to the same management practices (i.e., vegetation, tillage, and irrigation practices); (3) it collected soil samples during non-fertilization periods; and (4) it reported the mean abundance and SD of HONO- and NO-producing genes, and replicate numbers, or these data were extractable from its tables or figures. Data were extracted from figures using WebPlotDigitizer (https://automeris.io/WebPlotDigitizer/). This process afforded 52 studies (Table 3.1) for meta-analysis, which was performed using OpenMEE software(Wallace et al., 2017). The location of the sites in these studies are showed in Figure 3.5.

Table 3.1 The studies used for meta-analysis.

Refs	region	Latitude	longitude
Li et al (Li et al., 2020a)	Hunan	26.753	111.876
Sun et al (Sun et al., 2015)	Anhui	33.217	116.583
Wang et al (Wang et al., 2018)	Hebei	37.9	114.67
Sun et al (Sun et al., 2021)	Hebei	37.883	114.683
Wang et al (Wang et al., 2019b)	Shaanxi	35.2	107.667

Yang et al (Yang et al., 2017a)	Beijing	39.8	116.467
Chen et al (Chen et al., 2012)	Hunan	28.014	110.02
Hu et al (Hu et al., 2019)	Hubei	32.167	112.167
Liu et al (Liu et al., 2019a)	Chongqing	29.8	106.4
Fan et al (Fan et al., 2016)	Jiangsu	31.967	119.3
Yang et al (Yang et al., 2017b)	Hebei	37.617	116.383
Chen et al (Chen et al., 2010)	Hunan	28.867	111.2
Yin et al (Yin et al., 2014)	Shenyang	41.533	123.383
Gu et al (Gu et al., 2017)	Jiangsu	29.879	119.875
	Jiangsu	31.664	119.468
Xia et al (Xia et al., 2021)	Hunan	28.117	112.3
Tang et al (Tang et al., 2016)	Jiangxi	26.741	115.058
Yin et al (Yin et al., 2019)	Xinjiang	37.017	80.717
Tang et al (Tang et al., 2019a)	Hunan	28.117	112.3
Dong et al (Dong et al., 2015)	Sichuan	31.267	105.467
Yang et al (Yang et al., 2020)	Hunan	28.117	112.3
Tao et al (Tao et al., 2018)	Xinjiang	44.383	85.683
Wang et al (Wang et al., 2020b)	Shaanxi	35.2	107.667
Fang et al (Fang et al., 2020)	Fujian	26.225	119.069
Hu et al (Hu et al., 2020)	Jilin	43.517	124.8
Yu et al (Yu et al., 2018)	Heilongjiang	47.433	126.633
Ai et al (Ai et al., 2013)	Hebei	37.917	115.217
Duan et al (Duan et al., 2017)	Hunan	28.953	112.737
Tao et al (Tao et al., 2017)	Xinjiang	44.383	85.683
Zhou et al (Zhou et al., 2014)	Chongqing	29.8	106.4
Guo et al (Guo et al., 2017)	Anhui	33.617	116.75
Xue et al (Xue et al., 2016)	Jilin	43.506	124.809
Zhao et al (Zhao et al., 2016)	Jiangsu	31.3	120.617

Jin et al (Jin et al., 2014)	Jiangsu	31.085	120.773
Su et al (Su et al., 2015)	Hunan	28.917	111.45
Song et al (Song et al., 2017)	Hunan	26.759	111.872
Dai et al (Dai et al., 2021)	Jiangxi	28.567	115.933
Yao et al (Yao et al., 2016)	Zhejiang	29.017	119.45
Long et al (Long et al., 2021)	Yunnan	23.533	103.217
Chen et al (Chen et al., 2011)	Hunan	28.917	111.433
Bei et al (Bei et al., 2018)	Hebei	36.7	114.9
Fan et al (Fan et al., 2011)	Heilongjiang	50.25	127.48
Chen et al (Chen et al., 2014)	Inner Mongolia	42.03	116.28
Chen et al (Chen et al., 2013)	Inner Mongolia	42.03	116.28
Wang et al (Wang et al., 2014)	Jiangsu	31.3	120.62
Chen et al (Chen et al., 2019)	Hunan	28.55	113.33
Fang et al (Fang et al., 2018)	Fujian	26.23	119.07
Gu et al (Gu et al., 2018)	Zhejiang	29.02	119.47
Liu et al (Liu et al., 2018)	Zhejiang	30.83	120.67
	Hunan	28.62	113.33
	Jiangxi	28.57	115.57
	Jiangxi	28.25	116.92
Shen et al (Shen et al., 2011)	Inner Mongolia	42.04	116.29
Wang et al (Wang et al., 2019a)	Jiangxi	26.73	115.05
Wen et al (Wen et al., 2018)	Hubei	30.47	114.35
Zhang et al (Zhang et al., 2015b)	Fujian	26.23	119.07

Figure 3.5 Locations of studies used for meta-analysis.

The second step of the meta-analysis involved calculating the effect size y_i and the variance v_i of each study. The effect size represents the magnitude of the effect of long-term fertilization on the abundance of HONO- and NO-producing genes and is expressed as a natural logarithm response ratio (lnRR), which was calculated as follows(Luo et al., 2006;Dai et al., 2020) :

$$y_i = \ln(\mathrm{RR}) = \ln(\frac{\mathrm{X_{fer}}}{\mathrm{X_c}}), \quad (3.5)$$

where X_{fer} and X_c are the mean abundances of the target genes in the N-fertilization treatment group and in the control group, respectively. The variance (v_i) associated with each y_i was calculated as follows:

$$v_i = \frac{{S_{fer}}^2}{n_{fer}{X_{fer}}^2} + \frac{{S_c}^2}{n_c{X_c}^2}, \quad (3.6)$$

where S_{fer} and S_c are the SD of fertilization and control treatments, respectively; and n_{fer} and n_c are the number of replicates in the fertilization and non-fertilization group, respectively.

Finally, a random-effects model was used to calculate overall effect size (y_{mean}) by combining the y_i values from all of the studies, accounting for within-study sampling variance and between-study variance. A restricted maximum likelihood approach was used to determine the parameters of the meta-analysis. The y_{mean} was regarded as significant if its 95% confidence interval (CI) did not overlap with 0. Subsequently, y_{mean} was transformed back to a percentage change in gene abundance caused by long-term fertilization, as follows:

$$\text{Percentage change} = (e^{y_{mean}} - 1) \times 100\%. \quad (3.7)$$

Chapter 4. Impact of fertilization on soil HONO emissions

4.1 Introduction

China is the world's largest user of agricultural N fertilizers and accounts for approximately 30% of total global consumption of N fertilizers (FAOSTAT (Food and Agriculture Organization Corporate Statistical Database), 2019). In addition, China's total agricultural N fertilizer consumption increased from 9.3 Tg in 1980 to 20.7 Tg in 2018 (National Bureau of Statistics, 2019). Furthermore, China is one of three regions in the world with the highest levels of N deposition, which over the past 30 years have increased by approximately 60% (Yu et al., 2019). The use of agricultural fertilizers and high levels of N deposition increase soil N concentrations and the abundance and activities of soil microbes(Kautz et al., 2004;Tian et al., 2015), which inevitably lead to the release of a considerable amount of reactive N species, including HONO and NO, to the atmosphere. However, the effects of fertilization on soil HONO emissions have not been well studied.

As reviewed in chapter 2, HONO emitted from soil is produced through microbial processes of nitrification and denitrification (Oswald et al., 2013;Ermel et al., 2018;Wu et al., 2019). The regulating factors of these processes are complex and diverse, and mainly include availability of soil N, organic matter content, soil moisture, pH, and

temperature (Butterbach-Bahl et al., 2013;Ludwig et al., 2001). Soil moisture affects HONO production via controlling the availability of O_2 in soil that influences microbial activity (Bollmann and Conrad, 1998). Previous laboratory studies have shown that HONO fluxes from natural and agricultural soils typically peak at 0%–40% WHC and then decrease to a very low level at high SWC (Oswald et al., 2013). However, recent field measurements (Tang et al., 2019b;Xue et al., 2019;Liu et al., 2019b;Xue et al., 2021) observed a sharp increase in soil HONO emission immediately after fertilization when SWC is high as agricultural fertilization usually takes place along with rainfall or followed by irrigation (Gao et al., 2016a). This post-fertilization HONO source from soil has been suggested to be an important 'missing source' of ambient HONO in daytime (Su et al., 2011;Liu et al., 2019b). However, the effect of fertilizer types on HONO emission and its SWC dependence after fertilization are unknown, making it difficult to predict this HONO source and its atmospheric impact in air quality models.

In this chapter, we investigated the responses of HONO emissions from fertilized soil to SWC, fertilizer type, and the time since fertilization. We found that in addition to the promotion effect at a low SWC, fertilizer applications can also greatly stimulate soil HONO emissions at a high SWC– a common condition for fertilized soil. Based on the laboratory results, we derived a parameterization scheme linking HONO emission to SWC for three commonly used fertilizers and implement the scheme in a regional chemistry and transport model to quantify post-fertilization HONO emissions and its impact on air quality in the NCP. We show that the soil HONO emissions significantly

improved model HONO simulation and this source has important impact on regional air quality in the fertilization period.

4.2 Soil HONO and NO emissions from fertilized soils

We measured the HONO fluxes under different soil moisture for agricultural soil samples that were collected from Wangdu, Hebei province in Northern China (S_{WD}) and Hong Kong in Southern China (S_{HK}). Before fertilization, only one HONO emission peak was observed at a low SWC (the dry peak) in both soil samples. And the emission flux (F_N) was 341 ng m^{-2} s^{-1} at 41% WHC for S_{WD} (Figure 4.1a) and 78 ng m^{-2} s^{-1} at 18% WHC for S_{HK} (Figure 4.1b); it decreased to nearly zero at >60% WHC prior to fertilization for both samples. Similar phenomenon has been observed in previous study (Oswald et al., 2013), and nitrification ($NH_4^+ \rightarrow NO_2^- \rightarrow NO_3^-$) is thought to predominate at low SWC, producing NO_2^- and then HONO (chapter 4). The small peak at high SWC (the wet peak) reported by Wu et al (2019) did not occur or was too low to be observed in our soil samples.

We then separately applied three widely used N fertilizers, urea ($CO(NH_2)_2$), ammonium bicarbonate (NH_4HCO_3) and ammonium nitrate (NH_4NO_3) to the soil samples to investigate the response of soil HONO emissions to fertilization (see chapter 3). As shown in Figure 4.1c–1h, the dry peaks were significantly enhanced after fertilization and reached to a maximum 1–6 days later, with a maximum flux of 2100–3400 ng m^{-2} s^{-1} for S_{WD} and 5900–8300 ng m^{-2} s^{-1} for S_{HK} (Figure 4.2). The post-

fertilization HONO emissions at low SWC increased by approximately 10 and 100 times for S_{WD} and S_{HK}, respectively. The elevated HONO emissions at low SWC is due to the increase of NH_4^+ amount in the nitrification process after fertilization. The maximum dry peak occurred approximately 2 days later for urea use than NH_4HCO_3 and NH_4NO_3 for both samples, mainly because that urea is organic nitrogen and must be first hydrolyzed to NH_4^+-N by urease in soil within 2–3 days (Cartes et al., 2009;Bouwman et al., 1997).

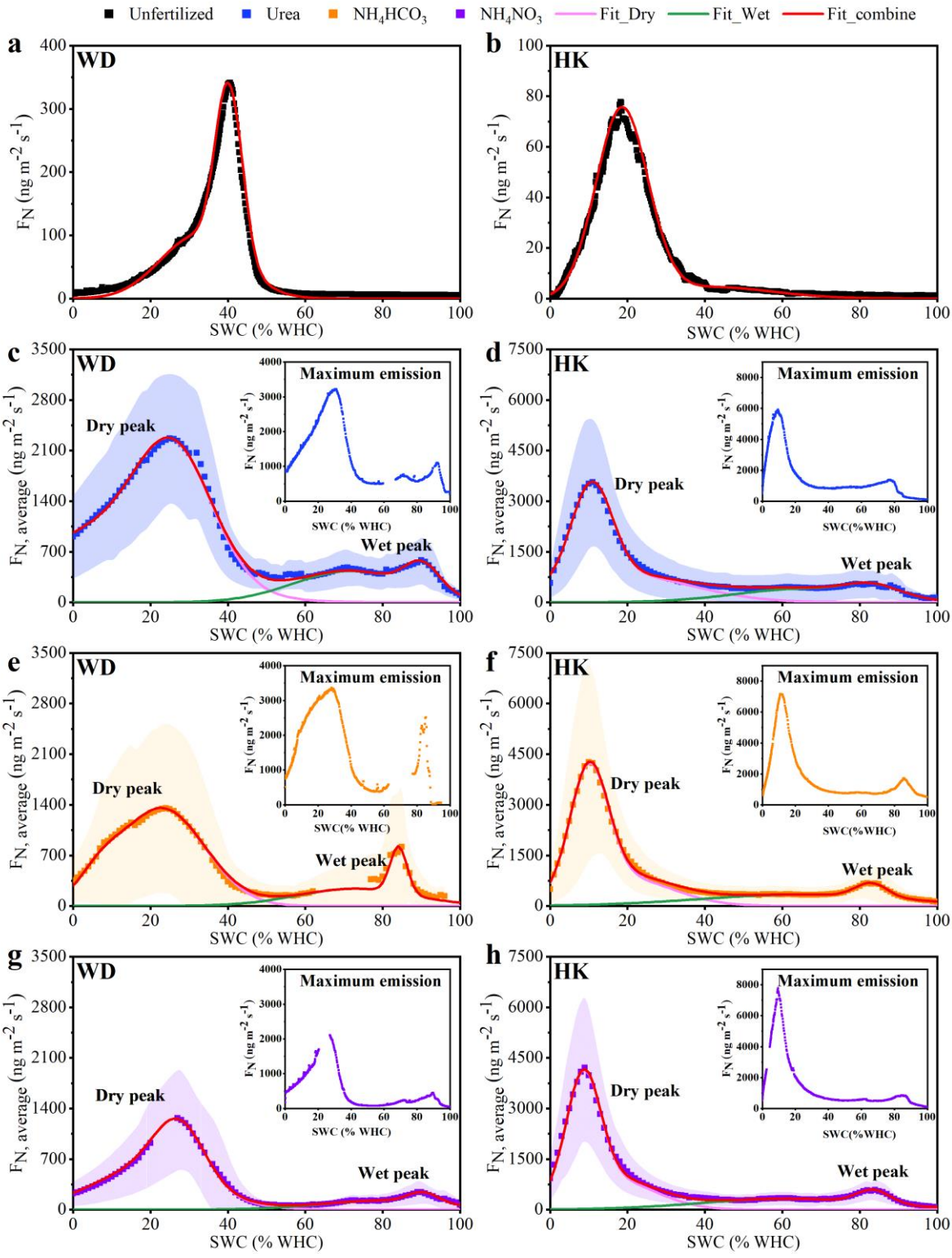

Figure 4.1 Soil emission fluxes of HONO as a function of the soil water content SWC (% water holding capacity, WHC). Soil HONO emissions before (a, b) and after

applying urea (blue squares, c, d), NH_4HCO_3 (orange squares, e, f), and NH_4NO_3 (purple squares, g, h) to soil samples from Wangdu, Hebei province in Northern China (S_{WD}) and Hong Kong in Southern China (S_{HK}). The solid squares indicate the averaged emission results during the fertilization-affected period. The shadow areas represent the standard deviations. The pink, green and red lines represent the soil HONO emission fitting results at low SWC, high SWC, and the entire SWC range, respectively, as multiple Gaussian functions (Table 4.1). The upper right corner of c–h shows the maximum emission of the fertilized subsamples.

Differing from the extremely low pre-fertilization HONO emissions at high SWC, significant wet peaks are observed at >60% WHC for all of the fertilized soil subsamples from both sites and for different days (Figure 4.1c–1h), and they exhibit similar variations with time after fertilization to the dry peaks (Figure 4.2a, b). After the application of urea, NH_4HCO_3 and NH_4NO_3, the maximum wet peaks reached 1100, 2516 and 450 ng m^{-2} s^{-1} at 85%–93% WHC for S_{WD}, respectively, and 1460, 1725 and 1048 ng m^{-2} s^{-1} at 77–87% WHC for S_{HK}. These values were considerably higher than the pre-fertilization dry peaks. We took a weighted average of the HONO emission fluxes of each subsample against all of the fertilization-affected days and obtain averaged emissions ($F_{N,average}$) in Figure 4.1. The averaged emissions ($F_{N,average}$) of the wet peaks during the entire fertilization-affected period were 240–820 ng m^{-2} s^{-1} (Figure 4.1c–1h). The boosted HONO emissions at high SWC may result from the addition of N fertilizer that provides substrate for microorganisms and increases the

abundances of their functional genes (Ouyang et al., 2018;Jin et al., 2014;Di et al., 2014), resulting in a wet peak of HONO emission via promoting both $NH_4^+ \rightarrow NO_2^-$ (Shen et al., 2013;Wrage et al., 2001;Zhu et al., 2013;Carrasco et al., 2004;Zhou et al., 2012) and $NO_3^- \rightarrow NO_2^-$ (Wu et al., 2019) at high SWC (unsaturated) with limited oxygen content. The greater promoting effects of N fertilizer on HONO emissions for S_{HK} than for S_{WD} are possibly due to the different soil properties between the two samples. The pH values of S_{WD} and S_{HK} were 7.9 and 5.7, respectively. The alkaline condition (high pH) of S_{WD} is likely to lead more conversion of NH_4^+-N in three fertilizers to NH_3 followed by its volatilization loss (Bolan et al., 2004;Rodriguez et al., 2019) and a low pH of S_{HK} favours HONO release from soil (Su et al., 2011).

In addition to HONO, post-fertilization NO emissions also increased for both S_{WD} and S_{HK} at low SWC, while the effect of fertilization on NO emission at high SWC is not obvious (Figure 4.3). The average NO fluxes at 60%–100% WHC are only 1.7% and 1.0% of HONO fluxes in S_{WD} and S_{HK}, respectively.

The application of urea leads to the highest cumulative HONO emission for the whole fertilization-affected period, whereas NH_4NO_3 has the lowest emission, for both the dry and wet conditions (Figure 4.2c, d). For S_{WD}, the cumulative HONO emissions after urea application are 219% and 319% higher than NH_4NO_3 at low and high SWC, respectively; for S_{HK}, the cumulative promotion effects after using urea are 7% and 66% higher than NH_4NO_3 for dry and wet peaks, respectively. At low SWC, HONO is

produced mainly by the nitrification process (chapter 4) and is boosted more by urea than NH_4NO_3 due to more abundant reduced N in urea ($CO(NH_2)_2$) than NH_4NO_3 (2:1). At high SWC, soil HONO production is from both $NH_4^+ \rightarrow NO_2^-$ and $NO_3^- \rightarrow NO_2^-$. The higher HONO emission for urea than for NH_4NO_3 suggests that $NH_4^+ \rightarrow NO_2^-$ (Shen et al., 2013;Zhu et al., 2013;Carrasco et al., 2004;Zhou et al., 2012;Liu et al., 2014;Wrage et al., 2001) is more important than $NO_3^- \rightarrow NO_2^-$ (Wu et al., 2019) because urea contains only reduced N. Additionally, urea can increase the content of soluble organic carbon (Mulvaney et al., 1997), which is conducive to the growth of heterotrophic microorganisms and leads to increased production of NO_2^- (Venterea, 2007). The smaller difference between urea and NH_4NO_3 in S_{HK} suggest increased importance of the $NO_3^- \rightarrow NO_2^-$ process compared to S_{WD}.

The loss of soil N to HONO in the atmosphere after fertilization can be estimated as follows. We assume that the HONO emissions during the entire fertilization period reach the wet peaks as shown in Figure 4.2a and 4.2b, the proportion of cumulative HONO emitted (as N) during the entire fertilization period (Figure 4.2c, d) in the fertilizer usage in S_{WD} are 1.7%, 0.6%, and 0.3% for urea, NH_4HCO_3, and NH_4NO_3, respectively, and in S_{HK} are 5.4%, 1.5%, and 2.4% for urea, NH_4HCO_3, and NH_4NO_3, respectively.

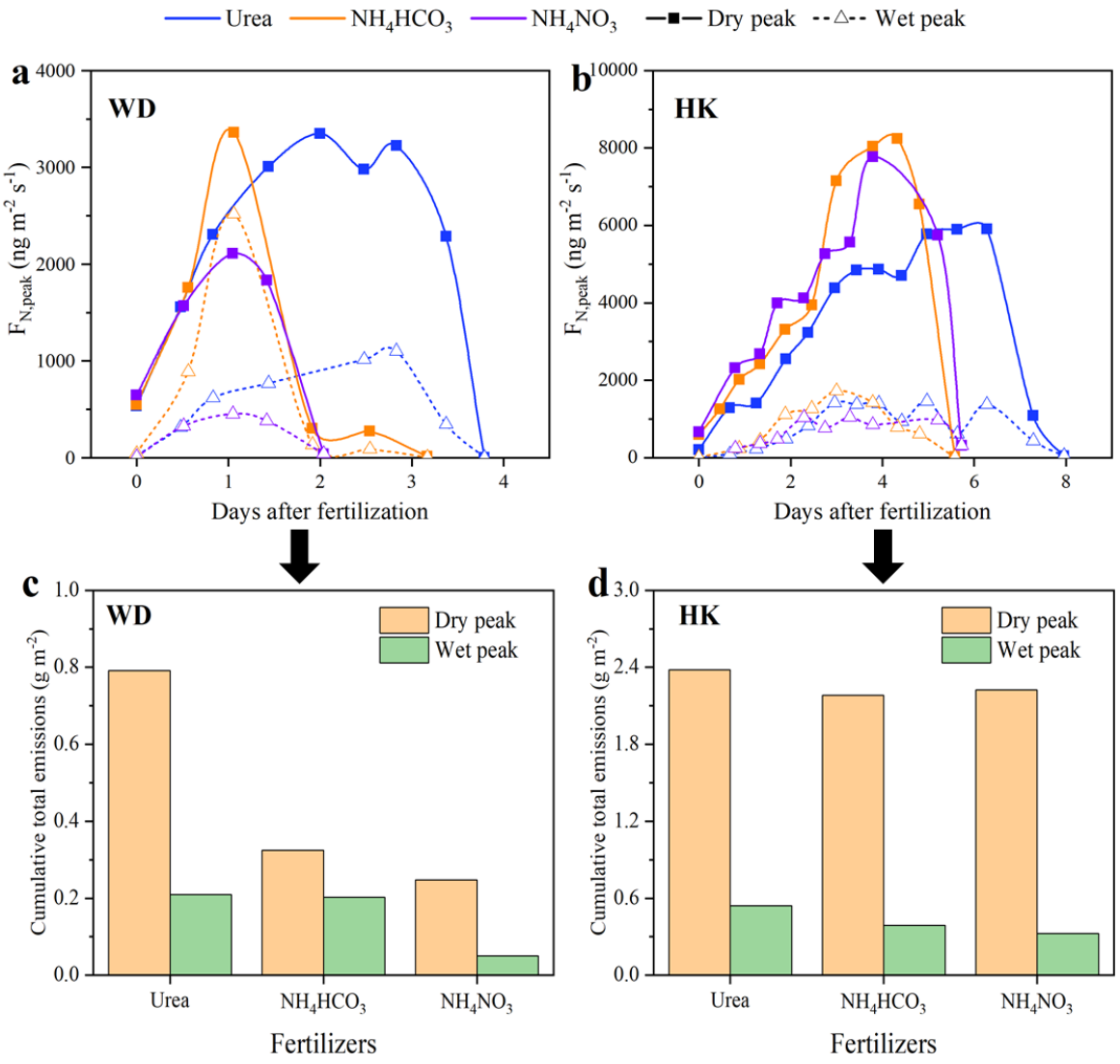

Figure 4.2 Variations of HONO emission peaks of subsamples and cumulative HONO emissions during the fertilization-affected period. a and b show the variation of the peak values as a function of days since fertilization for S_{WD} and S_{HK}, respectively (Dry peak: solid square, Wet peak: open triangle; urea: blue, NH_4HCO_3: orange, and NH_4NO_3: purple). c and d represent the integrated HONO emission after application of

urea, NH_4HCO_3, and NH_4NO_3 for S_{WD} and S_{HK}, respectively (Dry peak: yellow bars, wet peak: green bars).

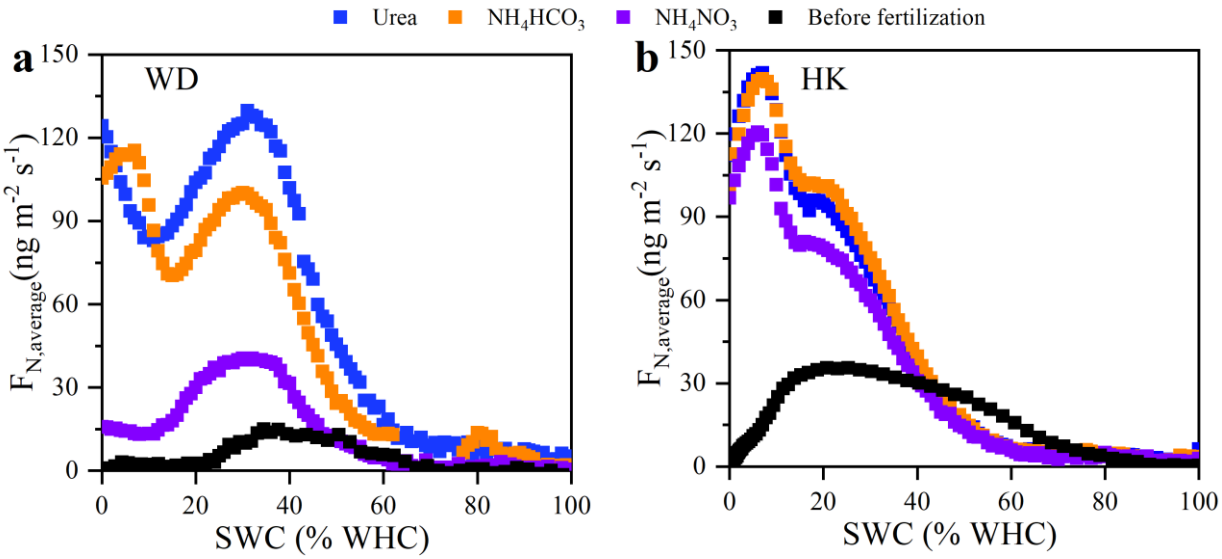

Figure 4.3 Soil NO emission before and after fertilization. The black squares indicate the NO emissions before fertilization for (a) S_{WD} and (b) S_{HK}. The blue, orange, purple squares represent the NO emissions after applying urea, NH_4HCO_3, and NH_4NO_3, respectively.

4.3 Impact of soil temperature

In addition to soil moisture and fertilization, soil temperature is also an important factor influencing soil nitrogen emissions (Oswald et al., 2013;Wu et al., 2019). An exponential increase in soil respiration with respect to temperature is commonly accepted and was observed for biological systems over a limited range of temperatures (O'Connel, 1990;Thierron and Laudelout, 1996;Winkler et al., 1996). To test the

response of HONO emissions to the variation of temperature, the temperature in chamber was regulated between 5 and 55 °C with a step of 10 °C. Figure 4.4 shows the relationship between the soil emission of the S_{HK} and the temperature. Previous study demonstrated that the soil biological process and soil nitrogen emission increases exponentially with respect to temperature (Winkler et al., 1996;Wu et al., 2019), so we use the result of S_{HK} to represent the effect of temperature that were fitted by using a Arrhenius equation:

$$F_N(T) = A \cdot \exp\left[\left(\frac{-Ea}{R}\right) \cdot \frac{1}{T}\right] \quad (4.1)$$

where R is the gas constant (8.314 J mol^{-1} K^{-1}), Ea is the activation energy and is determined, together with constant A, by exponential fitting the HONO emission and temperature data obtained in our experiments.

As shown in Figure 4.4, Fit 1 is exponential fit, and the inset in the figure is the log-transformation of the flux as the function of the inverse temperature with the red line representing the flux calculated using exponential fit parameter. Fit1 over predicts the HONO emission at temperatures below ~300 K (27 °C), but under predict it above ~310 K (37 °C). The other fitting (Fit 2) is to first log-transform the emission data and then linearly fit the data as a function of inverse temperature. We tried Fit 2, yielding $F_N(T) = 3.384 \cdot 10^{12} \cdot \exp\left[\left(\frac{-60642}{R}\right) \cdot \frac{1}{T}\right]$, which has a larger activation term compared to the exponential Fit1 ($F_N(T) = 6.182 \cdot 10^{9} \cdot \exp\left[\left(\frac{-43990}{R}\right) \cdot \frac{1}{T}\right]$). Fit 2 is better at temperature below 300 K but has under predict more at 310 K. The model simulated soil temperature

at Wandu is 19 - 43 °C (292 - 316 K)(see the model results in (Wang et al., 2021)), with daytime temperature in the range of 25 - 43 °C (298 - 316 K). Thus, we chose the Fit1 as it may better simulate daytime HONO flux. From the Arrhenius plot, we obtained the activation energies for HONO was 43.99 kJ mol^{-1}. This value is within the range reported for nitrification by ammonia-oxidizing bacteria (AOB) (25 to 149 kJ mol^{-1}) (Qiao and Bakken, 1999;Saad and Conrad, 1993), suggesting that the soil nitrification process is an important contributor to HONO.

$$\text{Fit1: } F_N(T) = 6.182 \cdot 10^9 \cdot \exp\left[\left(\frac{-43990}{R} \cdot \frac{1}{T}\right)\right] \quad R^2=0.97$$

$$\text{Fit2: } F_N(T) = 3.384 \cdot 10^{12} \cdot \exp\left[\left(\frac{-60642}{R} \cdot \frac{1}{T}\right)\right] \quad R^2=0.98$$

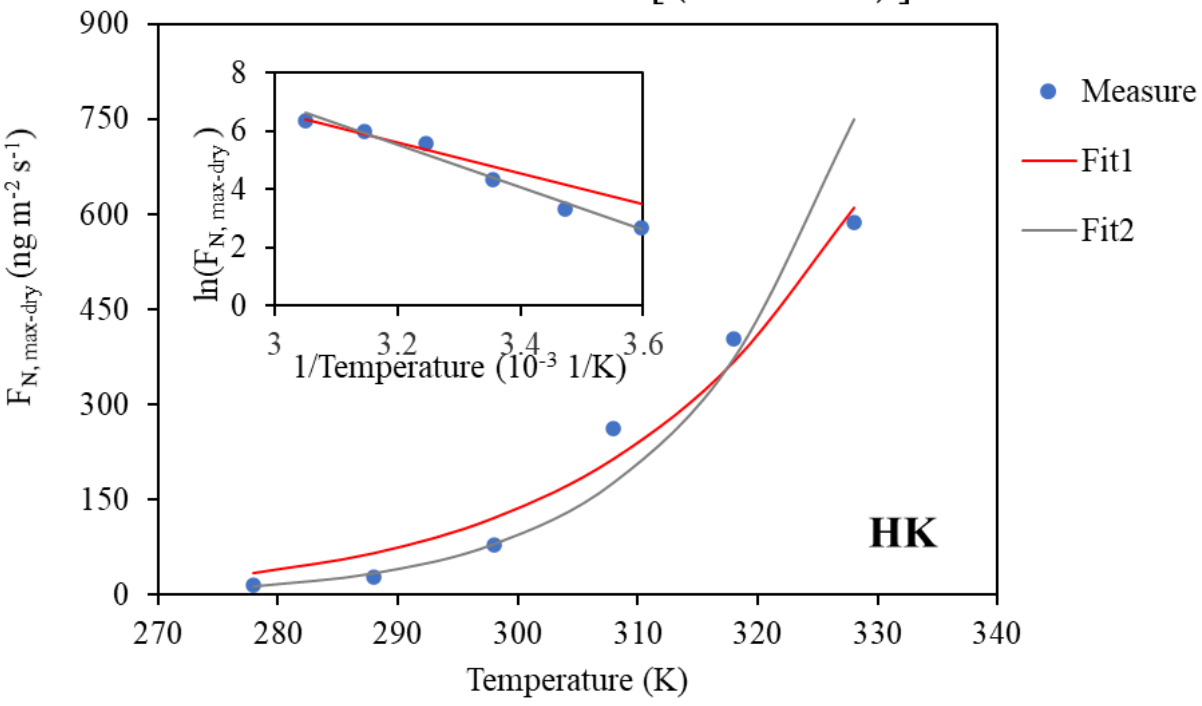

Figure 4.4 Impact of soil temperature on soil HONO emissions in Hong Kong. The blue dot is the flux measured in the laboratory, and the red and gray lines represent two different fitting results.

Another index to describe the temperature dependence of soil microbial activities, commonly referred to as the Q_{10} value, has been the focus of many studies. The value of Q_{10} is the factor by which the respiration rate differs for a temperature interval of 10 ℃, and is defined as:

$$Q_{10} = \frac{R_{T+10}}{R_T} \quad (4.2)$$

where R_T and R_{T+10} are respiration rates at temperatures of T and T + 10, respectively (Winkler et al., 1996). Many previous studies have reported an exponential increase in soil NO emission with increasing temperature, where the Q10 value is approximately 2 (Kirkman et al., 2001;Levine et al., 1996;Meixner and Yang, 2006). However, studies in Kalahari reported values of up to 4.6 (Aranibar et al., 2004). As shown in Figure 4.5, Q_{10} values of S_{HK} ranged from 0.4 to 3.4, which is within the range of previous studies. Q_{10} values increased first and then decreased with the increasing temperature. The maximum value was between 25 and 35℃, which means soil microbial activity increases with temperature and then decreases and optimum soil temperature of microbial activity in soil is 25 - 35℃. A previous study also indicates that the high temperatures may even be a negative relationship the NO emission and the soil temperature (Passianoto et al., 2004).

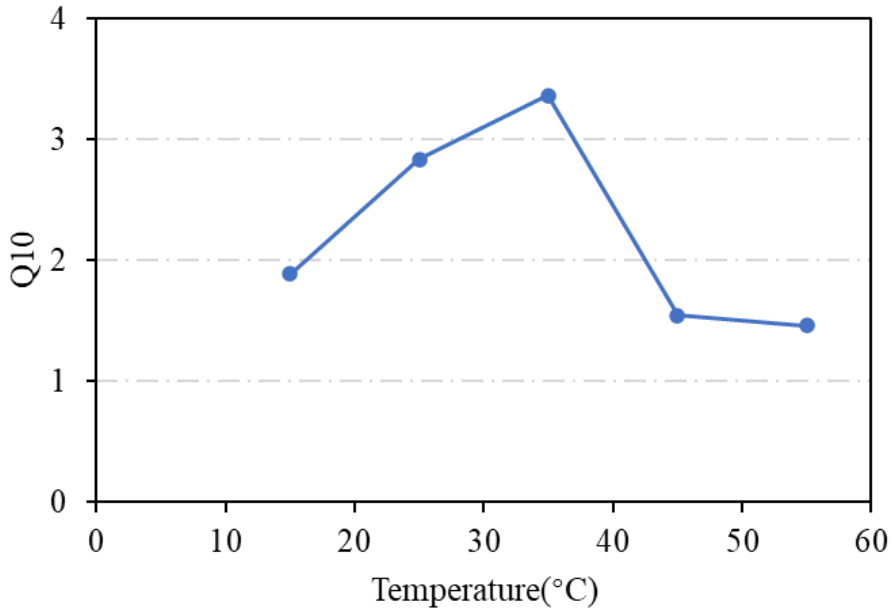

Figure 4.5 Q_{10} values of HK sample between 5 and 55 °C.

4.4 Parameterization scheme

The post-fertilization soil HONO emissions (F_N) are predicted as a function of soil temperature (T) and soil water content (SWC), similar to the parameterization for soil NO emissions(Behrendt et al., 2014;van Dijk et al., 2002;Mamtimin et al., 2016):

$$F_N = F_{N,max}(T_0, SWC_C) \cdot g(SWC_{fer}) \cdot h(T), \quad (4.3)$$

where $F_{N,max}$ is the maximum HONO flux at the optimum SWC (SWC_C) under a reference temperature T_0; $g(SWC_{fer})$ is the function of HONO emission as SWC; $h(T)$

is the temperature dependence of HONO emission and is expressed as ratio of HONO emission at T ($F_N(T)$) to that at T_0 ($F_N(T_0)$):

$$h(T)=\frac{F_N(T)}{F_N(T_0)}=\frac{A\cdot\exp\left[\left(\frac{-Ea}{R}\right)\cdot\frac{1}{T}\right]}{A\cdot\exp\left[\left(\frac{-Ea}{R}\right)\cdot\frac{1}{T_0}\right]}=\exp\left[\left(\frac{-Ea}{R}\right)\cdot\left(\frac{1}{T}-\frac{1}{T_0}\right)\right] \quad , \tag{4.4}$$

$F_N(T)$ takes the form of $A\cdot\exp\left[\left(\frac{-Ea}{R}\right)\cdot\frac{1}{T}\right]$, $F_{N,max}(T_0, SWC_C)\cdot g(SWC_{fer})$ (to be discussed later) and $h(T)$ are experimentally determined, and T_0 is 25 °C which is the room temperature under which the experiments are conducted.

To make use of the laboratory results to quantify the soil HONO emissions in the real ambient environment (F_{emis}), we used the following formula derived from a standard formalism that describes the atmosphere-soil exchange of trace gases (Meusel et al., 2018;Su et al., 2011):

$$F_{emis}= v_t \times [HONO]^* = v_t \times [HONO]_{measured} \quad , \tag{4.5}$$

where the transfer velocity (v_t) is from the CMAQ outputs, [HONO]* is the HONO equilibrium concentration at the soil surface (Meusel et al., 2018), and $[HONO]_{measured}$ is the measured HONO mixing ratio at the chamber outlet. In our chamber system, the zero-air inlets were evenly distributed and a small fan was used to mix the air in the chamber. We assume that the air was well mixed in the chamber and [HONO]* was equal to $[HONO]_{measured}$ (Figure 4.6). By combining equation (4.3-4.5 and 3.3), we can derive the soil HONO emissions in the real ambient environment (F_{emis}) as below:

$$F_{emis} = v_t \times [HONO]^* = v_t \times [HONO]_{measured} = v_t \times \frac{F_{N,max}(T_0, SWC_C) \cdot g(SWC_{fer})}{\frac{Q}{A} \cdot \frac{M_N}{V_m}} \times \exp\left[\left(\frac{-Ea}{R}\right) \cdot \left(\frac{1}{T} - \frac{1}{T_0}\right)\right] \quad , \quad (4.6)$$

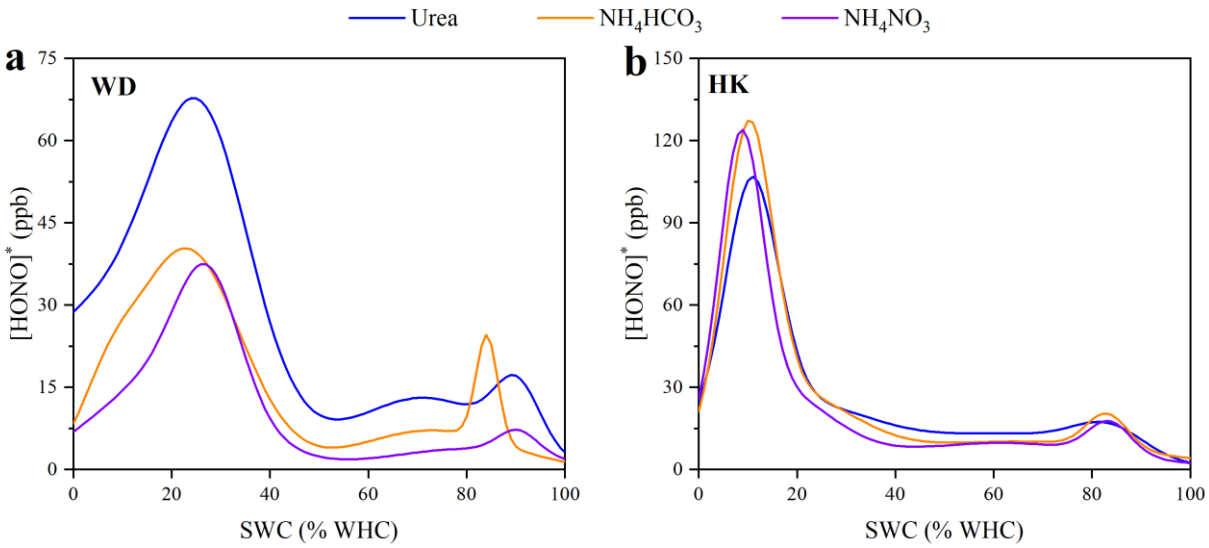

Figure 4.6 Measured [HONO]* for (a)Wangdu (WD) and (b) Hong Kong (HK) samples. [HONO]* is the equilibrium concentration at the soil surface (Meusel et al., 2018). Here we assumed the gas in the dynamic chamber was evenly mixed, and the measured HONO mixing ratio was used to represent [HONO]*. The [HONO]* shown here is the result obtained using multiple Gaussian fittings.

Based on our experimental results showed in Figure 4.1, we derived a parameterization that links the soil HONO emission flux at 25 °C (F_{N,T_0}) to SWC in equation (5.6) for air-quality model use. Gaussian fitting was applied in Matlab 8.6 (MathWorks Inc., Natick, MA, USA) to fit the experimental data shown in Figure 4.1 using the following formulation:

$$F_{N,T_0} = F_{N,max}(T_0, SWC_C) \cdot g(SWC_{fer}) = F_{N,max}(T_0, SWC_C)\exp\left(-\frac{(SWC-SWC_C)^2}{w^2}\right) \quad (4.7)$$

where SWC is the soil water content ranging from 0% to 100% WHC, SWC_C is the soil water content at which the maximum HONO release rate ($F_{N,max}$) occurred, and w characterizes the width of the fitting curves. As shown in Figure 4.1 and Figure 4.7, two Gaussian functions well fit the dry peak (Dry1 + Dry2) in the low SWC range (0%–60% WHC) and the wet peak (Wet1 + Wet2) in the high SWC range (60%–100% WHC), respectively, for both S_{WD} and S_{HK}, in the form of:

$$F_{N(\text{Dry peak}),T_0} = F_{N,max_{Dry1}} \cdot \exp\left(-\frac{\left(SWC-SWC_{C_{Dry1}}\right)^2}{{w_{Dry1}}^2}\right) + F_{N,max_{Dry2}} \cdot \exp\left(-\frac{\left(SWC-SWC_{C_{Dry2}}\right)^2}{{w_{Dry2}}^2}\right), \quad (4.8)$$

$$F_{N(\text{Wet peak}),T_0} = F_{N,max_{Wet1}} \cdot \exp\left(-\frac{\left(SWC-SWC_{C_{Wet1}}\right)^2}{{w_{Wet1}}^2}\right) + F_{N,max_{Wet2}} \cdot \exp\left(-\frac{\left(SWC-SWC_{C_{Wet2}}\right)^2}{{w_{Wet2}}^2}\right). \quad (4.9)$$

Based on the input of F_N and SWC, the fitting procedure yielded $F_{N,max}$, SWC_c, and w which are listed in Table 4.1 for low and high SWC conditions of S_{WD} and S_{HK}. After combining with the formula for the temperature effect (Equation 4.6). The final formulation for the HONO emission (unit: ppb m s^{-1}) after applying N fertilizer of 100 kg N ha^{-1} at soil water content (SWC) and temperature (T) is shown below:

$$F_{emis} = F_{emis(Dry\ peak)} + F_{emis(Wet\ peak)} = v_t \times \frac{F_{N,max}(T_0, SWC_C) \cdot g(SWC_{fer})}{\frac{Q}{A} \cdot \frac{M_N}{V_m}} \times \exp\left[\left(\frac{-Ea}{R}\right) \cdot \left(\frac{1}{T} - \frac{1}{T_0}\right)\right] = v_t \times \left[\frac{F_{N,max_{Dry1}} \cdot \exp\left(-\frac{\left(SWC - SWC_{C_{Dry1}}\right)^2}{w_{Dry1}{}^2}\right) + F_{N,max_{Dry2}} \cdot \exp\left(-\frac{\left(SWC - SWC_{C_{Dry2}}\right)^2}{w_{Dry2}{}^2}\right)}{\frac{6.3/60}{0.00196} \cdot \frac{14}{22.4}} + \frac{F_{N,max_{Wet1}} \cdot \exp\left(-\frac{\left(SWC - SWC_{C_{Wet1}}\right)^2}{w_{Wet1}{}^2}\right) + F_{N,max_{Wet2}} \cdot \exp\left(-\frac{\left(SWC - SWC_{C_{Wet2}}\right)^2}{w_{Wet2}{}^2}\right)}{\frac{6.3/60}{0.00196} \cdot \frac{14}{22.4}} \right] \times \exp\left[\left(\frac{-43990}{R}\right) \cdot \left(\frac{1}{T} - \frac{1}{298}\right)\right] \quad , \qquad (4.10)$$

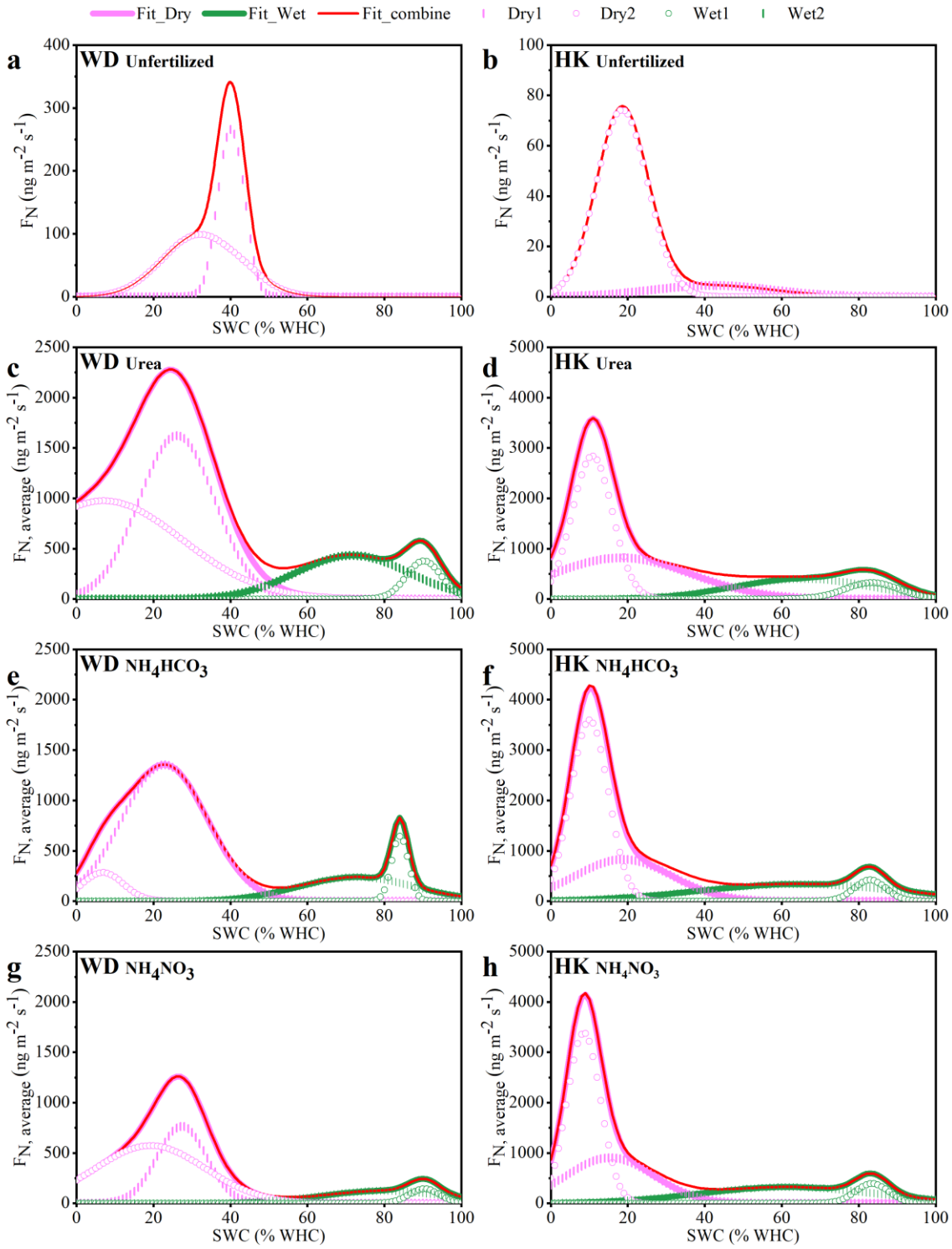

Figure 4.7 Gaussian fitting results of the soil HONO emission. The pink vertical lines and the pink hollow circles represent Dry1 and Dry2 at low SWC (0%–60% WHC),

respectively, and the pink lines represent summation of Dry1 and Dry2 (Dry1+Dry2). The green lines (Wet1 (green hollow circles) + Wet2 (green vertical lines)) represent the fitting results at high SWC (60%–100% WHC). The red lines are the fitting curves in entire SWC range.

Table 4.1 Conceptual model of soil HONO emissions as multiple Gaussian functions of the soil water content (SWC). Dry1 and Dry2 represent the HONO emissions at low SWC (0%–60% water holding capacity, WHC) and Wet1 and Wet2 represent the HONO emissions at high SWC (60%–100% WHC).

Sites	Fertilizers	Parameters	Dry1	Dry2	Wet1	Wet2
WD	Unfertilized	$F_{N,max}$	99.00	265.90	--	--
		SWC_c	29.71	36.65	--	--
		w	13.03	4.04	--	--
	Urea	$F_{N,max}$	975.31	1623.84	433.53	377.29
		SWC_c	7.06	26.12	71.71	90.28
		w	28.81	13.90	20.74	6.43
	NH_4HCO_3	$F_{N,max}$	284.29	1357.77	240.05	645.91
		SWC_c	6.84	22.91	72.83	84.11
		w	7.53	15.63	21.29	3.09
	NH_4NO_3	$F_{N,max}$	572.21	766.40	125.16	142.87
		SWC_c	19.21	27.38	79.92	90.43
		w	20.16	9.08	22.75	5.61
	Unfertilized	$F_{N,max}$	74.24	4.51	--	--
		SWC_c	18.55	42.02	--	--
		w	9.48	21.99	--	--

HK	Urea	$F_{N,max}$	2837.35	819.90	403.16	322.76
		SWC_c	10.79	18.39	65.66	83.45
		w	7.43	25.51	25.18	9.93
	NH_4HCO_3	$F_{N,max}$	3594.82	830.73	340.66	419.88
		SWC_c	10.09	18.88	64.81	83.00
		w	6.91	17.78	36.96	5.86
	NH_4NO_3	$F_{N,max}$	3388.2	908.04	324.72	390.58
		SWC_c	8.59	15.39	61.58	83.51
		w	6.19	16.08	32.03	6.12

4.5 Impact of post-fertilization HONO emissions on air quality

We next implement the parameterization scheme we derived in the Community Multiscale Air Quality (CMAQ) model and simulate the HONO during a typical fertilization event in the NCP. The model simulations were performed by collaborator (Dr. Xiao Fu). High ambient HONO levels were observed following fertilization during 27-30 June 2014 at an agricultural site in Wangdu (Liu et al., 2019b), with the peak HONO mixing ratio of ~2.4 ppb at nighttime and ~0.9 ppb at noon (Figure 4.8b). As the information on the fertilizer use for this fertilization event was not available, we adopted our lab measured HONO emission for 100 kg N ha^{-1} which is a typical fertilization use in the NCP (Zhang et al., 2014). Soil fertilization by individual farmers in a large agricultural region like NCP can take place at the different time, and the

impact of fertilization on the atmosphere is influenced by the average effect of these fertilization activities. In order to obtain the average effect of fertilization on HONO emissions, we used averaged emissions ($F_{N,average}$) shown in Figure 4.1 in the model simulations. As the NO emission does not show significant increase at high SWC after fertilization (Figure 4.3), we did not include soil NO emission in our model simulations.

The long-term observation data at 653 agriculture monitoring sites across China show that the SWC in most agricultural land is higher than 60% (Pan et al., 2019). In view of the difficulty of accurately simulating soil moisture during fertilization that typically occurs along with irrigation, we incorporated the average, lowermost and uppermost soil HONO emissions in the SWC range of 60%–100% WHC after using urea (the dominant fertilizer in China) to represent the average case (SoilHONO_avg), lower limit case (SoilHONO_min) and upper limit case (SoilHONO_max).

As shown in Figure 4.8b, the model simulation without soil emissions (Base) underestimates the ambient HONO levels by −54%, −76% and −45% for the daily, daytime (6:00–18:00) and nighttime averages, respectively, despite the fact that model has included most other known sources (e.g., heterogeneous reactions of NO_2 on the ground and aerosol surface, photolysis of nitrate, etc.). With the implementation of the soil emission assuming a uniform use of urea fertilizer of 100 kg N ha^{-1} in the model domain, the modelled soil HONO emissions (F_{emis}) show a pronounced diurnal variation (Figure 4.8a), with higher emissions in daytime than nighttime due to the

impacts of the increasing transfer velocity and soil temperature in daytime. The daytime peak values vary in the range of 20–196 ng N m^2 s^{-1} with an average of ~80 ng N m^2 s^{-1}. The lowest values at nighttime are in the range of 0.1–9 ng N m^2 s^{-1}, with an average of ~4 ng N m^2 s^{-1}. The diurnal pattern and magnitude of the soil HONO emissions are consistent with previous field observed HONO flux with open-top chambers at Wangdu site (Tang et al., 2019b;Xue et al., 2019). The inclusion of soil HONO emissions at high SWC improved the model performance for ambient HONO simulations at Wangdu for the study case. The observed values at night are generally in the range between the lower and upper simulated limits due to variation in the soil water content. The simulated nighttime average HONO levels by SoilHONO_avg increased from 0.8 ppb to 1.8 ppb, with the NMB decreasing from −45% to 33% (Figure 4.8b). The daytime HONO simulation was also improved, with the NMB decreasing from −76% to −29%. However, underestimation of HONO at noontime remains considerable, possibly due to the contributions of missing photosensitive sources and the difficulty in simulating local emissions and meteorology with a regional model.

With inclusion of the soil HONO emission under the typical fertilizer use, the simulated daytime average O_3 levels increased from 68.3 to 74.5 ppb, closer to the observed average at Wangdu (74.6 ppb) (Figure 4.8c). The maximum increase in the hourly O_3 level was above 9 ppb. The increased oxidation capacity enhanced secondary aerosol production. The simulated nitrate concentration increased by 49% (Figure 4.8d) due to an increase in the oxidation of NO_x by OH and O_3 to form nitric acid. The model

was able to capture the high nitrate concentrations, e.g., at night on 29 and 30 June. Here, we only examined nitrate because our model had been previously improved for the nitrate production processes, whereas the chemical processes for other secondary aerosols (e.g., sulfate and organics) are less certain in the current chemical transport models.

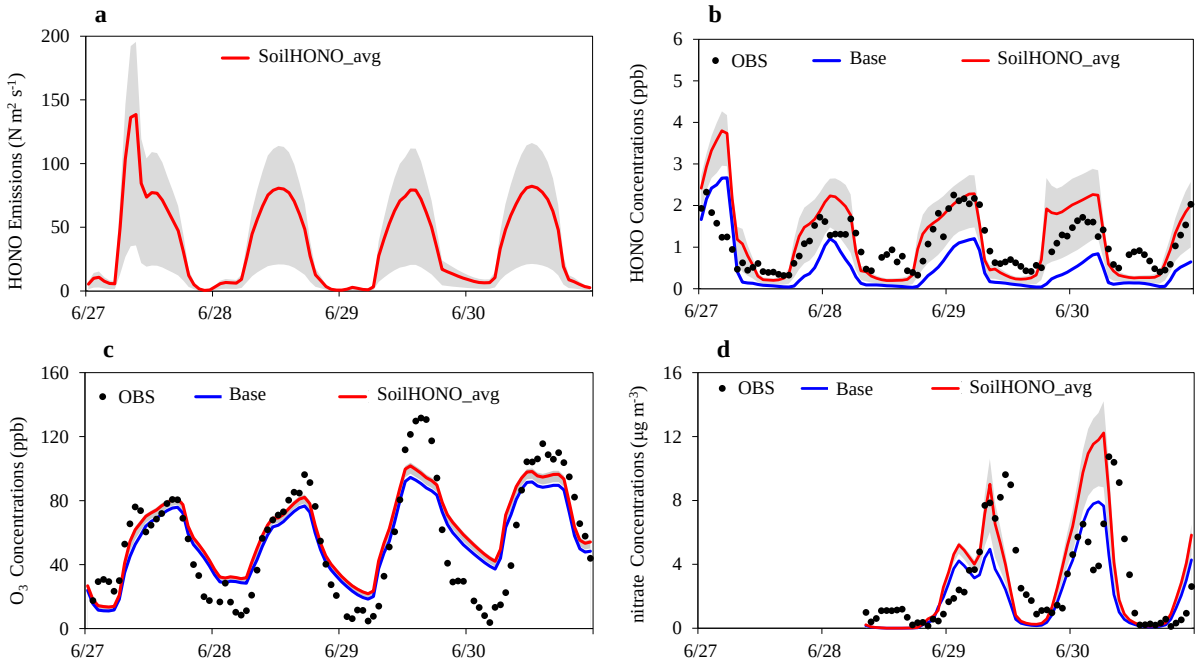

Figure 4.8 Impacts of soil HONO emissions after urea application at Wangdu in the North China Plain. (a) Soil HONO emissions (F_{emis}) and the impacts on (b) HONO mixing ratios, (c) O_3 mixing ratios, and (d) nitrate concentrations at the Wangdu site. Nitrate observation data were not available before 8:00 on 28 June 2014 due to instrument failure. The grey areas represent the range between the lowest (SoilHONO_min) and highest (SoilHONO_max) HONO emission with respect to SWC.

We also simulated the potential impacts of soil HONO emissions in the NCP region for the average case (SoilHONO_avg), which suggests that soil HONO emissions increased regionally averaged daytime OH, O_3, and daily fine particulate nitrate concentrations by 41%, 8%, and 47%, respectively (Figure 4.9). More details on the simulation results can be found in Wang et al. (2021).

It should be noted the above simulations of the regional soil HONO impact may subject to uncertainty due to the lack of information on fertilizer use in different croplands in the simulation period and limited soil samples whose emissions were tested in our study. Nonetheless, the soil parameterization scheme from our study enables emission-based air quality models to estimate the soil HONO emission and atmospheric impact after fertilization. Further studies are needed to quantify the soil HONO emissions from other agricultural lands and to develop a database on the gridded distribution of different fertilizer use in major agricultural regions.

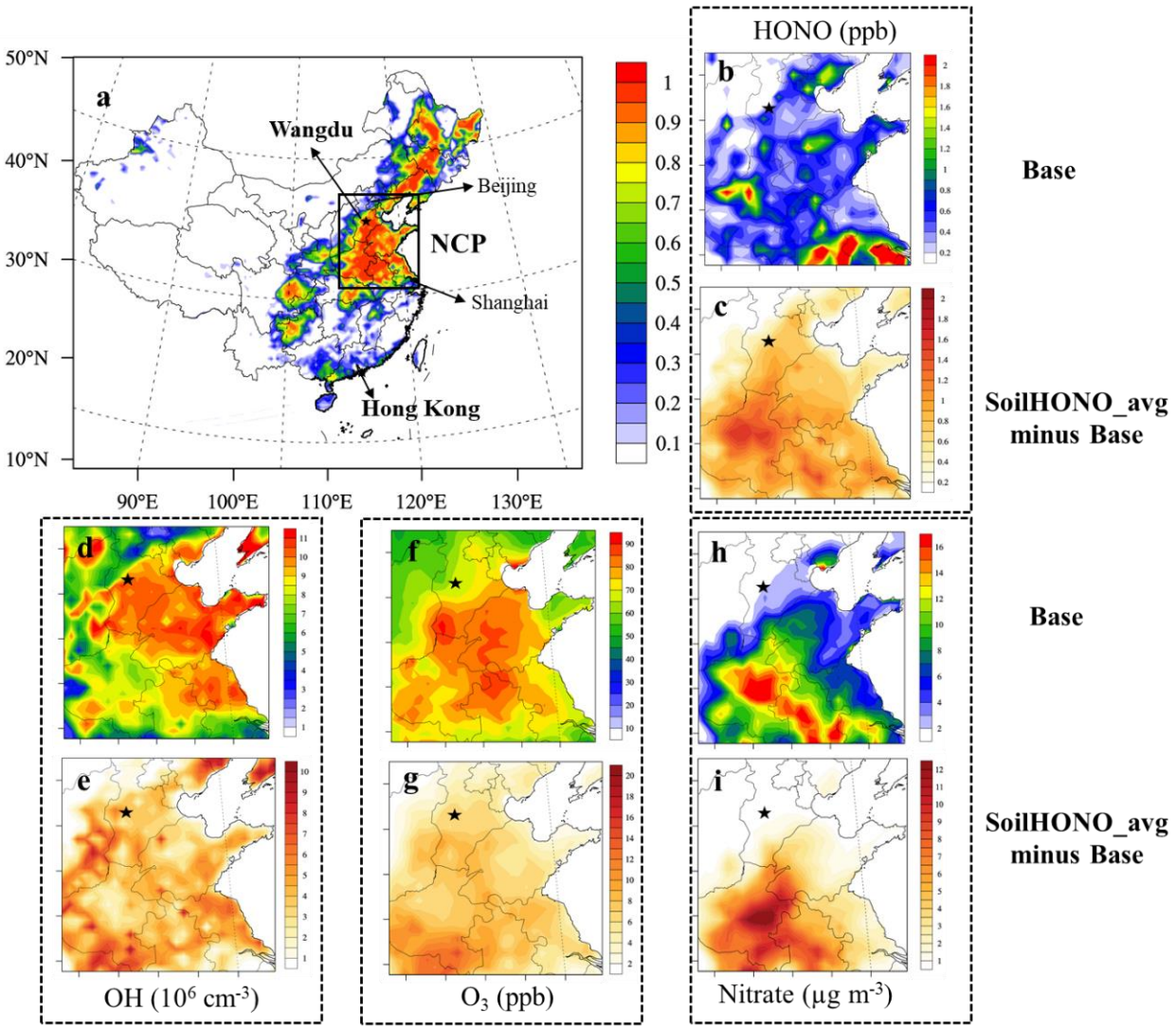

Figure 4.9 Model simulated impacts of soil HONO emissions after urea application in the North China Plain. a is the distribution of cropland (unit: fraction) in China and model domain. b-i are the spatial distributions of the (b, c) daily average HONO, (d, e) daytime average OH, (f, g) daytime average O_3 and (h, i) daily average nitrate in the Base case and the differences with SoilHONO_avg during 27–30 June 2014. The black stars represent the locations of the sampling sites in Wangdu.

4.6 Implications

This chapter demonstrates that fertilization of soils by three widely nitrogen-based fertilizers could have important contribution to ambient HONO and in turn aggravate air pollution in the agriculture intensive NCP region of China. As the most consumed chemical fertilizer type, nitrogen fertilizers have been extensively used in the world. According to the International Fertilizer Association (IFA) (IFA (International Fertilizer Association), 2000-2017) and China Statistical Yearbook (National Bureau of Statistics, 2019), China is the world's largest N fertilizers consumer, followed by India, the USA, western and central Europe, Brazil, and Russia (Figure 4.10). From year 2000 to 2017, nitrogen fertilizer consumption increased by 3%-114% in these countries and 18 % in the world (IFA (International Fertilizer Association), 2000-2017). And the global demand is projected to increase at a rate of 1.2%/year from 2017 to 2022 and will reach 112 Tg N yr^{-1} in 2022 (FAO (Food and Agriculture Organization), 2019). The potential high HONO emissions from fertilized soil and its impacts on air quality thus require worldwide attention.

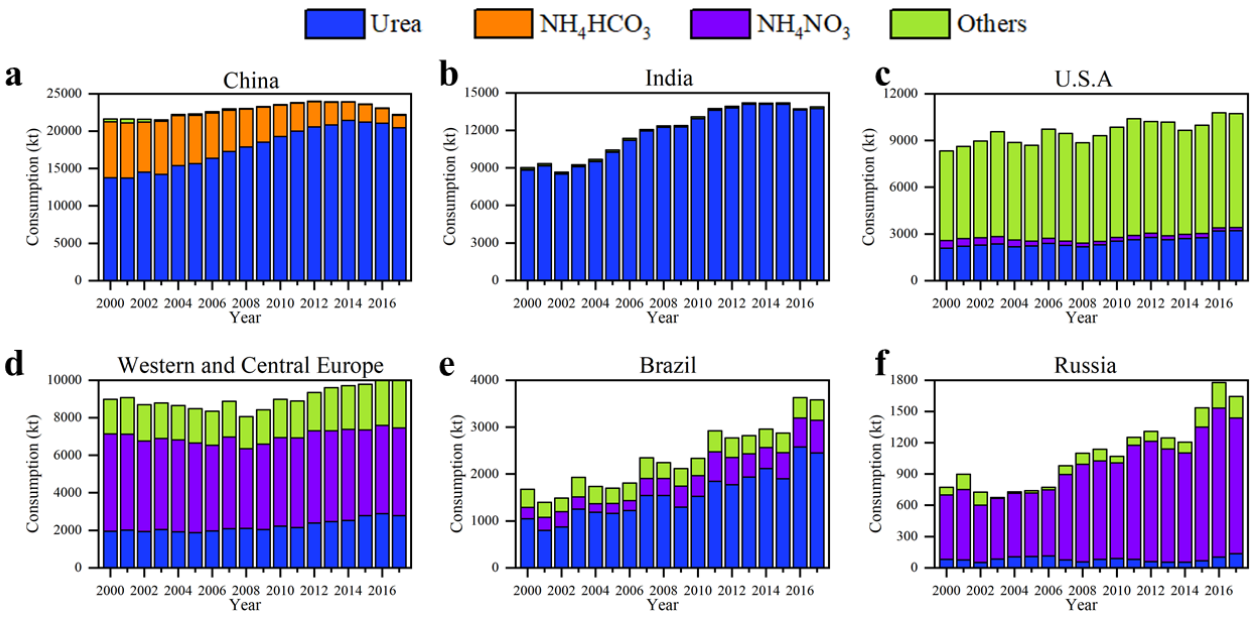

Figure 4.10 Consumptions of different N fertilizers in six regions with large areas of cultivated land in 2000-2017. The blue, orange, purple, and green bars represent the consumption of urea, NH_4HCO_3, NH_4NO_3 and other fertilizers, respectively.

Urea accounts for more than 60% of the global consumed N fertilizer (IFA (International Fertilizer Association), 2000-2017). In China, urea consumption has increased by approximately 49%, and its proportion in total fertilizer use increased from 63.6% in 2000 to 92.1% in 2017 (Figure 4.10a). In India, urea accounts for ~99% of the total N fertilizer consumption (Figure 4.10b). In comparison, the USA, Europe, and Russia use more ammonium nitrate and other N fertilizers (e.g., calcium ammonium nitrate, liquid ammonia, nitrogen solutions), with urea accounting for 5%–30%. Although urea has several advantages over other nitrogen fertilizers such as its higher nitrogen content and a longer residence in soil for absorption by plants, the same properties unfortunately lead to higher emission of HONO to the atmosphere. Thus, for

China and India, two countries with the highest urea use and severe air pollution, adding nitrification inhibitors (Woodward et al., 2021) along urea or replacing urea with low HONO emitting fertilizers would help alleviate air pollution during the fertilization periods. We also call for investigations of the HONO emissions potential from other nitrogen fertilizers, in addition to the three studied in this work, and their environmental impacts.

4.7 Summary

In this chapter, we measured the soil HONO emissions after applying three common fertilizers and found high HONO emissions from soils at 75%–95% WHC, which contrasts to previous lower predictions at high soil moisture. In terms of the effects of different fertilizer types, urea use leads to the largest release of HONO compared to the other two commonly used fertilizers (NH_4HCO_3 and NH_4NO_3). The significant promotion effect of fertilization lasted up to one week. Implementation of the lab-derived parametrization in CMAQ model significantly improved post-fertilization HONO predictions at a rural site in the agriculture intensive North China Plain, and increased regionally averaged daytime OH, O_3, and daily fine particulate nitrate concentrations by 41%, 8%, and 47%, respectively. The result of this chapter underscores the necessity to include this large post-fertilization HONO source in modeling air quality and atmospheric chemistry. We also proposed that fertilizer

structure adjustments may reduce HONO emissions and improve air quality in polluted regions with intense agriculture.

Chapter 5. Soil background emissions from different soil types across China

5.1 Introduction

Emissions from soils that are not fertilized in the current year or season are regarded as background emissions (Gu et al., 2009;Gu et al., 2007;Bouwman, 1996;Ding et al., 2013). In natural ecosystems, background emissions are one of the most critical nitrogen loss pathways due to the absence of anthropogenic disturbance. In agricultural systems. the application of N fertilizers increases soil emissions of nitrous oxide (N_2O), NO, and HONO, but this effect lasts for only about 2 weeks (Wang et al., 2021;Bouwman et al., 2002;Tian et al., 2020;Tang et al., 2019b;Xue et al., 2019;Xue et al., 2021;Liu et al., 2019b). In contrast, background emissions from agricultural soils remain at a low level but persist for most of the time (Tian et al., 2020;Zhang et al., 2014). As the result, background emissions of NO account for 40% of total annual emissions of NO (the sum of background and fertilizer-induced emissions)(Yan et al., 2003a). Therefore, it is important to quantify soil background emissions and their effect on air quality. However, only two studies have measured HONO emissions from soils collected in China during non-fertilization periods: a study that examined soils collected from Xinjiang, (Oswald et al., 2013) and a study that examined soils collected from Shanghai (Wu et al., 2022). There is an obvious need to quantify soil emissions of HONO and NO in vast regions of China with diverse soil

properties and agricultural practices and to develop a process-based parameterization of HONO and NO emissions for model use.

In this chapter, the HONO and NO emission fluxes of soil samples collected from various regions in China during a non-fertilization season were measured. The results showed that soil background emission fluxes of HONO were higher than those of NO. Based on the experimental results, we developed a parameterization scheme for background emissions of HONO and NO with respect to SWC. We then incorporated this scheme into a regional chemical transport model to estimate soil background emissions of HONO and NO and their effects over China in a summer month. Our study underlines the previously underappreciated contribution of HONO to total reactive oxidized N species emitted from soils.

5.2 Soil background HONO and NO emissions

All of the samples' emission fluxes of HONO and NO exhibited consistent water-dependent characteristics and were similar to those that have been reported in previous studies (Oswald et al., 2013). That is, the emission fluxes first increased and then decreased with decreasing SWC, and the highest emissions of HONO and NO were typically from soils with an SWC corresponding to 20%–36% WHC and 17%–43% WHC, respectively. In addition, all of the soil samples had similarly shaped emission profiles. The emission peak values of all samples are shown in Figure 5.1, which reveals that emission fluxes from cropland soil were higher than those from forest soil, possibly

due to the long-term fertilization of cropland soil causing it to have a higher N content and greater microbial activity than forest soil. In addition, soil samples collected in northern China had higher emission fluxes than those collected in southern China. This may be attributable to the presence of more cropland and the application of more fertilizer in northern than in southern China (Wang et al., 2020a;Tian et al., 2012), resulting in these regions exhibiting different increases in the abundances of HONO- and NO-producing genes in response to long-term fertilization, as discussed in chapter 4.

The maximum emission of HONO in our national samples ranged from 0.2 ng m^{-2} s^{-1} to 484 ng m^{-2} s^{-1}. The range is wider than the range of 5 samples in Xinjiang (5-250 ng m^{-2} s^{-1}) (Oswald et al., 2013) and of 35 samples in Shanghai (4-288 ng m^{-2} s^{-1}) (Wu et al., 2022), highlighting large variations of soil HONO emissions from the vast land of China. Resulting from the high N deposition in China, the HONO emissions from forest soils in the present study (range: 0.2-208 ng m^{-2} s^{-1}, mean: 50 ng m^{-2} s^{-1}) are higher than that from forest soils in Germany (<1.2 ng m^{-2} s^{-1}) (Sörgel et al., 2015), Australia (<5 ng m^{-2} s^{-1}) (Oswald et al., 2013), Suriname(<5 ng m^{-2} s^{-1}) (Oswald et al., 2013), and Finland (0-1 ng m^{-2} s^{-1}) (Maljanen et al., 2013). The HONO emission from cropland soil in other countries (e.g. Germany (~250 ng m^{-2} s^{-1}) and France (~20 ng m^{-2} s^{-1}) (Oswald et al., 2013)) are within the range (16-484 ng m^{-2} s^{-1}) of this study.

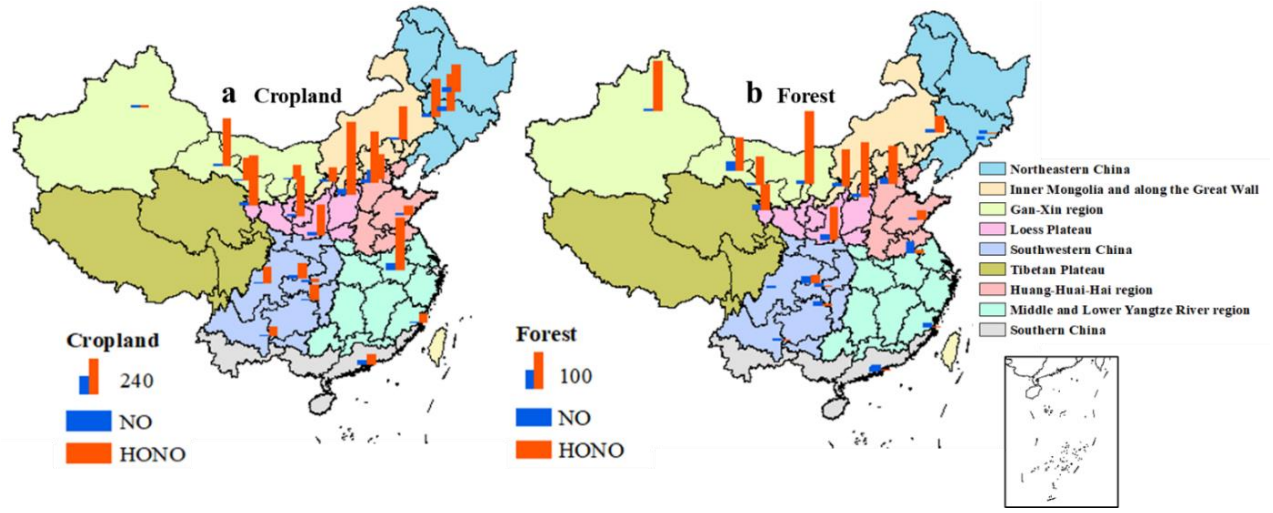

Figure 5.1 Laboratory-measured maximum emission fluxes (ng m^{-2} s^{-1}) of soil samples collected from (a) cropland and (b) forests in various regions of China. The orange and blue bars represent the fluxes of HONO and NO, respectively

We divided China's agricultural areas into nine major regions according to China Integrated Agricultural Regionalization report (NARC (National Agriculture Regionalization Committee), 1981). Each of these regions has similar cropping patterns (Qiu et al., 2022) as well as similar soil types and crop types (Chen et al., 2020). We averaged the emission fluxes of the samples collected from each of these regions to obtain an averaged emission flux curve for each region. The results are shown in Figure 6.2c–r. For cropland soil, the average maximum emission fluxes of HONO and NO in each of the nine regions ranged from 35 to 410 ng m^{-2} s^{-1} and from 6 to 43 ng m^{-2} s^{-1}, respectively. In addition, the peak emission fluxes for HONO were approximately 10 times those for NO. For forest soil, the average maximum emission fluxes of HONO and NO in each of the nine regions ranged from 1 to 145 ng m^{-2} s^{-1} and from 5 to 20

ng m^{-2} s^{-1}, respectively. We also averaged the fluxes of different SWC segments and thus found that the discrepancy between HONO and NO emission fluxes varied with the SWC, as shown in Figure 5.2a,b. That is, at SWC less than 40% WHC, the emission fluxes of HONO were generally significantly higher than those of NO, whereas at SWC greater than 40% WHC, the emission fluxes of HONO and NO were similar, due to a marked decrease in the emission flux of HONO.

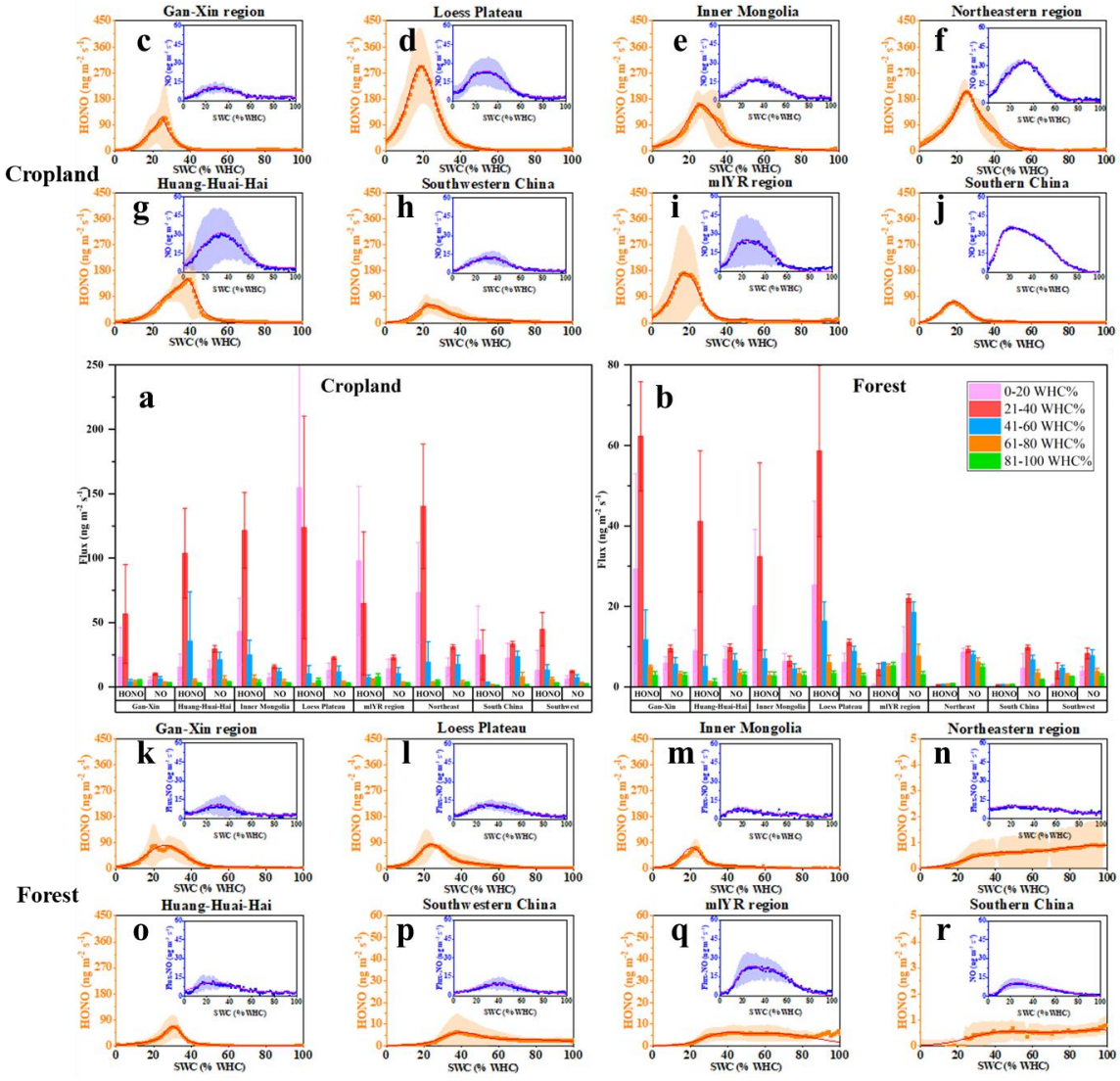

Figure 5.2 Average emission fluxes of HONO and NO as a function of the SWC of soil samples collected in eight regions of China. (a) and (b) represent the average fluxes of different SWC segments; and (c–r) depict the characteristics of the average emission fluxes of HONO (orange squares) and NO (blue squares) from cropland (c–j) and forest (k–r) soil as a function of SWC (% water holding capacity, WHC). The shaded areas represent the standard deviations, while the red and pink lines represent the results of fitting soil HONO and NO emissions as multiple Gaussian functions, respectively (Table 6.1).

Soil microbial HONO and NO emissions are caused by the nitrification and denitrification processes in soil, regulated by different microbial communities. As discussed in chapter 4, long-term fertilization in China increased more HONO-producing gene abundance than NO-producing gene abundance, which caused higher emission fluxes of HONO than of NO from soils, especially in the regions exposed to high levels of long-term fertilization and N deposition.

5.3 Results of meta-analysis

The results of our meta-analysis revealed the effects of long-term fertilization on the abundance of *AOA amoA*, *AOB amoA*, *narG*, *nirK*, and *nirS* in China (as only two studies have examined *napA*, we did not use the results for this gene). The overall effect sizes of long-term fertilization on the abundance of the above genes are presented in Figure 5.3, which shows that there was a greater enhancement in HONO-producing

gene abundance (*AOA amoA* (32%), *AOB amoA* (326%), and *narG* (99%)) than in NO-producing gene abundance (*nirK* (90%) and *nirS* (36%)) ($P < 0.05$). These effects were significant, as the 95% CIs did not overlap 0. Thus, we infer that long-term fertilization had a much greater effect on the abundance of HONO-producing genes (*amoA* and *narG*) than on the abundance of NO-producing genes (*nirK* and *nirS*).

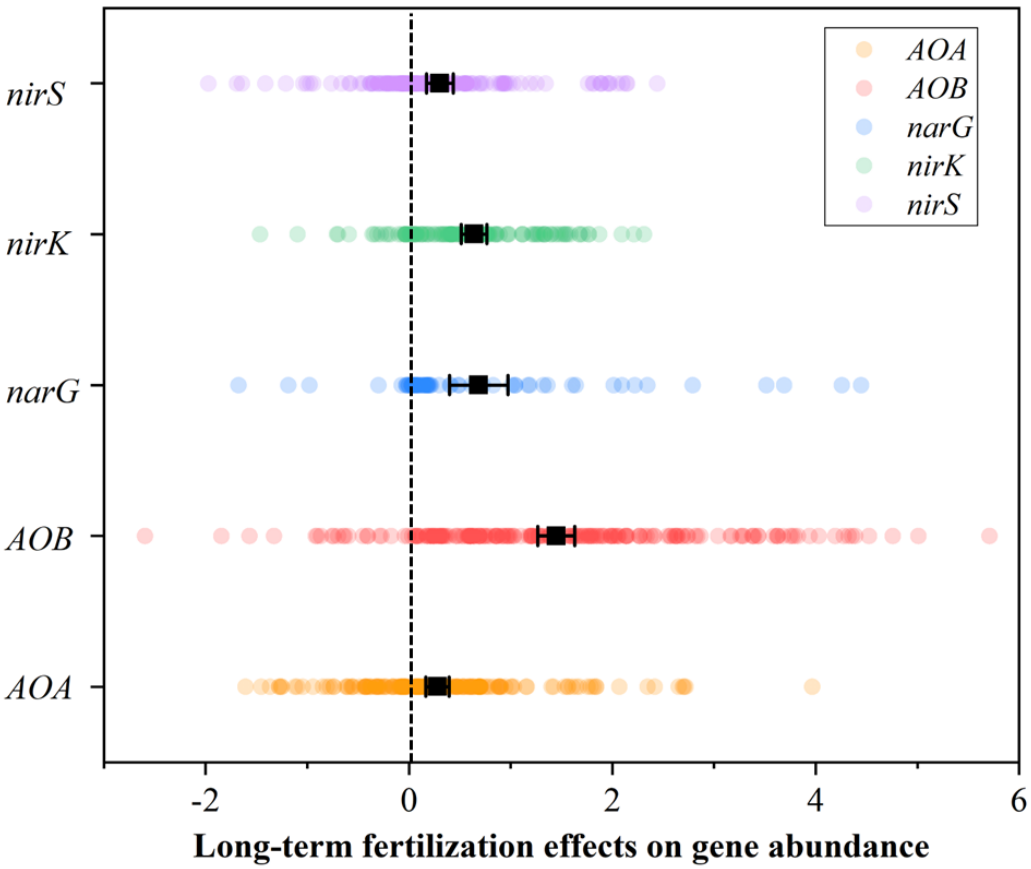

Figure 5.3 Effect of long-term fertilization on gene abundance. Each dot represents the effect size for a specific gene in one of the included studies. Black solid squares and associated error bars are effect sizes and 95% confidence intervals, respectively.

We next divided China into northern and southern parts, with 32°N latitude as the boundary, and classified the effect sizes in these two parts to determine the differences of the long-term fertilization effects on abundance of N-cycling microbial genes. The overall effect sizes after classification are shown in Figure 5.4. The increases in the abundances of *AOA amoA*, *AOB amoA*, *narG*, *nirK* and *nirS* were 36%, 448%, 129%, 119%, and 52%, respectively, in northern China; and 30%, 261%, 80%, 66%, and 19%, respectively, in southern China. This showed that long-term fertilization generated a more favorable microbial environment in soils in northern China than in those in southern China for the production and release of HONO and NO.

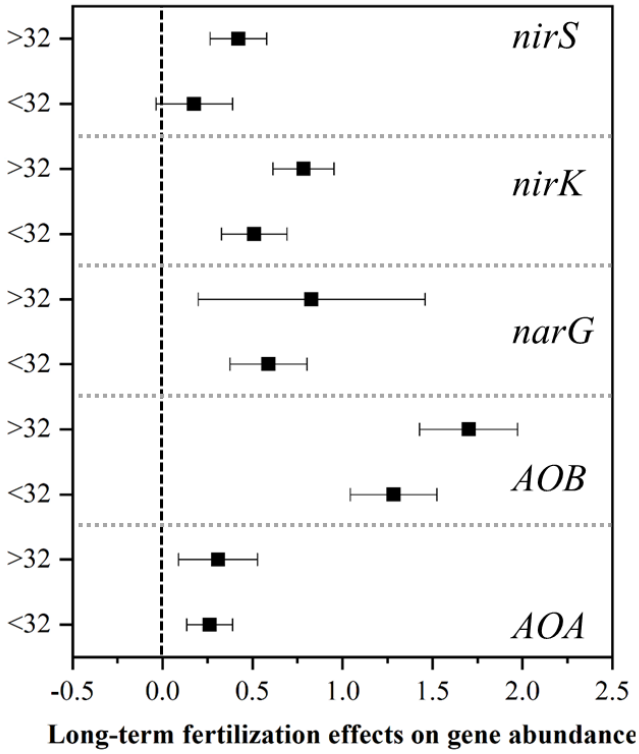

Figure 5.4 Effects of long-term fertilization on N-cycling gene abundance in northern China (> 32°N latitude) and southern China (< 32°N latitude). Black solid squares and associated error bars are effect sizes and 95% confidence intervals, respectively.

5.4 Parameterization scheme

Similar to section 5.4, we used SWC and T to quantify soil emission fluxes of these species (Mamtimin et al., 2016;van Dijk et al., 2002;Behrendt et al., 2014) via the following equations:

$$F_{N(HONO)} = F_{N,max\,(HONO)}(T_0, SWC_C) \cdot g(SWC)_{(HONO)} \cdot h(T), \quad (5.1)$$

$$F_{N(NO)} = F_{N,max\,(NO)}(T_0, SWC_C) \cdot g(SWC)_{(NO)} \cdot h(T), \quad (5.2)$$

where SWC_C is the optimal SWC where the maximum flux ($F_{N,max}(T_0, SWC_C)$) has been observed at a reference temperature T_0 (25 °C); $g(SWC)$ is the dependency of HONO or NO emissions on the SWC; and $h(T)$ is a dimensionless function of soil emissions with respect to soil T and is expressed as the ratio of emissions at T ($F_N(T)$) to that at T_0 ($F_N(T_0)$) (Wang et al., 2021), as follows:

$$h(T) = \frac{F_N(T)}{F_N(T_0)} = \frac{A \cdot \exp\left[\left(\frac{-Ea}{R}\right)\cdot\frac{1}{T}\right]}{A \cdot \exp\left[\left(\frac{-Ea}{R}\right)\cdot\frac{1}{T_0}\right]} = \exp\left[\left(\frac{-Ea}{R}\right) \cdot \left(\frac{1}{T} - \frac{1}{T_0}\right)\right] \quad , \quad (5.3)$$

where A is a constant, R is the gas constant (8.314 J mol^{-1} K^{-1}), and Ea is the activation energy. We used the average of the three Ea values (80, 75, and 44 kJ mol^{-1}) that have been reported by Oswald et al. (2013) and chapter 4. $F_{N,max}(T_0, SWC_C) \cdot g(SWC)$ was determined by our experiments, as described below.

The soil background emissions of HONO and NO in the real ambient environment were estimated using a standard formalism for the atmosphere–soil exchange of trace gases, as shown below:

$$F_{emis}(HONO) = v_t(HONO) \times [HONO]^* = \frac{1}{R_a(HONO) + R_b(HONO) + R_{soil}(HONO)} \times [HONO]_{measured}, \quad (5.4)$$

$$F_{emis}(NO) = v_t(NO) \times [NO]^* = \frac{1}{R_a(NO) + R_b(NO) + R_{soil}(NO)} \times [NO]_{measured}, \quad (5.5)$$

where v_t is transfer velocity, which equals the reciprocal of the sum of aerodynamic resistance (R_a), quasi-laminar layer resistance (R_b), and soil resistance (R_{soil}), where R_a, R_b, and R_{soil} were calculated using the formulae recommended by Pleim and Sakaguchi et al; and [HONO]* and [NO]* are the equilibrium concentrations of HONO and NO at the soil surface, which were assumed to be the mixing ratios of HONO and NO measured at the chamber outlet ($[HONO]_{measured}$ and $[NO]_{measured}$), given that air was well mixed in the chamber. Finally, by combining Eqs. (3.3), (5.1), (5.3), and (5.4) or (3.4), (5.2), (5.3), and (5.5), we deduced the soil emissions of HONO or NO, respectively, in the real ambient environment (F_{emis}), as follows:

$$F_{emis}(HONO) = v_t(HONO) \times [HONO]^* = \frac{1}{R_a(HONO) + R_b(HONO) + R_{soil}(HONO)} \times [HONO]_{measured} =$$

$$\frac{1}{R_a(HONO) + R_b(HONO) + R_{soil}(HONO)} \times \frac{F_{N,max\,(HONO)}(T_0, SWC_C) \cdot g(SWC)_{(HONO)}}{\frac{Q}{A} \cdot \frac{M_N}{V_m}} \times \exp\left[\left(\frac{-Ea}{R}\right) \cdot \left(\frac{1}{T} - \frac{1}{T_0}\right)\right], \quad (5.6)$$

$$F_{emis}(NO) = v_t(NO) \times [NO]^* = \frac{1}{R_a(NO)+R_b(NO)+R_{soil}(NO)} \times [NO]_{measured} =$$

$$\frac{1}{R_a(NO)+R_b(NO)+R_{soil}(NO)} \times \frac{F_{N,max\,(NO)}(T_0, SWC_C) \cdot g(SWC)_{(NO)}}{\frac{Q}{A} \cdot \frac{M_N}{V_m}} \times \exp\left[\left(\frac{-Ea}{R}\right) \cdot \left(\frac{1}{T} - \frac{1}{T_0}\right)\right]. \quad (5.7)$$

Based on the averaged experimental results shown in Figure 5.2c–r, we developed a parameterization of cropland and forest in various regions to link soil emission fluxes of HONO and NO at 25 °C with the SWC in Eqs. (5.6) and (5.7). We used a multiple Gaussian fitting approach in MATLAB 8.6 (MathWorks Inc., Natick, MA, USA) to fit the HONO and NO release profiles:

$$F_{N,max}(T_0, SWC_C) \cdot g(SWC) = F_{N,max_{Peak1}} \cdot \exp\left(-\frac{\left(SWC - SWC_{C_{Peak1}}\right)^2}{w_{Peak1}{}^2}\right) + F_{N,max_{Peak2}} \cdot \exp\left(-\frac{\left(SWC - SWC_{C_{Peak2}}\right)^2}{w_{Peak2}{}^2}\right), \quad (5.8)$$

where $F_{N,max_{Peak}}$ is the peak value of emission fluxes, SWC ranged from 0% to 100% WHC, SWC_C is the SWC at which the $F_{N,max_{Peak}}$ occurred, and *w* is the width of the fitting curves. As shown in Figure 5.2c–r, two Gaussian functions well fitted the experimental dependency of HONO emission on the SWC, and the fitting parameters are listed in Table 5.1.

Table 5.1 Parameterization schemes of soil background emissions of HONO and NO as multiple Gaussian functions of the SWC. Peak1 and Peak2 represent two Gaussian functions.

			HONO		NO	
Cropland	Region	Parameter	Peak1	Peak2	Peak1	Peak2
	Gan–Xin region	$F_{N,max}$	36.54	80.53	9.89	2.98
		SWC_c	25.04	23.56	27.94	88.19
		w	2.62	9.97	23.17	54.35
	Loess Plateau	$F_{N,max}$	72.57	219.9	22.58	2.98
		SWC_c	18.63	19.19	28.64	88.78
		w	21.35	9.00	23.69	63.18
	Southern China	$F_{N,max}$	72.24	4.51	20.5	29.81
		SWC_c	18.55	42.02	17.05	39.02
		w	9.48	21.99	11.95	26.21
	Inner Mongolia and along the Great Wall	$F_{N,max}$	130.17	31.32	15.41	2.53
		SWC_c	26.35	31.53	34.39	89.86
		w	10.08	36.83	24.57	95.38
	Huang–Huai–Ha region	$F_{N,max}$	108.76	59.59	30.86	3.71
		SWC_c	32.91	39.48	32.87	88.33
		w	14.35	4.82	24.52	44.35
	Northeastern China	$F_{N,max}$	136.5	69.72	4.93	28.57
		SWC_c	26.45	24.9	17.31	32.62
		w	17.56	5.14	69.65	22.18
	Southwestern China	$F_{N,max}$	52.89	13.27	12.11	2.31
		SWC_c	24.33	43.26	32.21	79.94
		w	10.14	30.78	23.33	43.93

	Middle and Lower Yangtze River region	$F_{N,max}$	159.75	12.86	6.98	22.71
		SWC_c	17.93	23.57	16.95	30.48
		w	9.97	66.62	8.18	22.98
Forest	Gan–Xin region	$F_{N,max}$	73.74	7.74	9.87	2.85
		SWC_c	26.05	41.53	28.58	85.25
		w	13.36	55.56	23.01	54.35
	Loess Plateau	$F_{N,max}$	64.34	21.77	8.67	4.14
		SWC_c	24.24	35.04	30.17	58.19
		w	9.24	30.5	24.37	54.35
	Southern China	$F_{N,max}$	0.43	0.61	7.28	6.21
		SWC_c	41.58	95.67	24.15	48.37
		w	23.34	41.22	15.17	31.35
	Inner Mongolia and along the Great Wall	$F_{N,max}$	61.42	12.55	5.39	3.88
		SWC_c	20.86	30.06	19.17	52.83
		w	6.91	28.63	19.01	58.54
	Huang–Huai–Hai region	$F_{N,max}$	20.25	47.17	9.39	3.37
		SWC_c	26.94	30.45	24.76	72.81
		w	18.13	5.61	25.02	60.41
	Northeastern China	$F_{N,max}$	0.38	0.89	8.23	3.47
		SWC_c	37.65	93.67	20.24	95.19
		w	20.58	47.31	47.57	95.06
	Southwestern China	$F_{N,max}$	4.68	3.01	8.36	1.76
		SWC_c	39.46	74.26	38.35	97.11
		w	13.84	41.6	29.67	75.68
	Middle and Lower Yangtze River region	$F_{N,max}$	3.60	5.61	10.44	20.3
		SWC_c	36.49	65.97	23.07	43.39
		w	14.26	31.16	10.79	27.62

We compared reported field-measured fluxes with the results from our laboratory-derived parameterization. Given the paucity of field measurements of soil background emissions of HONO, we collated 19 field studies that measured background emission fluxes of NO using a chamber (Table 5.2). The sites of these studies were distributed in various provinces in China and thus the results represented the overall profile of background soil emissions of NO in China. As shown in Figure 5.5a, the reported soil background emissions of NO ranged from 0.2 to 11.0 ng m^{-2} s^{-1}, with an average of 2.2 ng m^{-2} s^{-1}, and 73% ranged from 0.5 to 3.0 ng m^{-2} s^{-1}. Among them, we further selected nine studies that reported the SWC and T for field measurements and compared their emission fluxes with the values calculated by our parameterization for each region. The results are shown in Figure 5.5b. The median of the field-measured emission fluxes of NO was 1.7 ng m^{-2} s^{-1}, while that from our parameterization was 2.2 ng m^{-2} s^{-1}. We acknowledge limitations in the above comparison arising from the differences between our study and the other studies in terms of the sampling season, date, and location. Nevertheless, the estimated soil emission fluxes of NO generated by our parameterization are comparable to those that have been determined from field measurements.

Table 5.2 The 48 field measurements of soil background NO emissions recorded in 19 studies in China.

Refs	Province	Latitude	longitude
Fang & Mu, 2009 (Fang and Yujing, 2009)	Zhejiang	30.83	120.7
Deng et al., 2012[a] (Deng et al., 2012)	Jiangsu	31.62	120.47
Liu et al., 2011 (Liu et al., 2011)	Shanxi	34.93	110.71
Mei et al., 2009[a] (Mei et al., 2009)	Jiangsu	32.58	119.7
Zhou et al., 2010[a] (Zhou et al., 2010)	Jiangsu	31.61	120.49
Yan et al., 2013[a] (Yan et al., 2013)	Shandong	36.97	117.98
Zhang et al., 2019[a] (Zhang et al., 2019b)	Shandong	36.86	117.83
Tian et al., 2020[a] (Tian et al., 2020)	Hebei	38.02	115.08
Li et al., 2013[a] (Li and Slomp, 2013)	Guangdong	23.17	113.38
Zhang et al., 2016[a] (Zhang et al., 2016b)	Jiangsu	32.07	118.97
Zhang et al., 2021[a] (Zhang et al., 2021)	Sichuan	30.68	103.8
Zhang et al., 2021[a] (Zhang et al., 2021)	Sichuan	31.27	105.47
Pang et al., 2009 (Pang et al., 2009)	Zhejiang	30.83	120.7
Yan et al., 2015 (Yan et al., 2015)	Shangdong	36.97	117.98
Zhang et al., 2011 (Zhang et al., 2011)	Heibei	38.66	115.25
Zheng et al., 2003 (Zheng et al., 2003)	Jiangsu	31.27	120.63
Yu et al., 2010 (Yu et al., 2010)	Heilongjiang	44.2	125.53
Zhang et al., 2019 (Zhang et al., 2019c)	Jiangsu	32.07	118.97
Yao et al., 2015 (Yao et al., 2015)	Jiangsu	32.58	119.7
Gao et al., 2016 (Gao et al., 2016b)	Sichuan	33.05	102.6

[a] Studies reporting field soil water content and temperature simultaneously for parameterization validation.

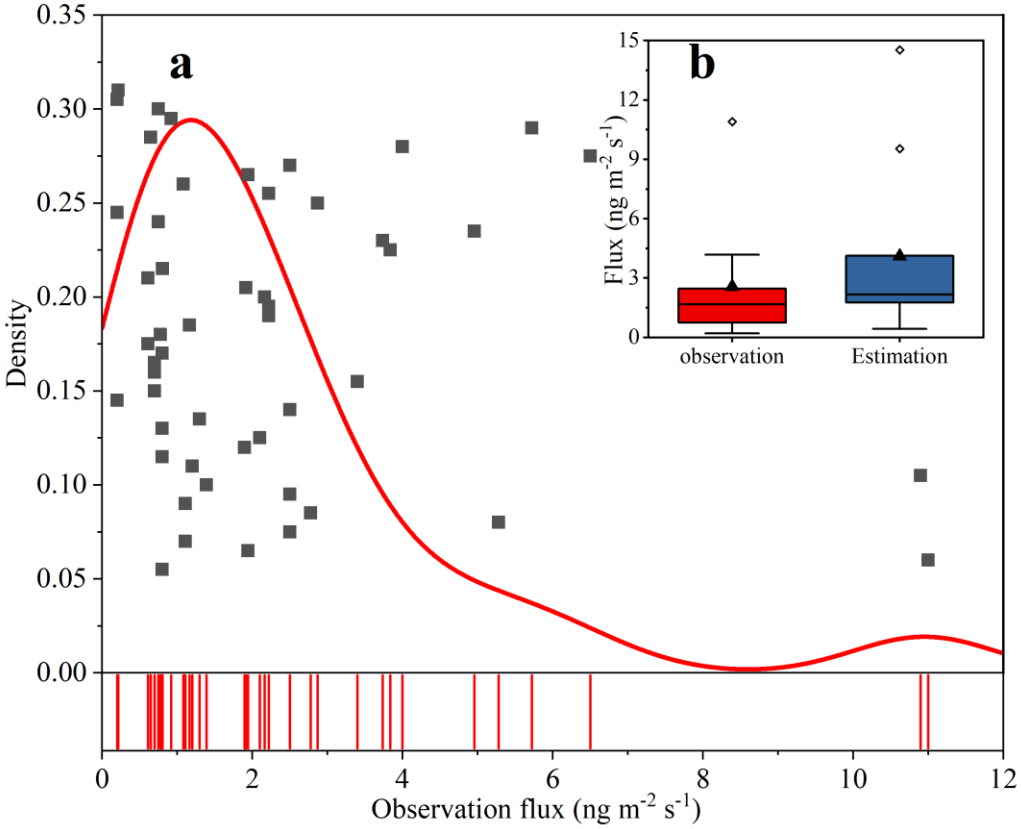

Figure 5.5 Range of field-measured background emission fluxes of NO in China. (a) Distribution of background emission flux of NO determined from 48 observations from 19 studies. Black solid squares are field-measured emission fluxes of NO, red curves are densities of field-measured emission fluxes of NO, and the rug at the bottom gives the count of observations. (b) Box plots of field-measured emission fluxes of NO and parameterization-estimated emission fluxes of NO. The middle, upper, and lower lines of the boxes show the median, upper, and lower quartiles, respectively, and the solid black triangle is the mean value. The whiskers show the value within the 1.5 interquartile range and the open rhombuses indicate the ranges of emission fluxes of NO.

5.5 Impact of soil background emissions on air quality

We next implement the HONO emission scheme in the CMAQ model to simulate the impact of soil background emissions on air quality in China. The model simulations were performed by collaborator (Dr. Xiao Fu). Detailed model simulation results can be found in Wang et al (Large contribution of nitrous acid to soil emitted reactive oxidized nitrogen and the impact on air quality, Published in Environ Sci Technol). Figure 5.6 shows the estimated average soil background emissions of HONO and NO for August 2016. The soil background emissions of HONO were higher than that those of NO. The high soil emissions were concentrated in regions with dense cropland, such as the NCP and Northeast Plain (NEP), with values greater than 2 ng N m^{-2} s^{-1} for HONO and greater than 1 ng N m^{-2} s^{-1} for NO. In the NCP region, where there are major anthropogenic sources, the background soil emissions of N accounted for approximately 3.2% of anthropogenic NO_x emissions. In contrast, in the NEP region, the background soil emissions of N reached approximately 10.8% of anthropogenic emissions of NO_x.

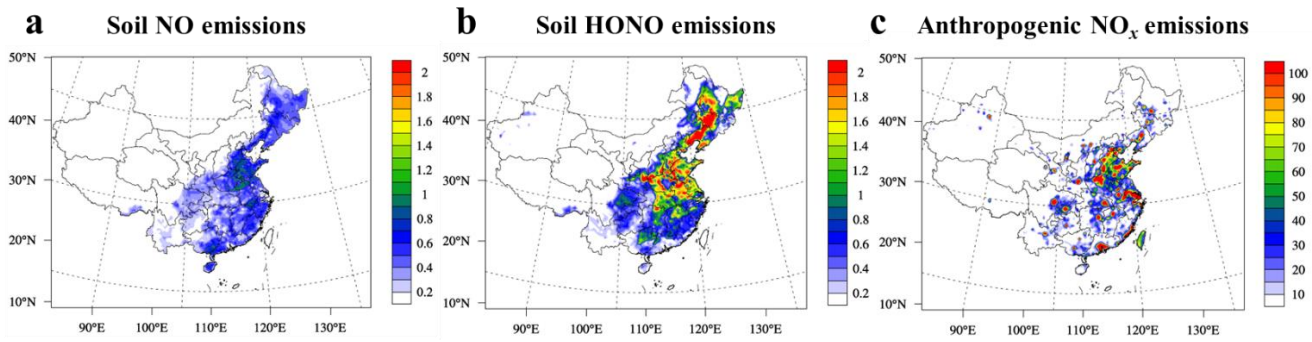

Figure 5.6 Model-simulated monthly average soil background emissions of (a) NO, (b) HONO (ng N m^{-2} s^{-1}) in August 2016, and (c) anthropogenic emissions of NO_x in 2015 in China.

We further evaluated the effect of soil background emissions on atmospheric oxidation capacity and air quality. As shown in Figure 5.7, the soil background emissions increased the monthly average concentrations of HONO by 0.08 and 0.07 ppb (21% and 47%) in the NCP and NEP regions, respectively. This indicates the important contribution of soil emissions to ambient HONO concentrations. Consequently, soil background emissions had a non-negligible effect on atmospheric oxidation capacity and secondary pollutants, especially in the NEP region, due its low anthropogenic emissions and dense cropland. We note that several previous studies in Europe suggest insignificant contributions of soil emissions to ambient HONO concentrations. For example, vertical measurements of HONO in a rural area of Germany using the aerodynamic gradient method indicated that soil acted as a sink of HONO in nighttime, and the soil emissions, based on the laboratory measured emissions from soil samples collected from the sites, contributed less to the daytime positive flux than other sources (Sörgel et al., 2015). Using the similar gradient method, another study also indicated soil being a net sink in an agricultural site of France during nighttime, and based on the correlation of the HONO flux with photolysis of NO_2 and the diurnal profile of the HONO flux (peaking in the late morning), the author attributed the positive HONO flux in daytime to light-induced HONO formation through

heterogeneous reaction of NO_2 on surface, rather than soil direct emission (Laufs et al., 2017). In that study, the soil HONO emissions were not measured but estimated based on soil moisture and temperature. Another recent study presented similar findings of the dominance of the NO_2 production pathway in a rural grassland following a rainfall (von der Heyden et al., 2022). Our model has considered HONO deposition and all known HONO sources including the light enhanced NO_2 heterogenous reactions on surface (see Method Section) and soil emissions based on the samples collected across China. The net positive contribution of soil to ambient HONO concentrations in our study may be partially explained by the high emissions of HONO from forest and cropland in China.

Figure 5.7 shows simulated contributions of soil background HONO and NO emissions to ambient OH, O_3, and particulate nitrate (NO_3^-) in August 2016. In the NEP region, the soil background emissions increased the maximum 1-hour (max-1h) OH, max-1h O_3, and daily average NO_3^- concentrations by 7.5%, 2.0%, and 5.0%, respectively, with the contributions in specific grid squares being greater than 25%, 4%, and 16%, respectively. In the NCP region, the presence of high anthropogenic emissions meant that the soil background emissions made smaller relative contributions to the concentrations of these pollutants. Moreover, soil background emissions of HONO had a larger effect than those of NO on air quality in northern China, while the emissions of these two species had similar effects on air quality in southern China.

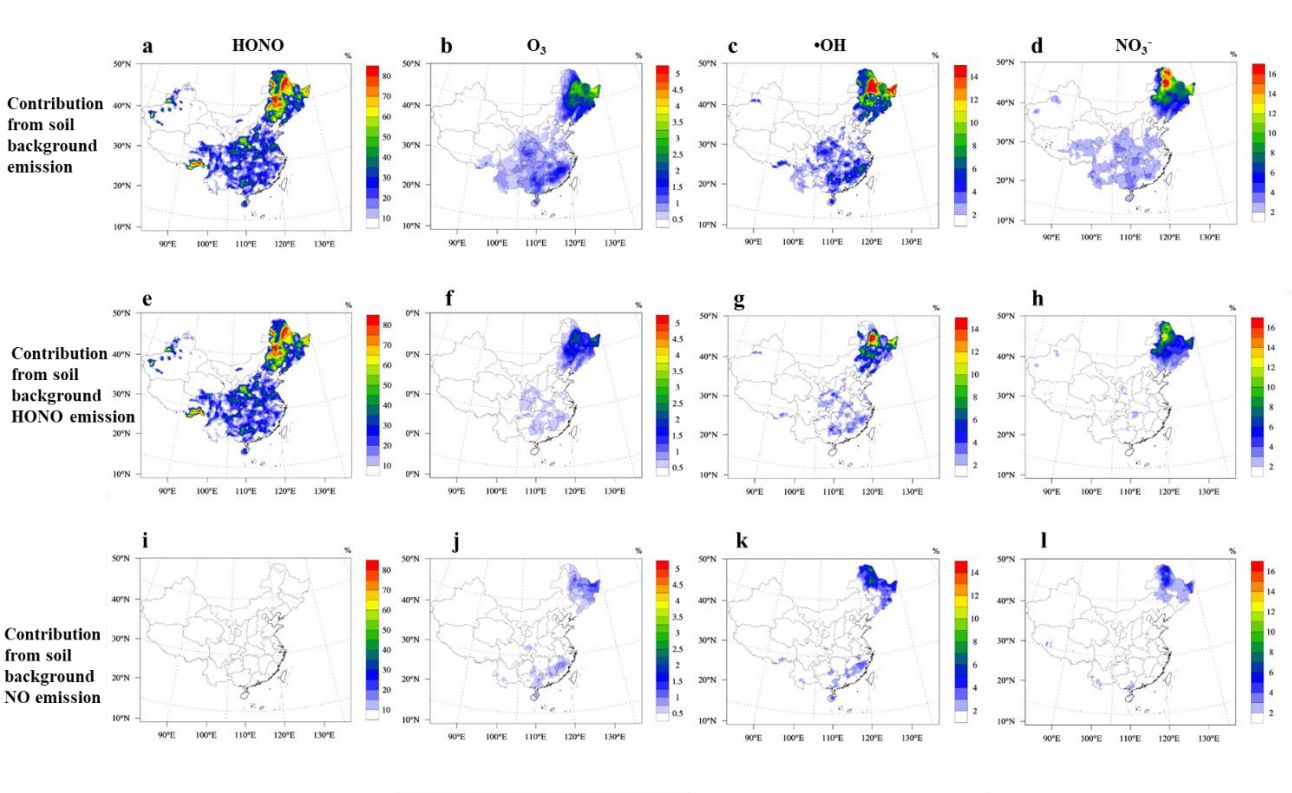

Figure 5.7 Simulated effects of soil background emissions on air quality. (a–d) Overall effect of soil background emissions of HONO and NO on monthly average concentrations of HONO, max-1h O_3, max-1h OH, and daily average concentrations of particulate nitrate ions (NO_3^-), respectively. (e–h) and (i–l) represent the contributions of soil background emissions of HONO and NO, respectively, to the above species.

Anthropogenic NO_x emissions have gradually declined in China since 2012, due to efforts to reduce anthropogenic emissions that were implemented in recent years (Wang et al., 2022). In anticipation of a continuous decrease in anthropogenic emissions, the effects of soil emissions of N species on atmospheric chemistry and air pollution control will become increasingly significant. If anthropogenic emissions of NO_x, VOCs,

SO_2, NH_3, $PM_{2.5}$, and BC decrease by 70%, 54%, 78%, 24%, 75%, and 90%, respectively, under low-carbon energy policies and maximum end-of-pipe control strategies (CBE–MFR in Xing et al. (2020)), the monthly average contributions of soil background HONO and NO emissions to max-1h OH, max-1h O_3, and daily average NO_3^- will increase to 17%, 4.6%, and 14%, respectively, in the NEP region (Figure 5.8). In addition, the corresponding contributions of soil background HONO emissions will be 12%, 3.0% and 9.3%, respectively. In the NCP region, the monthly average contributions of soil background HONO and NO emissions to max-1h OH, max-1h O_3, and daily average NO_3^- will increase to 4.4%, 2.0% and 6.6%, respectively.

We note that uncertainties exist in the above simulations, resulting from limited soil samples to represent the vast territory of China. Additionally, the emissions were determined from soil samples collected in March, whose soil characteristics are possibly different from those in August or other months. Fertilization activities are active from April to July, so the effect of soil emissions on air quality in August is possibly even larger due to more N residue in soil. Nonetheless, our results demonstrate the unignored impacts of soil background emissions on air quality in a month with active photochemistry.

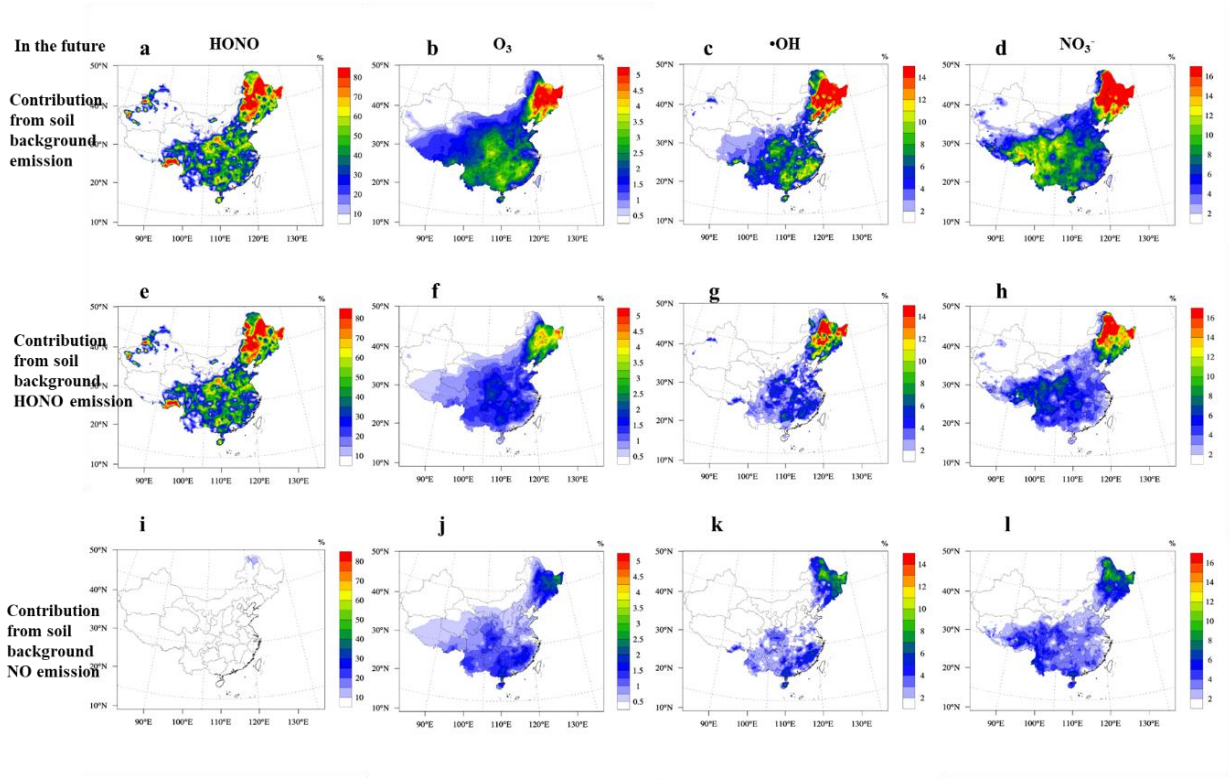

Figure 5.8 Simulated impacts of soil background on air quality in the future with the reduction of anthropogenic emissions under the low-carbon energy policies and maximal end-of-pipe control strategies. a-d are the overall impact of soil background HONO and NO emissions on monthly average HONO, max-1h O_3, max-1h OH, and NO_3^-, respectively. e-h and i-l represent the contribution from soil background HONO and NO emissions, respectively.

5.6 Implications

Many studies have shown that soil emissions of NO have a significant effect on air quality, especially during fertilization periods. For example, it was suggested that soil NO emissions during fertilization in the NCP region accounted for 11%–20% of anthropogenic emissions of NO_x and increased the concentrations of O_3 by 9.5 ppb (Lu

et al., 2019b). Moreover, a study in California showed that soil emissions accounted for 40% of the NO_x emissions in July, thereby increasing the monthly concentrations of NO_2 and O_3 by 176% and 23%, respectively (Sha et al., 2021). Another study in the southeastern U.S. revealed that nearly half of the increase in the concentration of O_3 at a rural site in summer was attributable to temperature-driven increases in emissions of NO_x (Romer et al., 2018).

Based on measurements of 48 soil samples collected across China, our study revealed that soil emissions of HONO were higher than soil emissions of NO in most of these samples, and our model simulations showed larger impact of HONO than NO on air quality. However, HONO has not been considered in many previous investigations of soil emissions of reactive oxidized N and their effect on air quality. Thus, the total amount of N lost from soil to the atmosphere may have been underestimated, and its effect on the atmosphere may have been underappreciated. We call for reappraisals of the roles of reactive N species in atmospheric chemistry and air quality by inclusion of HONO in assessments, particularly in countries or regions with vast agricultural lands, such as the U.S., India, Europe, and Brazil (Ramankutty et al., 2008), in addition to China. As anthropogenic emissions of NO_x are gradually decreasing due to strict emission controls, the contribution of soil emissions of N to the N budget and atmospheric environment will become increasingly important in the future. We call for more research on soil HONO emissions around the world and suggest

that future N emission control strategies should also consider soil HONO and NO emissions.

5.7 Summary

In this chapter, we measured background emission fluxes of HONO and NO from soil samples collected from 48 sites across China. The results showed much higher emissions of HONO than those of NO, which were caused by the higher promotion effects of long-term fertilization on the abundance of HONO-producing genes than NO-producing genes. Besides, this enhancement was greater in northern China than in southern China, which accounts for the higher emission fluxes in the former region than in the latter region. In simulations using a chemical transport model with laboratory-derived parametrization, we found that HONO emissions had a greater effect than NO emissions on air quality. With projected continuous reductions in anthropogenic emissions, the contribution of soil emissions will increase significantly. Our findings highlight the need to consider HONO in the assessment of reactive nitrogen loss from soils to the atmosphere and its effect on air quality.

Chapter 6. Summary and future work

6.1 Summary of the thesis

Soil emissions make a significant contribution to atmospheric HONO levels, but their impact on air quality is often overlooked due to a lack of parameterization to accurately quantify soil HONO emissions. This thesis addresses this gap by developing a parameterization for HONO emissions from both fertilized and unfertilized soils. The key findings and summaries of this thesis are presented below.

We measured post-fertilization HONO emissions from soil samples collected from two typical agricultural regions in China. Besides, we investigated the impact of different fertilizer types and the duration since fertilization on HONO emissions. The results showed that agricultural fertilization stimulate the soil HONO emissions significantly, and the promotion effects of fertilization lasted up to one week. Interestingly, high HONO emissions from soils at high SWC (75%–95% WHC) were found, which contrasts to previous lower predictions at high soil moisture. Based on the results of laboratory experiments, we developed a parameterization scheme linking HONO emission to SWC for three commonly used fertilizers. The implementation of the parametrization in a regional chemical and transport model (CMAQ) model significantly improved post-fertilization HONO predictions during fertilization period. The simulation results showed that the post-fertilization HONO emissions increased regionally averaged daytime OH, O_3, and daily fine particulate nitrate concentrations

by 41%, 8%, and 47%, respectively, in the NCP region. In terms of the effects of different fertilizer types, the largest release of HONO were found after urea applications compared to the other two commonly used fertilizers (NH_4HCO_3 and NH_4NO_3). We therefore recommend adjusting the type of fertilizer application to reduce HONO emissions and their impact on air quality, especially in the polluted regions with intense agriculture.

We measured background (unfertilized) HONO and NO emissions from soil samples collected from 48 sites across China. Results showed that cropland soils have higher emissions than forest soils that are not affected by anthropogenic activities. Because long-term fertilization had a greater increase in HONO-producing genes compared to NO-producing genes, higher emissions of HONO than those of NO were found. The greater enhancement of long-term fertilization to genes in northern China resulted in higher emission fluxes in comparison to southern China. We developed a parameterization scheme to accurately assess background soil HONO and NO emissions in various regions of China. The simulation results showed that HONO emissions had a greater effect than NO emissions on air quality and the contribution of soil emissions will increase significantly with the continuous reductions of anthropogenic emissions. Our study highlights the need to consider HONO in the evaluation of reactive nitrogen loss from soils to the atmosphere and its impact on air quality. Neglecting soil HONO emissions in previous studies may lead to an underestimation of total N emissions from soil to the atmosphere. Future studies of

nitrogen cycle and atmospheric chemistry should consider the influence of soil HONO emissions.

6.2 Future works

While this thesis discusses the importance of soil HONO emissions, there are still many topics that warrant further investigation in future research.

1. Effects of different fertilizer application rates on soil HONO emissions. As an important supplier of nitrogen in the soil, different application rates of chemical fertilizers directly affect soil nitrogen content, thereby affecting soil reactive nitrogen emissions, including HONO. While this thesis has explored the effects of fertilizer types and timing of fertilization on soil HONO emissions, the role of fertilizer application rates remains unexplored.

2. Global soil HONO emissions and their implications for air quality. Soils have been demonstrated to be an important source of global NO_x emissions. A global inventory shows that soil emissions account for 22% of global NO_x emissions (Jaegle et al., 2005). Such considerable amounts of soil NO emissions are an important contributor to global atmospheric NO_x and have a significant impact on air quality. However, the global-scale study of soil HONO emissions and their influence on air quality has been lacking. In this thesis, we have demonstrated that soil emissions have a more pronounced effect on regions with low anthropogenic emissions and intensive

cropland compared to regions with high anthropogenic emissions. Therefore, we hypothesize that the impact of soil emissions on air quality may be particularly significant in countries and regions with extensive agricultural land but limited anthropogenic sources, such as the United States, Brazil, and Europe. Future studies can employ the parameterization scheme we have developed to evaluate the impact of soil HONO emissions in a global-scale model.

3. Using isotopic techniques to quantify the relative contributions of various microbial processes to soil emissions of HONO. This paper has reviewed the microbial mechanisms of soil HONO emissions. Both soil nitrification and denitrification processes can produce HONO. However, the specific contribution of each process to HONO emissions remains unknown. By employing isotopic techniques, we aim to quantify the individual contributions of these processes, thereby providing a basis for controlling soil emissions and their impact on air quality.

4. Nitrogen deposition has significant impacts on soil emissions. It provides N to the soil, resulting in an increase in soil N content. This, in turn, leads to increased emission of reactive nitrogen from the soil. As a crucial source of nitrogen input in agricultural soil, the amount of nitrogen deposition is continuously rising. However, the specific impact of nitrogen deposition on soil HONO emissions remains uncertain. Therefore, in the future, a combination of laboratory experiments and modeling can be

used to simulate the effects of nitrogen deposition on soil HONO emissions and its consequences on air quality.

5. Precipitation can stimulate pulsed soil emissions when the soil remains drying for a long time. Previous studies on soil NO emissions connected pulse emissions with the duration of drought periods. The longer the drought, the more significant the impact of precipitation pulses. In our study, however, we simulated a relatively short time frame, focusing only on one week following fertilizer application or one month of background emissions. Hence, I believe the influence of pulses would not be highly observable in this study. Nonetheless, it is undeniable that this is an important question, and we can explore the influence of pulses in future studies.

6. The impacts of the use of nitrification inhibitors on the emission of reactive nitrogen in soil. By inhibiting nitrification, these inhibitors can decrease the formation of nitrite and nitrate in the soil, thereby suppressing the emission of gases such as HONO, NO, and N_2O. However, the inhibitors also hinder the conversion of ammonium nitrogen in the soil, leading to the accumulation of ammonium nitrogen and an increase in NH_3 emissions. Therefore, in the future, we can conduct research to understand the comprehensive impact of nitrification inhibitors on the emission of reactive nitrogen and evaluate their overall effect on air quality.

Reference

Acker, K., Möller, D., Wieprecht, W., Meixner, F. X., and Berresheim, H.: Strong daytime production of OH from HNO_2 at a rural mountain site, Geophysical Research Letters, 33, 2006.

Ai, C., Liang, G., Sun, J., Wang, X., He, P., and Zhou, W.: Different roles of rhizosphere effect and long-term fertilization in the activity and community structure of ammonia oxidizers in a calcareous fluvo-aquic soil, Soil Biology and Biochemistry, 57, 30-42, 10.1016/j.soilbio.2012.08.003, 2013.

Alicke, B., Geyer, A., Hofzumahaus, A., Holland, F., Konrad, S., Patz, H. W., Schafer, J., Stutz, J., Volz-Thomas, A., and Platt, U.: OH formation by HONO photolysis during the BERLIOZ experiment, Journal of Geophysical Research, 108, 2003.

Ammann, M., Kalberer, M., Jost, D. T., Tobler, L., and Rössler, E.: Heterogeneous production of nitrous acid on soot in polluted air masses, Nature, 395, 157-160, 1998.

Aranibar, J. N., Otter, L., Macko, S. A., Feral, C. J. W., and Swap, R. J.: Nitrogen Cycling in the Soil–Plant System along a Precipitation Gradient in the Kalahari Sands, Global Change Biology, 10, 359-373, 2004.

Atkinson, R., Baulch, D. L., Cox, R. A., Crowley, J. N., Hampson, R. F., Hynes, R. G., Jenkin, M. E., Rossi, M. J., and Troe, J.: Evaluated kinetic and photochemical data for atmospheric chemistry: Volume II–gas phase reactions of organic species, Atmospheric chemistry and physics, 6, 3625-4055, 2006.

Bao, F., Li, M., Zhang, Y., Chen, C., and Zhao, J.: Photochemical Aging of Beijing Urban $PM_{2.5}$: HONO Production, Environ Sci Technol, 52, 6309-6316, 10.1021/acs.est.8b00538, 2018.

Behrendt, T., Veres, P. R., Ashuri, F., Song, G., Flanz, M., Mamtimin, B., Bruse, M., Williams, J., and Meixner, F. X.: Characterisation of NO production and consumption: new insights by an improved laboratory dynamic chamber technique, Biogeosciences, 11, 5463-5492, 10.5194/bg-11-5463-2014, 2014.

Bei, S., Zhang, Y., Li, T., Christie, P., Li, X., and Zhang, J.: Response of the soil microbial community to different fertilizer inputs in a wheat-maize rotation on a calcareous soil, Agriculture, Ecosystems & Environment, 260, 58-69, 10.1016/j.agee.2018.03.014, 2018.

Bhadha, J. H., Capasso, J. M., Khatiwada, R., Swanson, S., and LaBorde, C.: Raising soil organic matter content to Improve water holding capacity, UF/IFAS Extension, SL447, 2017.

Bhattarai, H. R., Virkajärvi, P., Yli-Pirilä, P., and Maljanen, M.: Emissions of atmospherically important nitrous acid (HONO) gas from northern grassland soil increases in the presence of nitrite (NO_2^-), Agriculture, Ecosystems & Environment, 256, 194-199, 10.1016/j.agee.2018.01.017, 2018.

Bhattarai, H. R., Wanek, W., Siljanen, H. M. P., Ronkainen, J. G., Liimatainen, M., Hu, Y., Nykänen, H., Biasi, C., and Maljanen, M.: Denitrification is the major nitrous acid production pathway in boreal agricultural soils, Communications Earth & Environment, 2, 54, 10.1038/s43247-021-00125-7, 2021.

Bøckman, O. C.: Fertilizers and biological nitrogen fixation as sources of plant nutrients: perspectives for future agriculture, Plant and Soil, 194, 11-14, 1997.

Bolan, N. S., Saggar, S., Luo, J. F., Bhandral, R., and Singh, J.: Gaseous emissions of nitrogen from grazed pastures: processes, measurements and modelling, environmental implications, and mitigation, Advances in Agronomy, 84, 288-295, 2004.

Bollmann, A., and Conrad, R.: Influence of O_2 availability on NO and N_2O release by nitrification and denitrification in soils, Global Change Biology, 4, 387-396, 1998.

Bouwman, A. F.: Direct emission of nitrous oxide from agricultural soils, Nutrient Cycling in Agroecosystems, 46, 53-70, 1996.

Bouwman, A. F., Lee, D. S., Asman, W. A. H., Dentener, F. J., Van Der Hoek, K. W., and Olivier, J. G. J.: A global high-resolution emission inventory for ammonia, Global Biogeochemical Cycles, 11, 561-587, 1997.

Bouwman, A. F., Boumans, L. J. M., and Batjes, N. H.: Emissions of N_2O and NO from fertilized fields: Summary of available measurement data, Global Biogeochemical Cycles, 16, 6-1-6-13, 2002.

Burling, I. R., Yokelson, R. J., Griffith, D. W. T., Johnson, T. J., Veres, P., Roberts, J. M., Warneke, C., Urbanski, S. P., Reardon, J., Weise, D. R., Hao, W. M., and de Gouw, J.: Laboratory measurements of trace gas emissions from biomass burning of fuel types from the southeastern and southwestern United States, Atmospheric Chemistry and Physics, 10, 11115-11130, 10.5194/acp-10-11115-2010, 2010.

Butterbach-Bahl, K., Baggs, E. M., Dannenmann, M., Kiese, R., and Zechmeister-Boltenstern, S.: Nitrous oxide emissions from soils: how well do we understand the processes and their controls?, Philos Trans R Soc Lond B Biol Sci, 368, 20130122, 10.1098/rstb.2013.0122, 2013.

Carrasco, D., Fernandez-Valiente, E., Ariosa, Y., and Quesada, A.: Measurement of coupled nitrification-denitrification in paddy fields affected by Terrazole, a nitrification inhibitor, Biology and Fertility of Soils, 39, 186-192, 2004.

Cartes, P., Jara, A. A., Demanet, R., and María, L. M.: Urease activity and nitrogen mineralization kinetics as affected by temperature and urea input rate in southern Chilean Andisols, Journal of Soil Science and Plant Nutrition, 9, 14, 2009.

Chan, W. H., Nordstrom, R. J., Calvert, J. G., and Shaw, J. H.: Kinetic study of nitrous acid formation and decay reactions in gaseous mixtures of nitrous acid, nitrogen oxide (NO), nitrogen oxide (NO_2), water, and nitrogen, Environmental Science & Technology, 10, 674-682, 1976.

Chen, D., Li, Y., Wang, C., Liu, X., Wang, Y., Shen, J., Qin, J., and Wu, J.: Dynamics and underlying mechanisms of N_2O and NO emissions in response to a transient land-use conversion of Masson pine forest to tea field, Sci Total Environ, 693, 133549, 10.1016/j.scitotenv.2019.07.355, 2019.

Chen, X., Zhang, L.-M., Shen, J.-P., Wei, W.-X., and He, J.-Z.: Abundance and community structure of ammonia-oxidizing archaea and bacteria in an acid paddy soil, Biology and Fertility of Soils, 47, 323-331, 10.1007/s00374-011-0542-8, 2011.

Chen, X., Li, T., Lu, D., Cheng, L., Zhou, J., and Wang, H.: Estimation of soil available potassium in Chinese agricultural fields using a modified sodium tetraphenyl boron method, Land Degradation & Development, 31, 1737-1748, 10.1002/ldr.3535, 2020.

Chen, Y., Xu, Z., Hu, H., Hu, Y., Hao, Z., Jiang, Y., and Chen, B.: Responses of ammonia-oxidizing bacteria and archaea to nitrogen fertilization and precipitation increment in a typical temperate steppe in Inner Mongolia, Applied Soil Ecology, 68, 36-45, 10.1016/j.apsoil.2013.03.006, 2013.

Chen, Y. L., Hu, H. W., Han, H. Y., Du, Y., Wan, S. Q., Xu, Z. W., and Chen, B. D.: Abundance and community structure of ammonia-oxidizing Archaea and Bacteria in response to fertilization and mowing in a temperate steppe in Inner Mongolia, FEMS Microbiol Ecol, 89, 67-79, 10.1111/1574-6941.12336, 2014.

Chen, Z., Luo, X., Hu, R., Wu, M., Wu, J., and Wei, W.: Impact of long-term fertilization on the composition of denitrifier communities based on nitrite reductase analyses in a paddy soil, Microb Ecol, 60, 850-861, 10.1007/s00248-010-9700-z, 2010.

Chen, Z., Liu, J., Wu, M., Xie, X., Wu, J., and Wei, W.: Differentiated response of denitrifying communities to fertilization regime in paddy soil, Microb Ecol, 63, 446-459, 10.1007/s00248-011-9909-5, 2012.

Correa-Galeote, D., Tortosa, G., Moreno, S., Bru, D., Philippot, L., and Bedmar, E. J.: Spatiotemporal variations in the abundance and structure of denitrifier communities in sediments differing in nitrate content, Curr Issues Mol Biol, 24, 71-102, 10.21775/cimb.024.071, 2017.

Dai, X., Guo, Q., Song, D., Zhou, W., Liu, G., Liang, G., He, P., Sun, G., Yuan, F., and Liu, Z.: Long-term mineral fertilizer substitution by organic fertilizer and the effect on the abundance and community structure of ammonia-oxidizing archaea and bacteria in paddy soil of south China, European Journal of Soil Biology, 103, 10.1016/j.ejsobi.2021.103288, 2021.

Dai, Z., Yu, M., Chen, H., Zhao, H., Huang, Y., Su, W., Xia, F., Chang, S. X., Brookes, P. C., Dahlgren, R. A., and Xu, J.: Elevated temperature shifts soil N cycling from microbial immobilization to enhanced mineralization, nitrification and denitrification across global terrestrial ecosystems, Glob Chang Biol, 26, 5267-5276, 10.1111/gcb.15211, 2020.

Deng, J., Zhou, Z., Zheng, X., Liu, C., Yao, Z., Xie, B., Cui, F., Han, S., and Zhu, J.: Annual emissions of nitrous oxide and nitric oxide from rice-wheat rotation and vegetable fields: a case study in the Tai-Lake region, China, Plant and Soil, 360, 37-53, 10.1007/s11104-012-1223-6, 2012.

Di, H. J., Cameron, K. C., Podolyan, A., and Robinson, A.: Effect of soil moisture status and a nitrification inhibitor, dicyandiamide, on ammonia oxidizer and denitrifier growth and nitrous oxide emissions in a grassland soil, Soil Biology and Biochemistry, 73, 59-68, 10.1016/j.soilbio.2014.02.011, 2014.

Ding, W., Luo, J., Li, J., Yu, H., Fan, J., and Liu, D.: Effect of long-term compost and inorganic fertilizer application on background N_2O and fertilizer-induced N_2O emissions from an intensively cultivated soil, Sci Total Environ, 465, 115-124, 10.1016/j.scitotenv.2012.11.020, 2013.

Dong, Z., Zhu, B., Hua, K., and Jiang, Y.: Linkage of N_2O emissions to the abundance of soil ammonia oxidizers and denitrifiers in purple soil under long-term fertilization, Soil Science and Plant Nutrition, 61, 799-807, 10.1080/00380768.2015.1049930, 2015.

Duan, R., Long, X.-E., Tang, Y.-f., Wen, J., Su, S., Bai, L., Liu, R., and Zeng, X.: Effects of different fertilizer application methods on the community of nitrifiers and denitrifiers in a paddy soil, Journal of Soils and Sediments, 18, 24-38, 10.1007/s11368-017-1738-9, 2017.

Elshorbany, Y. F., Kurtenbach, R., Wiesen, P., Lissi, E., Rubio, M., Villena, G., Gramsch, E., Rickard, A. R., Pilling, M. J., and Kleffmann, J.: Oxidation capacity of the city air of Santiago, Chile, Atmos. Chem. Phys., , 9, 2257-2273, 2009.

Elshorbany, Y. F., Kleffmann, J., Kurtenbach, R., Lissi, E., Rubio, M., Villena, G., Gramsch, E., Rickard, A. R., Pilling, M. J., and Wiesen, P.: Seasonal dependence of the oxidation capacity of the city of Santiago de Chile, Atmospheric Environment, 44, 5383-5394, 2010.

Ermel, M., Behrendt, T., Oswald, R., Derstroff, B., Wu, D., Hohlmann, S., Stönner, C., Pommerening-Röser, A., Könneke, M., Williams, J., Meixner, F. X., Andreae, M. O., Trebs, I., and Sörgel, M.: Hydroxylamine released by nitrifying microorganisms is a precursor for HONO emission from drying soils, Scientific Reports, 8, 1877, 2018.

Fan, F., Yang, Q., Li, Z., Wei, D., Cui, X., and Liang, Y.: Impacts of organic and inorganic fertilizers on nitrification in a cold climate soil are linked to the bacterial ammonia oxidizer community, Microb Ecol, 62, 982-990, 10.1007/s00248-011-9897-5, 2011.

Fan, X., Yu, H., Wu, Q., Ma, J., Xu, H., Yang, J., and Zhuang, Y.: Effects of fertilization on microbial abundance and emissions of greenhouse gases (CH_4 and N_2O) in rice paddy fields, Ecol Evol, 6, 1054-1063, 10.1002/ece3.1879, 2016.

Fang, S., and Yujing, M.: NO_X fluxes from several typical agricultural fields during summer-autumn in the Yangtze Delta, China, Atmospheric Environment, 43, 2665-2671, 10.1016/j.atmosenv.2009.02.027, 2009.

Fang, Y., Wang, F., Jia, X., and Chen, J.: Distinct responses of ammonia-oxidizing bacteria and archaea to green manure combined with reduced chemical fertilizer in a paddy soil, Journal of Soils and Sediments, 19, 1613-1623, 10.1007/s11368-018-2154-5, 2018.

Fang, Y., Wang, F., Jia, X., Zhang, H., Lin, C., Chen, L., and Chen, J.: Differential response of denitrifying community to the application of green manure and reduced chemical fertilizer in a paddy soil, Chilean journal of agricultural research, 80, 393-404, 10.4067/s0718-58392020000300393, 2020.

FAO (Food and Agriculture Organization): World fertilizer trends and outlook to 2022, Available at http://www.fao.org/3/ca6746en/CA6746EN.pdf?eloutlink=imf2fao (accessed 28th Aug 2021), 2019.

FAOSTAT (Food and Agriculture Organization Corporate Statistical Database): FAO online database, Available at http://faostat3.fao.org/browse/G1/*/E (accessed 24th Jun 2020), 2019.

Finlayson-Pitts, B. J., and Pitts J., J. N.: Tropospheric air pollution: Ozone, airborne toxics, polycyclic aromatic hydrocarbons, and particles, Science, 276, 1045-1051, 1997.

Finlayson-Pitts, B. J., Wingen, L. M., Sumner, A. L., Syomin, D., and Ramazan, K. A.: The heterogeneous hydrolysis of NO_2 in laboratory systems and in outdoor and indoor atmospheres: An integrated mechanism, Phys. Chem. Chem. Phys., 5, 223-242, 2003.

Fu, X., Wang, T., Zhang, L., Li, Q., and Wang, Z.: The significant contribution of HONO to secondary pollutants during a severe winter pollution event in southern China, Atmospheric Chemistry Physics, 19, 1-14, 2019.

Gao, J., Xie, Y., Jin, H., Liu, Y., Bai, X., Ma, D., Zhu, Y., Wang, C., and Guo, T.: Nitrous oxide emission and denitrifier abundance in two agricultural soils amended with crop residues and urea in the north china plain, PLoS One, 11, e0154773, 2016a.

Gao, Y., Ma, X., and Cooper, D. J.: Short-term effect of nitrogen addition on nitric oxide emissions from an alpine meadow in the Tibetan Plateau, Environ Sci Pollut Res Int, 23, 12474-12479, 10.1007/s11356-016-6763-5, 2016b.

Geets, J., de Cooman, M., Wittebolle, L., Heylen, K., Vanparys, B., De Vos, P., Verstraete, W., and Boon, N.: Real-time PCR assay for the simultaneous quantification of nitrifying and denitrifying bacteria in activated sludge, Appl Microbiol Biotechnol, 75, 211-221, 10.1007/s00253-006-0805-8, 2007.

George, C., Strekowski, R. S., Kleffmann, J., Stemmler, K., and Ammann, M.: Photoenhanced uptake of gaseous NO_2 on solid organic compounds: a photochemical source of HONO?, Faraday Discussions, 130, 195, 2005.

Gheysari, M., Mirlatifi, S. M., Homaee, M., Asadi, M. E., and Hoogenboom, G.: Nitrate leaching in a silage maize field under different irrigation and nitrogen fertilizer rates, Agricultural Water Management, 96, 946, 2009.

Gu, C., Zhou, H., Zhang, Q., Zhao, Y., Di, H., and Liang, Y.: Effects of various fertilization regimes on abundance and activity of anaerobic ammonium oxidation bacteria in rice-wheat cropping systems in China, Sci Total Environ, 599-600, 1064-1072, 10.1016/j.scitotenv.2017.04.240, 2017.

Gu, J., Zheng, X., Wang, Y., Ding, W., Zhu, B., Chen, X., Wang, Y., Zhao, Z., Shi, Y., and Zhu, J.: Regulatory effects of soil properties on background N_2O emissions from agricultural soils in China, Plant and Soil, 295, 53-65, 10.1007/s11104-007-9260-2, 2007.

Gu, J., Zheng, X., and Zhang, W.: Background nitrous oxide emissions from croplands in China in the year 2000, Plant and Soil, 320, 307-320, 10.1007/s11104-009-9896-1, 2009.

Gu, R., Zheng, P., Chen, T., Dong, C., Wang, Y. n., Liu, Y., Liu, Y., Luo, Y., Han, G., Wang, X., Zhou, X., Wang, T., Wang, W., and Xue, L.: Atmospheric nitrous acid (HONO) at a rural coastal site in North China: Seasonal variations and effects of biomass burning, Atmospheric Environment, 229, 10.1016/j.atmosenv.2020.117429, 2020.

Gu, R., Shen, H., Xue, L., Wang, T., Gao, J., Li, H., Liang, Y., Xia, M., Yu, C., Liu, Y., and Wang, W.: Investigating the sources of atmospheric nitrous acid (HONO)

in the megacity of Beijing, China, Sci Total Environ, 812, 152270, 10.1016/j.scitotenv.2021.152270, 2021.

Gu, R., Wang, W., Peng, X., Xia, M., Zhao, M., Zhang, Y., Wang, Y., Liu, Y., Shen, H., Xue, L., Wang, T., and Wang, W.: Nitrous acid in the polluted coastal atmosphere of the South China Sea: Ship emissions, budgets, and impacts, Sci Total Environ, 826, 153692, 10.1016/j.scitotenv.2022.153692, 2022.

Gu, Y., Mi, W., Xie, Y., Ma, Q., Wu, L., Hu, Z., and Dai, F.: Nitrapyrin affects the abundance of ammonia oxidizers rather than community structure in a yellow clay paddy soil, Journal of Soils and Sediments, 19, 872-882, 10.1007/s11368-018-2075-3, 2018.

Guo, J., Ling, N., Chen, H., Zhu, C., Kong, Y., Wang, M., Shen, Q., and Guo, S.: Distinct drivers of activity, abundance, diversity and composition of ammonia-oxidizers: evidence from a long-term field experiment, Soil Biology and Biochemistry, 115, 403-414, 10.1016/j.soilbio.2017.09.007, 2017.

Harper, L. A., Denmead, O. T., and Flesch, T. K.: Micrometeorological techniques for measurement of enteric greenhouse gas emissions, Animal Feed Science and Technology, 166-167, 227-239, 10.1016/j.anifeedsci.2011.04.013, 2011.

Harrison, R. M., Peak, J. D., and Collins, G. M.: Tropospheric cycle of nitrous acid, JOURNAL OF GEOPHYSICAL RESEARCH, 101, 14429, 1996.

Heland, J., Kleffmann, J., Kurtenbach, R., and Wiesen, P.: A New Instrument To Measure Gaseous Nitrous Acid (HONO) in the Atmosphere, Environ Sci Technol, 35, 3207-3212, 2001.

Horst, T. W., and Weil, J. C.: How Far is Far Enough? The Fetch Requirements for Micrometeorological Measurement of Surface Fluxes, Journal of Atmospheric Oceanic Technology, 11, 1018-1025, 1994.

Hou, S., Tong, S., Ge, M., and An, J.: Comparison of atmospheric nitrous acid during severe haze and clean periods in Beijing, China, Atmospheric Environment, 124, 199-206, 10.1016/j.atmosenv.2015.06.023, 2016.

Hu, Q., Liu, T., Jiang, S., Cao, C., Li, C., Chen, B., and Liu, J.: Combined effects of straw returning and chemical N fertilization on greenhouse gas emissions and yield from paddy fields in northwest Hubei province, China, Journal of Soil Science and Plant Nutrition, 20, 392-406, 10.1007/s42729-019-00120-0, 2019.

Hu, X., Liu, J., Wei, D., Zhu, P., Cui, X. a., Zhou, B., Chen, X., Jin, J., Liu, X., and Wang, G.: Chronic effects of different fertilization regimes on nirS-type denitrifier communities across the black soil region of Northeast China, Pedosphere, 30, 73-86, 10.1016/s1002-0160(19)60840-4, 2020.

Huang, R. J., Yang, L., Cao, J., Wang, Q., Tie, X., Ho, K. F., Shen, Z., Zhang, R., Li, G., Zhu, C., Zhang, N., Dai, W., Zhou, J., Liu, S., Chen, Y., Chen, J., and O'Dowd,

C. D.: Concentration and sources of atmospheric nitrous acid (HONO) at an urban site in Western China, Sci Total Environ, 593-594, 165-172, 10.1016/j.scitotenv.2017.02.166, 2017.

Huang, Z., Wan, X., He, Z., Yu, Z., Wang, M., Hu, Z., and Yang, Y.: Soil microbial biomass, community composition and soil nitrogen cycling in relation to tree species in subtropical China, Soil Biology and Biochemistry, 62, 68-75, 10.1016/j.soilbio.2013.03.008, 2013.

IFA (International Fertilizer Association): World nitrogen fertilizer consumption, Available at http://www.fertilizer.org (accessed 9th Aug 2020), 2000-2017.

Jaegle, L., Steinberger, L., Martin, R. V., and Chance, K.: Global partitioning of NO_x sources using satellite observations: relative roles of fossil fuel combustion, biomass burning and soil emissions, Faraday Discuss, 130, 407-423; discussion 491-517, 519-424, 10.1039/b502128f, 2005.

Jin, Z. J., Li, L. Q., Liu, X. Y., Pan, G. X., Qaiser, H., and Liu, Y. Z.: Impact of long-term fertilization on community structure of ammonia oxidizing and denitrifying bacteria based on amoA and nirK Genes in a rice paddy from Tai Lake region, China, Journal of Integrative Agriculture, 13, 2286-2298, 10.1016/s2095-3119(14)60784-x, 2014.

Ju, X., and Zhang, C.: Nitrogen cycling and environmental impacts in upland agricultural soils in North China: A review, Journal of Integrative Agriculture, 16, 2848-2862, 10.1016/s2095-3119(17)61743-x, 2017.

Kalberer, M., Ammann, M., Arens, F., Gäggeler, H. W., and Baltensperger, U.: Heterogeneous formation of nitrous acid (HONO) on soot aerosol particles, JOURNAL OF GEOPHYSICAL RESEARCH, 1999.

Kautz, T., Wirth, S., and Ellmer, F.: Microbial activity in a sandy arable soil is governed by the fertilization regime, European Journal of Soil Biology, 40, 87-94, 10.1016/j.ejsobi.2004.10.001, 2004.

Kim, D.-G., Giltrap, D., and Hernandez-Ramirez, G.: Background nitrous oxide emissions in agricultural and natural lands: a meta-analysis, Plant and Soil, 373, 17-30, 10.1007/s11104-013-1762-5, 2013.

Kim, S., Vandenboer, T. C., Young, C. J., Riedel, T. P., Thornton, J. A., Swarthout, B., Sive, B., Lerner, B., Gilman, J., and Warneke, C.: The primary and recycling sources of OH during the NACHTT-2011 campaign: HONO as an important OH primary source in the wintertime, Journal of Geophysical Research, 119, 6886-6896, 2014.

Kirchstetter, T. W., Harley, R. A., and Littlejohn, D.: Measurement of nitrous acid in motor vehicle exhaust, Environmental science & technology, 30, 2843-2849, 1996.

Kirkman, G. A., Yang, W. X., and Meixner, F. X.: Biogenic nitric oxide emissions upscaling: An approach for Zimbabwe, Global Biogeochemical Cycles, 15, 1005-1020, 10.1029/2000gb001287, 2001.

Kleffmann, J., Becker, K. H., Lackhoff, M., and Wiesen, P.: Heterogeneous conversion of NO_2 on carbonaceous surfaces, Phys. Chem. Chem. Phys., 1, 5443-5450, 1999.

Kleffmann, J., Heland, J., Kurtenbach, R., Lrzer, J. C., and Wiesen, P.: A new instrument (LOPAP) for the detection of nitrous acid (HONO), Environmental Science & Pollution Research, 9, 48-54, 2002.

Kleffmann, J., Gavriloaiei, T., Hofzumahaus, A., Holland, F., and Wahner, A.: Daytime formation of nitrous acid: a major source of OH radicals in a forest, GEOPHYSICAL RESEARCH LETTERS, 32, 1-4, 2005.

Kleffmann, J.: Daytime sources of nitrous acid (HONO) in the atmospheric boundary layer, Chemphyschem, 8, 1137-1144, 10.1002/cphc.200700016, 2007.

Kurtenbach, R., Becker, K. H., Gomes, J. A. G., Kleffmann, J., Lörzer, J. C., Spittler, M., Wiesen, P., Ackermann, R., Geyer, A., and Platt, U.: Investigations of emissions and heterogeneous formation of HONO in a road traffic tunnel, Atmospheric Environment, 35, 3385-3394, 2001.

Lammel, G., and NeiláCape, J.: Nitrous acid and nitrite in the atmosphere, Chemical Society Reviews, 25, 361-369, 1996.

Laufs, S., Cazaunau, M., Stella, P., Kurtenbach, R., Cellier, P., Mellouki, A., Loubet, B., and Kleffmann, J.: Diurnal fluxes of HONO above a crop rotation, Atmospheric Chemistry and Physics, 17, 6907-6923, 10.5194/acp-17-6907-2017, 2017.

Levine, J. S., Winstead, E., Parsons, D. A. B., Scholes, M. C., Scholes, R. J., Cofer, W. R., Cahoon, D. R., and Sebacher, D. I.: Biogenic emissions of nitric oxide (NO) and nitrous oxide (N_2O) from savannas in South Africa: The impact of wetting and burning, J. Geophys. Res, 101, 6, 1996.

Levy-Booth, D. J., Prescott, C. E., and Grayston, S. J.: Microbial functional genes involved in nitrogen fixation, nitrification and denitrification in forest ecosystems, Soil Biology and Biochemistry, 75, 11-25, 10.1016/j.soilbio.2014.03.021, 2014.

Li, D., and Slomp, C. P.: Emissions of NO and NH3 from a Typical Vegetable-Land Soil after the Application of Chemical N Fertilizers in the Pearl River Delta, Plos One, 8, e59360, 2013.

Li, W. X., Wang, C., Zheng, M. M., Cai, Z. J., Wang, B. R., and Shen, R. F.: Fertilization strategies affect soil properties and abundance of N-cycling functional genes in an acidic agricultural soil, Applied Soil Ecology, 156, 10.1016/j.apsoil.2020.103704, 2020a.

Li, X., Brauers, T., Häseler, R., Bohn, B., Fuchs, H., Hofzumahaus, A., Holland, F., Lou, S., Lu, K. D., Rohrer, F., Hu, M., Zeng, L. M., Zhang, Y. H., Garland, R. M., Su, H., Nowak, A., Wiedensohler, A., Takegawa, N., Shao, M., and Wahner, A.: Exploring the atmospheric chemistry of nitrous acid (HONO) at a rural site in Southern China, Atmospheric Chemistry and Physics, 12, 1497-1513, 10.5194/acp-12-1497-2012, 2012.

Li, Z., Zeng, Z., Tian, D., Wang, J., Fu, Z., Zhang, F., Zhang, R., Chen, W., Luo, Y., and Niu, S.: Global patterns and controlling factors of soil nitrification rate, Glob Chang Biol, 26, 4147-4157, 10.1111/gcb.15119, 2020b.

Liu, C., Wang, K., Meng, S., Zheng, X., Zhou, Z., Han, S., Chen, D., and Yang, Z.: Effects of irrigation, fertilization and crop straw management on nitrous oxide and nitric oxide emissions from a wheat–maize rotation field in northern China, Agriculture, Ecosystems & Environment, 140, 226-233, 10.1016/j.agee.2010.12.009, 2011.

Liu, H., Li, J., Zhao, Y., Xie, K., Tang, X., Wang, S., Li, Z., Liao, Y., Xu, J., Di, H., and Li, Y.: Ammonia oxidizers and nitrite-oxidizing bacteria respond differently to long-term manure application in four paddy soils of south of China, Sci Total Environ, 633, 641-648, 10.1016/j.scitotenv.2018.03.108, 2018.

Liu, J., Liu, Z., Ma, Z., Yang, S., Yao, D., Zhao, S., Hu, B., Tang, G., Sun, J., Cheng, M., Xu, Z., and Wang, Y.: Detailed budget analysis of HONO in Beijing, China:

Implication on atmosphere oxidation capacity in polluted megacity, Atmospheric Environment, 244, 10.1016/j.atmosenv.2020.117957, 2021.

Liu, R., He, J., and Zhang, L.: Response of nitrification/denitrification and their associated microbes to soil moisture change in paddy soil (in Chinese), Environmental Science, 35, 4275-4283, 2014.

Liu, T., Wang, Z., Wang, S., Zhao, Y., Wright, A. L., and Jiang, X.: Responses of ammonia-oxidizers and comammox to different long-term fertilization regimes in a subtropical paddy soil, European Journal of Soil Biology, 93, 10.1016/j.ejsobi.2019.103087, 2019a.

Liu, Y., Lu, K., Li, X., Dong, H., Tan, Z., Wang, H., Zou, Q., Wu, Y., Zeng, L., Hu, M., Min, K. E., Kecorius, S., Wiedensohler, A., and Zhang, Y.: A comprehensive model test of the HONO sources constrained to field measurements at rural North China Plain, Environmental Science & Technology, 53, 3517-3525, 10.1021/acs.est.8b06367, 2019b.

Long, G., Li, L., Wang, D., Zhao, P., Tang, L., Zhou, Y., and Yin, X.: Nitrogen levels regulate intercropping-related mitigation of potential nitrate leaching, Agriculture, Ecosystems & Environment, 319, 10.1016/j.agee.2021.107540, 2021.

Lu, C., and Tian, H.: Global nitrogen and phosphorus fertilizer use for agriculture production in the past half century: Shifted hot spots and nutrient imbalance, Earth System Science Data, 9, 181-192, 2017.

Lu, K., Guo, S., Tan, Z., Wang, H., Shang, D., Liu, Y., Li, X., Wu, Z., Hu, M., and Zhang, Y.: Exploring atmospheric free-radical chemistry in China: the self-cleansing capacity and the formation of secondary air pollution, Natl Sci Rev, 6, 579-594, 10.1093/nsr/nwy073, 2019a.

Lu, X., Zhang, L., Chen, Y., Zhou, M., Zheng, B., Li, K., Liu, Y., Lin, J., Fu, T.-M., and Zhang, Q.: Exploring 2016–2017 surface ozone pollution over China: source contributions and meteorological influences, Atmospheric Chemistry and Physics, 19, 8339-8361, 10.5194/acp-19-8339-2019, 2019b.

Ludwig, J., Meixner, F. X., Vogel, B., and Forstner, J.: Soil-air exchange of nitric oxide: An overview of processes, environmental factors, and modeling studies, Biogeochemistry, 52, 33, 2001.

Luo, Y., Hui, D., and Zhang, D.: Elevated CO_2 stimulates net accumulations of carbon and nitrogen in land ecosystems: A meta-analysis, Ecology, 87, 53-63, 2006.

Ma, F., Gao, H., Eneji, A. E., Jin, Z., Han, L., and Liu, J.: An economic valuation of groundwater management for agriculture in Luancheng county, North China, Agricultural Water Management, 163, 28-36, 10.1016/j.agwat.2015.08.027, 2016.

Maljanen, M., Yli-Pirilä, P., Hytönen, J., Joutsensaari, J., and Martikainen, P. J.: Acidic northern soils as sources of atmospheric nitrous acid (HONO), Soil Biology and Biochemistry, 67, 94-97, 10.1016/j.soilbio.2013.08.013, 2013.

Mamtimin, B., Meixner, F. X., Behrendt, T., Badawy, M., and Wagner, T.: The contribution of soil biogenic NO and HONO emissions from a managed hyperarid ecosystem to the regional NO_x emissions during growing season, Atmospheric Chemistry and Physics, 16, 10175-10194, 10.5194/acp-16-10175-2016, 2016.

Martens-Habbena, W., Berube, P. M., Urakawa, H., de la Torre, J. R., and Stahl, D. A.: Ammonia oxidation kinetics determine niche separation of nitrifying Archaea and Bacteria, Nature, 461, 976-979, 10.1038/nature08465, 2009.

Mei, B., Zheng, X., Xie, B., Dong, H., Zhou, Z., Wang, R., Deng, J., Cui, F., Tong, H., and Zhu, J.: Nitric oxide emissions from conventional vegetable fields in southeastern China, Atmospheric Environment, 43, 2762-2769, 10.1016/j.atmosenv.2009.02.040, 2009.

Meixner, F. X.: Surface exchange of odd nitrogen oxides, Nova Acta Leopoldina, 49, 1994.

Meixner, F. X., and Yang, W. X.: Biogenic emissions of nitric oxide and nitrous oxide from arid and semi-arid land. In: Dryland Ecohydrology, Springer, Dordrecht, 66, 23, 2006.

Meusel, H., Tamm, A., Kuhn, U., Wu, D., Leifke, A. L., Fiedler, S., Ruckteschler, N., Yordanova, P., Lang-Yona, N., Pöhlker, M., Lelieveld, J., Hoffmann, T., Pöschl, U., Su, H., Weber, B., and Cheng, Y.: Emission of nitrous acid from soil and biological soil crusts represents an important source of HONO in the remote atmosphere in Cyprus, Atmospheric Chemistry and Physics, 18, 799-813, 10.5194/acp-18-799-2018, 2018.

Michoud, V., Colomb, A., Borbon, A., Miet, K., Beekmann, M., Camredon, M., Aumont, B., Perrier, S., Zapf, P., Siour, G., Ait-Helal, W., Afif, C., Kukui, A., Furger, M., Dupont, J. C., Haeffelin, M., and Doussin, J. F.: Study of the unknown HONO daytime source at a European suburban site during the MEGAPOLI summer and winter field campaigns, Atmospheric Chemistry and Physics, 14, 2805-2822, 10.5194/acp-14-2805-2014, 2014.

Ministry of Agriculture and Rural Affairs of the People's Republic of China: Notice of the Ministry of Agriculture General Office on Issuing the Guiding Opinions on Scientific Fertilization of Major Crops in 2010 (in Chinese). available at http://www.moa.gov.cn/ztzl/ctpfsf/gzdt/201003/t20100326_1455875.htm, 2010.

Monge, M. E., D'Anna, B., Mazri, L., Giroir-Fendler, A., Ammann, M., Donaldson, D. J., and George, C.: Light changes the atmospheric reactivity of soot, Proceedings of the National Academy of Sciences of the United States of America, 107, 6605 – 6609, 2010.

Mueller, N. D., Lassaletta, L., Runck, B. C., Billen, G., Garnier, J., and Gerber, J. S.: Declining spatial efficiency of global cropland nitrogen allocation, Global Biogeochemical Cycles, 31, 245-257, 2017.

Muller, J. B. A., Percival, C. J., Gallagher, M. W., Fowler, D., Coyle, M., and Nemitz, E.: Sources of uncertainty in eddy covariance ozone flux measurements made by dry chemiluminescence fast response analysers, Atmos Meas Tech, 14, 2010.

Mulvaney, R. L., Khan, S. A., and Mulvaney, C. S.: Nitrogen fertilizers promote denitrification, Biology and Fertility of Soils, 24, 211-220, 1997.

Mulvaney, R. L., Khan, S. A., and Ellsworth, T. R.: Synthetic nitrogen fertilizers deplete soil nitrogen: a global dilemma for sustainable cereal production, Journal of Environmental Quality, 38, 2295-2314, 10.2134/jeq2008.0527, 2009.

Mushinski, R. M., Phillips, R. P., Payne, Z. C., Abney, R. B., Jo, I., Fei, S., Pusede, S. E., White, J. R., Rusch, D. B., and Raff, J. D.: Microbial mechanisms and ecosystem flux estimation for aerobic NOy emissions from deciduous forest soils, Proceedings of the National Academy of Sciences of the United States of America, 116, 2138-2145, 10.1073/pnas.1814632116, 2019.

Myers, R. J. K.: Temperature effects on ammonification and nitrification in a tropical soil, Soil Biology and Biochemistry, 7, 83-86, 1975.

NARC (National Agriculture Regionalization Committee): China integrated agricultural regionalization, Beijing: China Agriculture Press, 10.11821/dlxb201802001, 1981.

National Bureau of Statistics: China Statistical Yearbooks, Statistical Press: Beijing, 2019.

Nguyen, M. T., Sumathi, R., Sengupta, D., and Peeters, J.: Theoretical analysis of reactions related to the HNO_2 energy surface: OH + NO and H + NO_2, Chemical Physics Letters, 230, 1-11, 1998.

Nie, W., Ding, A. J., Xie, Y. N., Xu, Z., Mao, H., Kerminen, V. M., Zheng, L. F., Qi, X. M., Huang, X., Yang, X. Q., Sun, J. N., Herrmann, E., Petäjä, T., Kulmala, M., and Fu, C. B.: Influence of biomass burning plumes on HONO chemistry in eastern China, Atmospheric Chemistry and Physics, 15, 1147-1159, 10.5194/acp-15-1147-2015, 2015.

Notholt, J., Hjorth, J., and Raes, F.: Formation of HNO_2 on aerosol surfaces during foggy periods in the presence of NO and NO_2, Atmospheric Environment. Part A. General Topics, 26, 211-217, 1992.

O'Connel, A. M.: Microbial decomposition (respiration) of litter in eucalypt forests of south-western Australia: an empirical model based on laboratory incubations, Soil Biology and Biochemistry, 8, 1990.

Oswald, R., Behrendt, T., Ermel, M., Wu, D., Su, H., Cheng, Y., Breuninger, C., Moravek, A., Mougin, E., and Delon, C.: HONO emissions from soil bacteria as a major source of atmospheric reactive nitrogen, Science, 341, 3, 2013.

Ouyang, Y., Evans, S. E., Friesen, M. L., and Tiemann, L. K.: Effect of nitrogen fertilization on the abundance of nitrogen cycling genes in agricultural soils: A meta-analysis of field studies, Soil Biology and Biochemistry, 127, 71-78, 10.1016/j.soilbio.2018.08.024, 2018.

Pagsberg, P., Bjergbakke, E., Ratajczak, E., and Sillesen, A.: Kinetics of the gas phase reaction OH + NO(+M)→HONO(+M) and the determination of the UV absorption cross sections of HONO, Chemical Physics Letters 272, 383-390, 1997.

Pan, H. X., Zhu, G. F., ZHang, Y., Guo, H. W., Yong, L. L., Wan, Q. Z., Ma, H. Y., and Li, S.: Spatial and temporal variations of relative soil moisture in China's farmland (in Chinese), Acta Geographica Sinica, 74, 13, 10.11821/dlxb201901009, 2019.

Pang, X., Mu, Y., Lee, X., Fang, S., Yuan, J., and Huang, D.: Nitric oxides and nitrous oxide fluxes from typical vegetables cropland in China: Effects of canopy, soil properties and field management, Atmospheric Environment, 43, 2571-2578, 10.1016/j.atmosenv.2009.02.016, 2009.

Passianoto, C. C., Ahrens, T., Feigl, B. J., Streudler, P. A., Melillo, J. M., and Carmo, J. B.: Diurnal changes in nitric oxide emissions from conventional tillage and pasture sites in the Amazon Basin: influence of soil temperature, Plant Soil, 9, 2004.

Perner, D., and Platt, U.: Detection of nitrous acid in the atmosphere by differential optical absorption, Geophysical Research Letters, 6, 917-920, 1979.

Philippot, L.: Denitrifying genes in bacterial and Archaeal genomes, Biochimica et Biophysica Acta, 1577, 355– 376, 2002.

Plake, D., Stella, P., Moravek, A., Mayer, J. C., Ammann, C., and Held, A.: Comparison of ozone deposition measured with the dynamic chamber and the eddy covariance method, Agric Meteorol, 206, 15, 2015.

Platt, U., Perner, D., Harris, G. W., Winer, A. M., and Pitts, J. N.: Observations of nitrous acid in an urban atmosphere by differential optical absorption, Nature, 285, 312-314, 1980.

Qiao, J. Q., and Bakken, L. R.: Comparison of Nitrosospira strains isolated from terrestrial environments, FEMS Microbiology Ecology, 30, 16, 1999.

Qiu, B., Hu, X., Chen, C., Tang, Z., Yang, P., Zhu, X., Yan, C., and Jian, Z.: Maps of cropping patterns in China during 2015-2021, Sci Data, 9, 479, 10.1038/s41597-022-01589-8, 2022.

Qu, Y., Chen, Y., Liu, X., Zhang, J., Guo, Y., and An, J.: Seasonal effects of additional HONO sources and the heterogeneous reactions of N_2O_5 on nitrate in the North China Plain, Sci Total Environ, 690, 97-107, 10.1016/j.scitotenv.2019.06.436, 2019.

Ramankutty, N., Evan, A. T., Monfreda, C., and Foley, J. A.: Farming the planet: 1. Geographic distribution of global agricultural lands in the year 2000, Global Biogeochemical Cycles, 22, GB1003, 10.1029/2007gb002952, 2008.

Rappengluck, B., Lubertino, G., Alvarez, S., Golovko, J., Czader, B., and Ackermann, L.: Radical precursors and related species from traffic as observed and modeled at an urban highway junction, J Air Waste Manag Assoc, 63, 1270-1286, 10.1080/10962247.2013.822438, 2013.

Reisinger, A. R.: Observations of HNO_2 in the polluted winter atmosphere: possible heterogeneous production on aerosols, Atmospheric Environment, 34, 3865-3874, 2000.

Remde, A., Ludwig, J., Meixner, F. X., and Conrad, R.: A study to explain the emission of nitric oxide from a marsh soil, Journal of Atmospheric Chemistry, 17, 249-275, 1993.

Rodriguez, M. J., Saggar, S., Berben, P., Palmada, T., Lopez-Villalobos, N., and Pal, P.: Use of a urease inhibitor to mitigate ammonia emissions from urine patches, Environmental Technology, 1-12, 10.1080/09593330.2019.1620345, 2019.

Romer, P. S., Duffey, K. C., Wooldridge, P. J., Edgerton, E., Baumann, K., Feiner, P. A., Miller, D. O., Brune, W. H., Koss, A. R., de Gouw, J. A., Misztal, P. K., Goldstein, A. H., and Cohen, R. C.: Effects of temperature-dependent NO_x emissions on continental ozone production, Atmospheric Chemistry and Physics, 18, 2601-2614, 10.5194/acp-18-2601-2018, 2018.

Saad, O. A. L. O., and Conrad, R.: Temperature dependence of nitrification, denitrification, and turnover of nitric oxide in different soils, Biology & Fertility of Soils, 15, 7, 1993.

Sakamaki, F., Hatakeyama, S., and Akimoto, H.: Formation of nitrous acid and nitric oxide in the heterogeneous dark reaction of nitrogen dioxide and water vapor in a smog chamber, International Journal of Chemical Kinetics, 15, 1013-1029, 1983.

Scharko, N. K., Schuette, U. M. E., Berke, A. E., Banina, L., Peel, H. R., Donaldson, M. A., Hemmerich, C., White, J. R., and Raff, J. D.: Combined flux chamber and genomics approach links nitrous acid emissions to ammonia oxidizing bacteria and archaea in urban and agricultural soil, Environmental Science Technology, 49, 13825-13834, 2015.

Sepaskhah, A. R., and Tafteh, A.: Yield and nitrogen leaching in rapeseed field under different nitrogen rates and water saving irrigation, Agricultural Water Management, 112, 55-62, 2012.

Sha, T., Ma, X., Zhang, H., Janechek, N., Wang, Y., Wang, Y., Castro Garcia, L., Jenerette, G. D., and Wang, J.: Impacts of soil NO_x emission on O_3 air quality in rural California, Environ Sci Technol, 55, 7113-7122, 10.1021/acs.est.0c06834, 2021.

Shen, L. D., Liu, S., Lou, L. P., Liu, W. P., Xu, X. Y., Zheng, P., and Hu, B. L.: Broad distribution of diverse anaerobic ammonium-oxidizing bacteria in chinese agricultural soils, Appl Environ Microbiol, 79, 6167-6172, 10.1128/AEM.00884-13, 2013.

Shen, X.-Y., Zhang, L.-M., Shen, J.-P., Li, L.-H., Yuan, C.-L., and He, J.-Z.: Nitrogen loading levels affect abundance and composition of soil ammonia oxidizing prokaryotes in semiarid temperate grassland, Journal of Soils and Sediments, 11, 1243-1252, 10.1007/s11368-011-0375-y, 2011.

Smith, K. A., Clayton, H., Arab, J. R. M., Christensen, S., Ambus, P., Fowler, D., Hargreaves, K. J., Skiba, U., Harris, G. W., Wienhold, F. G., Klemedtsson, L., and Galle, B.: Micrometeorological and chamber methods for measurement of nitrous oxide fluxes between soils and the atmosphere: Overview and conclusions, Journal of Geophysical Research, 99, 10.1029/94jd00619, 1994.

Song, A., Fan, F., Yin, C., Wen, S., Zhang, Y., Fan, X., and Liang, Y.: The effects of silicon fertilizer on denitrification potential and associated genes abundance in paddy soil, Biology and Fertility of Soils, 53, 627-638, 10.1007/s00374-017-1206-0, 2017.

Sörgel, M., Trebs, I., Wu, D., and Held, A.: A comparison of measured HONO uptake and release with calculated source strengths in a heterogeneous forest environment, Atmospheric Chemistry and Physics, 15, 9237-9251, 10.5194/acp-15-9237-2015, 2015.

Spataro, F., and Ianniello, A.: Sources of atmospheric nitrous acid: state of the science, current research needs, and future prospects, J Air Waste Manag Assoc, 64, 1232-1250, 10.1080/10962247.2014.952846, 2014.

Stemmler, K., Ammann, M., Donders, C., Kleffmann, J., and George, C.: Photosensitized reduction of nitrogen dioxide on humic acid as a source of nitrous acid, Nature letters, 440, 195-198, 2006.

Stockwell, W. R., and Calvert, J. G.: The near ultraviolet absorption spectrum of gaseous HONO and N2O3, Journal of Photochemistry, 8, 193-203, 1978.

Stone, D., Whalley, L. K., and Heard, D. E.: Tropospheric OH and HO_2 radicals: field measurements and model comparisons, Chem Soc Rev, 41, 6348-6404, 10.1039/c2cs35140d, 2012.

Stutz, J., Kim, E. S., Platt, U., Bruno, P., Perrino, C., and Febo, A.: UV-visible absorption cross sections of nitrous acid, Journal of Geophysical Research: Atmospheres, 105, 14585-14592, 10.1029/2000jd900003, 2000.

Su, H., Cheng, Y., Oswald, R., Behrendt, T., Trebs, I., Meixner, F. X., Andreae, M., Cheng, P., and Zhang, Y.: Soil nitrite as a source of atmospheric HONO and OH radicals, Science, 333, p.1616-1618, 2011.

Su, J. Q., Ding, L. J., Xue, K., Yao, H. Y., Quensen, J., Bai, S. J., Wei, W. X., Wu, J. S., Zhou, J., Tiedje, J. M., and Zhu, Y. G.: Long-term balanced fertilization increases the soil microbial functional diversity in a phosphorus-limited paddy soil, Mol Ecol, 24, 136-150, 10.1111/mec.13010, 2015.

Sun, R., Guo, X., Wang, D., and Chu, H.: Effects of long-term application of chemical and organic fertilizers on the abundance of microbial communities involved in the nitrogen cycle, Applied Soil Ecology, 95, 171-178, 10.1016/j.apsoil.2015.06.010, 2015.

Sun, R., Wang, F., Hu, C., and Liu, B.: Metagenomics reveals taxon-specific responses of the nitrogen-cycling microbial community to long-term nitrogen fertilization, Soil Biology and Biochemistry, 156, 10.1016/j.soilbio.2021.108214, 2021.

Tafteh, A., and Sepaskhah, A. R.: Application of HYDRUS-1D model for simulating water and nitrate leaching from continuous and alternate furrow irrigated rapeseed and maize fields, Agricultural Water Management, 113, 19-29, 2012.

Tang, H., Xiao, X., Li, C., Tang, W., Cheng, K., Wang, K., Pan, X., and Li, W.: Effects of rhizosphere and long-term fertilization practices on the activity and community structure of denitrifiers under double-cropping rice field, Communications in Soil Science and Plant Analysis, 50, 682-697, 10.1080/00103624.2019.1589480, 2019a.

Tang, K., Qin, M., Duan, J., Fang, W., Meng, F., Liang, S., Xie, P., Liu, J., Liu, W., Xue, C., and Mu, Y.: A dual dynamic chamber system based on IBBCEAS for measuring fluxes of nitrous acid in agricultural fields in the North China Plain, Atmospheric Environment, 196, 10-19, 10.1016/j.atmosenv.2018.09.059, 2019b.

Tang, Y., Zhang, X., Li, D., Wang, H., Chen, F., Fu, X., Fang, X., Sun, X., and Yu, G.: Impacts of nitrogen and phosphorus additions on the abundance and community structure of ammonia oxidizers and denitrifying bacteria in Chinese fir plantations, Soil Biology and Biochemistry, 103, 284-293, 10.1016/j.soilbio.2016.09.001, 2016.

Tao, R., Wakelin, S. A., Liang, Y., and Chu, G.: Response of ammonia-oxidizing archaea and bacteria in calcareous soil to mineral and organic fertilizer application and

their relative contribution to nitrification, Soil Biology and Biochemistry, 114, 20-30, 10.1016/j.soilbio.2017.06.027, 2017.

Tao, R., Wakelin, S. A., Liang, Y., Hu, B., and Chu, G.: Nitrous oxide emission and denitrifier communities in drip-irrigated calcareous soil as affected by chemical and organic fertilizers, Sci Total Environ, 612, 739-749, 10.1016/j.scitotenv.2017.08.258, 2018.

Thierron, V., and Laudelout, H.: Contribution of root respiration to total CO_2 eflux from the soil of a deciduous forest, Canadian Journal of Forest Research, 7, 1996.

Tian, D., Zhang, Y., Mu, Y., Liu, J., and He, K.: Effect of N fertilizer types on N_2O and NO emissions under drip fertigation from an agricultural field in the North China Plain, Sci Total Environ, 715, 136903, 10.1016/j.scitotenv.2020.136903, 2020.

Tian, H., Lu, C., Melillo, J., Ren, W., Huang, Y., Xu, X., Liu, M., Zhang, C., Chen, G., Pan, S., Liu, J., and Reilly, J.: Food benefit and climate warming potential of nitrogen fertilizer uses in China, Environmental Research Letters, 7, 044020, 10.1088/1748-9326/7/4/044020, 2012.

Tian, W., Wang, L., Li, Y., Zhuang, K., Li, G., Zhang, J., Xiao, X., and Xi, Y.: Responses of microbial activity, abundance, and community in wheat soil after three years of heavy fertilization with manure-based compost and inorganic nitrogen,

Agriculture, Ecosystems & Environment, 213, 219-227, 10.1016/j.agee.2015.08.009, 2015.

Trinh, H. T., Imanishi, K., Morikawa, T., Hagino, H., and Takenaka, N.: Gaseous nitrous acid (HONO) and nitrogen oxides (NO_x) emission from gasoline and diesel vehicles under real-world driving test cycles, Journal of the Air & Waste Management Association, 67, 412-420, 2017.

van Dijk, S. M., Gut, A., Kirkman, G. A., Meixner, F. X., and Andreae, M. O.: Biogenic NO emissions from forest and pasture soils: Relating laboratory studies to field measurements, Journal of Geophysical Research, 107, 2002.

VandenBoer, T. C., Young, C. J., Talukdar, R. K., Markovic, M. Z., Brown, S. S., Roberts, J. M., and Murphy, J. G.: Nocturnal loss and daytime source of nitrous acid through reactive uptake and displacement, Nature Geoscience, 8, 55-60, 10.1038/ngeo2298, 2014.

Venterea, R. T.: Nitrite-driven nitrous oxide production under aerobic soil conditions: kinetics and biochemical controls, Global Change Biology, 13, 1798-1809, 10.1111/j.1365-2486.2007.01389.x, 2007.

Villena, G., Kleffmann, J., Kurtenbach, R., Wiesen, P., Lissi, E., Rubio, M. A., Croxatto, G., and Rappengliick, B.: Vertical gradients of HONO, NO_x and O_3 in Santiago de Chile, Atmospheric Environment, 45, 3867-3873, 2011.

von der Heyden, L., Wißdorf, W., Kurtenbach, R., and Kleffmann, J.: A relaxed eddy accumulation (REA) LOPAP system for flux measurements of nitrous acid (HONO), Atmospheric Measurement Techniques, 15, 1983-2000, 10.5194/amt-15-1983-2022, 2022.

Wallace, B. C., Lajeunesse, M. J., Dietz, G., Dahabreh, I. J., Trikalinos, T. A., Schmid, C. H., Gurevitch, J., and Poisot, T.: OpenMEE: Intuitive, open-source software for meta-analysis in ecology and evolutionary biology, Methods in Ecology and Evolution, 8, 941-947, 10.1111/2041-210x.12708, 2017.

Wang, F., Chen, S., Wang, Y., Zhang, Y., Hu, C., and Liu, B.: Long-Term nitrogen fertilization elevates the activity and abundance of nitrifying and denitrifying microbial communities in an upland soil: implications for nitrogen loss from intensive agricultural systems, Front Microbiol, 9, 2424, 10.3389/fmicb.2018.02424, 2018.

Wang, J., Wang, E., Yang, X., Zhang, F., and Yin, H.: Increased yield potential of wheat-maize cropping system in the North China Plain by climate change adaptation, Climatic Change, 113, 825-840, 10.1007/s10584-011-0385-1, 2012.

Wang, J., Zhang, L., Lu, Q., Raza, W., Huang, Q., and Shen, Q.: Ammonia oxidizer abundance in paddy soil profile with different fertilizer regimes, Applied Soil Ecology, 84, 38-44, 10.1016/j.apsoil.2014.06.009, 2014.

Wang, J., Wang, J., Rhodes, G., He, J. Z., and Ge, Y.: Adaptive responses of comammox Nitrospira and canonical ammonia oxidizers to long-term fertilizations: Implications for the relative contributions of different ammonia oxidizers to soil nitrogen cycling, Sci Total Environ, 668, 224-233, 10.1016/j.scitotenv.2019.02.427, 2019a.

Wang, S., Zhang, X., Wang, C., Zhang, X., Reis, S., Xu, J., and Gu, B.: A high-resolution map of reactive nitrogen inputs to China, Sci Data, 7, 379, 10.1038/s41597-020-00718-5, 2020a.

Wang, T., Xue, L., Feng, Z., Dai, J., Zhang, Y., and Tan, Y.: Ground-level ozone pollution in China: a synthesis of recent findings on influencing factors and impacts, Environmental Research Letters, 17, 063003, 10.1088/1748-9326/ac69fe, 2022.

Wang, Y., Ji, H., Wang, R., and Guo, S.: Responses of nitrification and denitrification to nitrogen and phosphorus fertilization: does the intrinsic soil fertility matter?, Plant and Soil, 440, 443-456, 10.1007/s11104-019-04108-8, 2019b.

Wang, Y., Ji, H., Wang, R., Hu, Y., and Guo, S.: Synthetic fertilizer increases denitrifier abundance and depletes subsoil total N in a long-term fertilization experiment, Front Microbiol, 11, 2026, 10.3389/fmicb.2020.02026, 2020b.

Wang, Y., Fu, X., Wu, D., Wang, M., Lu, K., Mu, Y., Liu, Z., Zhang, Y., and Wang, T.: Agricultural fertilization aggravates air pollution by stimulating soil nitrous

acid emissions at high soil moisture, Environ Sci Technol, 55, 14556-14566, 10.1021/acs.est.1c04134, 2021.

Wen, X., Hu, C., Sun, X., Zhao, X., Tan, Q., Liu, P., Xin, J., Qin, S., and Wang, P.: Characterization of vegetable nitrogen uptake and soil nitrogen transformation in response to continuous molybdenum application, Journal of Plant Nutrition and Soil Science, 181, 516-527, 10.1002/jpln.201700556, 2018.

Wertz, S., Poly, F., Le Roux, X., and Degrange, V.: Development and application of a PCR-denaturing gradient gel electrophoresis tool to study the diversity of Nitrobacter-like nxrA sequences in soil, FEMS Microbiol Ecol, 63, 261-271, 10.1111/j.1574-6941.2007.00416.x, 2008.

Winer, A. M., and Biermann, H. W.: Long pathlength differential optical absorption spectroscopy (DOAS) measurements of gaseous HONO, NO_2 and HCNO in the California South Coast Air Basin, 20, 423-445, 1994.

Winkler, J. P., Cherry, R. S., and Schlesinger, W. H.: The Q10 relationship of microbial respiration in a temperate forest soil, Soil Biology and Biochemistry, 6, 1996.

Wong, S. C., Li, X. D., Zhang, G., Qi, S. H., and Min, Y. S.: Heavy metals in agricultural soils of the Pearl River Delta, South China Environmental Pollution, 119, 33-44, 2001.

Woodward, E. E., Edwards, T. M., Givens, C. E., Kolpin, D. W., and Hladik, M. L.: Widespread Use of the Nitrification Inhibitor Nitrapyrin: Assessing Benefits and Costs to Agriculture, Ecosystems, and Environmental Health, Environ Sci Technol, 55, 1345-1353, 10.1021/acs.est.0c05732, 2021.

Wrage, N., Velthof, M. L., Beusichem, v., and Oenema, O.: Role of nitrifier denitrification in the production of nitrous oxide, Soil Biology and Biochemistry, 33, 1723-1732, 2001.

Wu, D., Horn, M. A., Behrendt, T., Muller, S., Li, J., Cole, J. A., Xie, B., Ju, X., Li, G., Ermel, M., Oswald, R., Frohlich-Nowoisky, J., Hoor, P., Hu, C., Liu, M., Andreae, M. O., Poschl, U., Cheng, Y., Su, H., Trebs, I., Weber, B., and Sorgel, M.: Soil HONO emissions at high moisture content are driven by microbial nitrate reduction to nitrite: tackling the HONO puzzle, The ISME Journal, 13, 1688-1699, 10.1038/s41396-019-0379-y, 2019.

Wu, D., Zhang, J., Wang, M., An, J., Wang, R., Haider, H., Xu-Ri, Huang, Y., Zhang, Q., Zhou, F., Tian, H., Zhang, X., Deng, L., Pan, Y., Chen, X., Yu, Y., Hu, C., Wang, R., Song, Y., Gao, Z., Wang, Y., Hou, L., and Liu, M.: Global and regional patterns of soil nitrous acid emissions and their acceleration of rural photochemical reactions, Journal of Geophysical Research: Atmospheres, 127, e2021JD036379, 10.1029/2021jd036379, 2022.

Xia, Y., Chen, X., Zheng, S., Gunina, A., Ning, Z., Hu, Y., Tang, H., Rui, Y., Zhang, Z., He, H., Huang, D., and Su, Y.: Manure application accumulates more nitrogen in paddy soils than rice straw but less from fungal necromass, Agriculture, Ecosystems & Environment, 319, 10.1016/j.agee.2021.107575, 2021.

Xing, J., Lu, X., Wang, S., Wang, T., Ding, D., Yu, S., Shindell, D., Ou, Y., Morawska, L., Li, S., Ren, L., Zhang, Y., Loughlin, D., Zheng, H., Zhao, B., Liu, S., Smith, K. R., and Hao, J.: The quest for improved air quality may push China to continue its CO_2 reduction beyond the Paris Commitment, Proceedings of the National Academy of Sciences of the United States of America, 117, 29535-29542, 10.1073/pnas.2013297117, 2020.

Xu, Z., Wang, T., Wu, J., Xue, L., Chan, J., Zha, Q., Zhou, S., Louie, P. K. K., and Luk, C. W. Y.: Nitrous acid (HONO) in a polluted subtropical atmosphere: Seasonal variability, direct vehicle emissions and heterogeneous production at ground surface, Atmospheric Environment, 106, 100-109, 10.1016/j.atmosenv.2015.01.061, 2015.

Xue, C., Zhang, X., Zhu, C., Zhao, J., Zhu, P., Peng, C., Ling, N., and Shen, Q.: Quantitative and compositional responses of ammonia-oxidizing archaea and bacteria to long-term field fertilization, Sci Rep, 6, 28981, 10.1038/srep28981, 2016.

Xue, C., Ye, C., Zhang, Y., Ma, Z., Liu, P., Zhang, C., Zhao, X., Liu, J., and Mu, Y.: Development and application of a twin open-top chambers method to measure soil

HONO emission in the North China Plain, Science of the Total Environment, 659, 621-631, 10.1016/j.scitotenv.2018.12.245, 2019.

Xue, C., Zhang, C., Ye, C., Liu, P., Catoire, V., Krysztofiak, G., Chen, H., Ren, Y., Zhao, X., Wang, J., Zhang, F., Zhang, C., Zhang, J., An, J., Wang, T., Chen, J., Kleffmann, J., Mellouki, A., and Mu, Y.: HONO Budget and Its Role in Nitrate Formation in the Rural North China Plain, Environ Sci Technol, 54, 11048-11057, 10.1021/acs.est.0c01832, 2020.

Xue, C., Ye, C., Zhang, C., Catoire, V., Liu, P., Gu, R., Zhang, J., Ma, Z., Zhao, X., Zhang, W., Ren, Y., Krysztofiak, G., Tong, S., Xue, L., An, J., Ge, M., Mellouki, A., and Mu, Y.: Evidence for strong HONO emission from fertilized agricultural fields and its remarkable impact on regional O_3 pollution in the summer North China Plain, ACS Earth and Space Chemistry, 5, 340-347, 10.1021/acsearthspacechem.0c00314, 2021.

Yan, G., Zheng, X., Cui, F., Yao, Z., Zhou, Z., Deng, J., and Xu, Y.: Two-year simultaneous records of N_2O and NO fluxes from a farmed cropland in the northern China plain with a reduced nitrogen addition rate by one-third, Agriculture, Ecosystems & Environment, 178, 39-50, 10.1016/j.agee.2013.06.016, 2013.

Yan, G., Yao, Z., Zheng, X., and Liu, C.: Characteristics of annual nitrous and nitric oxide emissions from major cereal crops in the North China Plain under

alternative fertilizer management, Agriculture, Ecosystems & Environment, 207, 67-78, 10.1016/j.agee.2015.03.030, 2015.

Yan, X., Akimoto, H., and Ohara, T.: Estimation of nitrous oxide, nitric oxide and ammonia emissons from croplands in East, Southeast and South Asia, Glob Chang Biol, 9, 1080-1096, 2003a.

Yan, X. Y., Akimoto, H., and Ohara, T.: Estimation of nitrous oxide, nitric oxide and ammonia emissions from croplands in east, southeast and south asia, Global Change Biology, 9, 1080-1096, 2003b.

Yang, L., Zhang, X., and Ju, X.: Linkage between N_2O emission and functional gene abundance in an intensively managed calcareous fluvo-aquic soil, Sci Rep, 7, 43283, 10.1038/srep43283, 2017a.

Yang, Y., Zhao, J., Jiang, Y., Hu, Y., Zhang, M., and Zeng, Z.: Response of bacteria harboring nirS and nirK genes to different N fertilization rates in an alkaline northern Chinese soil, European Journal of Soil Biology, 82, 1-9, 10.1016/j.ejsobi.2017.05.006, 2017b.

Yang, Y., Nie, J., Wang, S., Shi, L., Li, Z., Zeng, Z., and Zang, H.: Differentiated responses of nirS- and nirK-type denitrifiers to 30 years of combined inorganic and organic fertilization in a paddy soil, Archives of Agronomy and Soil Science, 67, 79-92, 10.1080/03650340.2020.1714032, 2020.

Yao, H., Huang, S., Qiu, Q., Li, Y., Wu, L., Mi, W., and Dai, F.: Effects of different fertilizers on the abundance and community structure of ammonia oxidizers in a yellow clay soil, Appl Microbiol Biotechnol, 100, 6815-6826, 10.1007/s00253-016-7502-z, 2016.

Yao, Z., Liu, C., Dong, H., Wang, R., and Zheng, X.: Annual nitric and nitrous oxide fluxes from Chinese subtropical plastic greenhouse and conventional vegetable cultivations, Environ Pollut, 196, 89-97, 10.1016/j.envpol.2014.09.010, 2015.

Ye, C., Gao, H., Zhang, N., and Zhou, X.: Photolysis of nitric acid and nitrate on natural and artificial Surfaces, Environmental Science & Technology, 50, 3530-3536, 10.1021/acs.est.5b05032, 2016a.

Ye, C., Zhou, X., Pu, D., Stutz, J., Festa, J., Spolaor, M., Tsai, C., Cantrell, C., Mauldin, R. L., 3rd, Campos, T., Weinheimer, A., Hornbrook, R. S., Apel, E. C., Guenther, A., Kaser, L., Yuan, B., Karl, T., Haggerty, J., Hall, S., Ullmann, K., Smith, J. N., Ortega, J., and Knote, C.: Rapid cycling of reactive nitrogen in the marine boundary layer, Nature, 532, 489-491, 10.1038/nature17195, 2016b.

Ye, C., Zhang, N., Gao, H., and Zhou, X.: Photolysis of particulate nitrate as a source of HONO and NO_x, Environmental Science & Technology, 51, 6849-6856, 10.1021/acs.est.7b00387, 2017.

Yin, C., Fan, F., Song, A., Li, Z., Yu, W., and Liang, Y.: Different denitrification potential of aquic brown soil in Northeast China under inorganic and organic fertilization accompanied by distinct changes of nirS- and nirK-denitrifying bacterial community, European Journal of Soil Biology, 65, 47-56, 10.1016/j.ejsobi.2014.09.003, 2014.

Yin, M., Gao, X., Tenuta, M., Kuang, W., Gui, D., and Zeng, F.: Manure application increased denitrifying gene abundance in a drip-irrigated cotton field, PeerJ, 7, e7894, 10.7717/peerj.7894, 2019.

Yokelson, R. J., Crounse, J. D., DeCarlo, P. F., Karl, T., Urbanski, S., Atlas, E., Campos, T., Shinozuka, Y., Kapustin, V., Clarke, A. D., Weinheimer, A., Knapp, D. J., Montzka, D. D., Holloway, J., Weibring, P., Flocke, F., Zheng, W., Toohey, D., Wennberg, P. O., Wiedinmyer, C., Mauldin, L., Fried, A., Richter, D., Walega, J., Jimenez, J. L., Adachi, K., Buseck, P. R., Hall, S. R., and Shetter, R.: Emissions from biomass burning in the Yucatan, Atmospheric Chemistry and Physics, 9, 5785-5812, 2009.

Yu, G., Jia, Y., He, N., Zhu, J., Chen, Z., Wang, Q., Piao, S., Liu, X., He, H., Guo, X., Wen, Z., Li, P., Ding, G., and Goulding, K.: Stabilization of atmospheric nitrogen deposition in China over the past decade, Nature Geoscience, 12, 424-429, 10.1038/s41561-019-0352-4, 2019.

Yu, J., Meixner, F. X., Sun, W., Mamtimin, B., Wang, G., Qi, X., Xia, C., and Xie, W.: Nitric oxide emissions from black soil, northeastern China: A laboratory study revealing significantly lower rates than hitherto reported, Soil Biology and Biochemistry, 42, 1784-1792, 10.1016/j.soilbio.2010.06.016, 2010.

Yu, Z., Liu, J., Li, Y., Jin, J., Liu, X., and Wang, G.: Impact of land use, fertilization and seasonal variation on the abundance and diversity of nirS-type denitrifying bacterial communities in a Mollisol in Northeast China, European Journal of Soil Biology, 85, 4-11, 10.1016/j.ejsobi.2017.12.001, 2018.

Yun, H., Wang, Z., Zha, Q., Wang, W., Xue, L., Zhang, L., Li, Q., Cui, L., Lee, S., Poon, S. C. N., and Wang, T.: Nitrous acid in a street canyon environment: Sources and contributions to local oxidation capacity, Atmospheric Environment, 167, 223-234, 10.1016/j.atmosenv.2017.08.018, 2017.

Zha, Q., Xue, L., Wang, T., Xu, Z., Yeung, C., Louie, P. K. K., and Luk, C. W. Y.: Large conversion rates of NO_2 to HNO_2 observed in air masses from the South China Sea: Evidence of strong production at sea surface?, Geophysical Research Letters, 41, 7710-7715, 10.1002/2014gl061429, 2014.

Zhang, B.-w., Zhou, M.-h., and Zhu, B.: Simultaneous quantification of greenhouse gas and nitric oxide emissions from subtropical conventional vegetable

systems: a 2-site field case study in Sichuan Basin, Journal of Mountain Science, 18, 671-682, 10.1007/s11629-020-6088-1, 2021.

Zhang, B., and Tao, F. M.: Direct homogeneous nucleation of NO_2, H2O, and NH3 for the production of ammonium nitrate particles and HONO gas, Chemical Physics Letters, 489, 143-147, 2010.

Zhang, J., Chen, J., Xue, C., Chen, H., Zhang, Q., Liu, X., Mu, Y., Guo, Y., Wang, D., Chen, Y., Li, J., Qu, Y., and An, J.: Impacts of six potential HONO sources on HO_x budgets and SOA formation during a wintertime heavy haze period in the North China Plain, Science of the Total Environment, 681, 110-123, 10.1016/j.scitotenv.2019.05.100, 2019a.

Zhang, L., Wang, T., Zhang, Q., Zheng, J., Xu, Z., and Lv, M.: Potential sources of nitrous acid (HONO) and their impacts on ozone: A WRF-Chem study in a polluted subtropical region, Journal of Geophysical Research: Atmospheres, 121, 3645-3662, 10.1002/2015jd024468, 2016a.

Zhang, M., Wang, W., Tang, L., Heenan, M., and Xu, Z.: Effects of nitrification inhibitor and herbicides on nitrification, nitrite and nitrate consumptions and nitrous oxide emission in an Australian sugarcane soil, Biology and Fertility of Soils, 54, 697-706, 10.1007/s00374-018-1293-6, 2018.

Zhang, W., Tong, S., Jia, C., Wang, L., Liu, B., Tang, G., Ji, D., Hu, B., Liu, Z., Li, W., Wang, Z., Liu, Y., Wang, Y., and Ge, M.: Different HONO Sources for Three Layers at the Urban Area of Beijing, Environ Sci Technol, 54, 12870-12880, 10.1021/acs.est.0c02146, 2020.

Zhang, X., Davidson, E. A., Mauzerall, D. L., Searchinger, T. D., Dumas, P., and Shen, Y.: Managing nitrogen for sustainable development, Nature, 528, 51, 2015a.

Zhang, X., Meng, F., Li, H., Wang, L., Wu, S., Xiao, G., and Wu, W.: Optimized fertigation maintains high yield and mitigates N2O and NO emissions in an intensified wheat–maize cropping system, Agricultural Water Management, 211, 26-36, 10.1016/j.agwat.2018.09.045, 2019b.

Zhang, Y., Liu, J., Mu, Y., Pei, S., Lun, X., and Chai, F.: Emissions of nitrous oxide, nitrogen oxides and ammonia from a maize field in the North China Plain, Atmospheric Environment, 45, 2956-2961, 10.1016/j.atmosenv.2010.10.052, 2011.

Zhang, Y., Mu, Y., Zhou, Y., Liu, J., and Zhang, C.: Nitrous oxide emissions from maize–wheat field during 4 successive years in the North China Plain, Biogeosciences, 11, 1717-1726, 10.5194/bg-11-1717-2014, 2014.

Zhang, Y., Wang, F., Zhang, J., Zhu, T., Lin, C., Müller, C., and Cai, Z.: Cattle manure and straw have contrasting effects on organic nitrogen mineralization pathways

in a subtropical paddy soil, Acta Agriculturae Scandinavica, Section B — Soil & Plant Science, 65, 619-628, 10.1080/09064710.2015.1039054, 2015b.

Zhang, Y., Lin, F., Jin, Y., Wang, X., Liu, S., and Zou, J.: Response of nitric and nitrous oxide fluxes to N fertilizer application in greenhouse vegetable cropping systems in southeast China, Scientific Reports, 6, 20700, 10.1038/srep20700, 2016b.

Zhang, Y., Wang, H., Maucieri, C., Liu, S., and Zou, J.: Annual nitric and nitrous oxide emissions response to biochar amendment from an intensive greenhouse vegetable system in southeast China, Scientia Horticulturae, 246, 879-886, 10.1016/j.scienta.2018.11.070, 2019c.

Zhao, J., Ni, T., Li, J., Lu, Q., Fang, Z., Huang, Q., Zhang, R., Li, R., Shen, B., and Shen, Q.: Effects of organic–inorganic compound fertilizer with reduced chemical fertilizer application on crop yields, soil biological activity and bacterial community structure in a rice–wheat cropping system, Applied Soil Ecology, 99, 1-12, 10.1016/j.apsoil.2015.11.006, 2016.

Zheng, X., Huang, Y., Wang, Y., and Wang, M.: Seasonal characteristics of nitric oxide emission from a typical Chinese rice wheat rotation during the non-waterlogged period, Global Change Biology, 9, 219-227, 2003.

Zhou, S., Sakiyama, Y., Riya, S., Song, X., Terada, A., and Hosomi, M.: Assessing nitrification and denitrification in a paddy soil with different water dynamics and

applied liquid cattle waste using the ^{15}N isotopic technique, Science of the Total Environment, 430, 93-100, 10.1016/j.scitotenv.2012.04.056, 2012.

Zhou, X., Zhang, N., Teravest, M., Tang, D., Hou, J., Bertman, S., Alaghmand, M., Shepson, P. B., Carroll, M. A., and Griffith, S.: Nitric acid photolysis on forest canopy surface as a source for tropospheric nitrous acid, Nature Geoscience, 4, 440-443, 2011.

Zhou, X. L., Gao, H. L., He, Y., Huang, G., Bertman, S. B., Civerolo, K., and Schwab, J.: Nitric acid photolysis on surfaces in low-NO_x environments: Significant atmospheric implications, Geophysical Research Letters, 30, 2003.

Zhou, Z., Zheng, X., Xie, B., Liu, C., Song, T., Han, S., and Zhu, J.: Nitric oxide emissions from rice-wheat rotation fields in eastern China: effect of fertilization, soil water content, and crop residue, Plant and Soil, 336, 87-98, 10.1007/s11104-010-0450-y, 2010.

Zhou, Z., Shi, X., Zheng, Y., Qin, Z., Xie, D., Li, Z., and Guo, T.: Abundance and community structure of ammonia-oxidizing bacteria and archaea in purple soil under long-term fertilization, European Journal of Soil Biology, 60, 24-33, 10.1016/j.ejsobi.2013.10.003, 2014.

Zhu, X., Burger, M., Doane, T. A., and Horwath, W. R.: Ammonia oxidation pathways and nitrifier denitrification are significant sources of N_2O and NO under low

oxygen availability, Proceedings of the National Academy of Sciences of the United States of America, 110, 6328-6333, 10.1073/pnas.1219993110, 2013.

Zhu, X., Zhang, W., Chen, H., and Mo, J.: Impacts of nitrogen deposition on soil nitrogen cycle in forest ecosystems: A review, Acta Ecologica Sinica, 35, 35-43, 10.1016/j.chnaes.2015.04.004, 2015.